Effect of the form of the overhang of a recurve seawall to reduce wave overtopping

by
Marcus Malan Kretschmer

Thesis presented in fulfilment of the requirements for the degree of Master of Engineering in the Faculty of Civil Engineering at Stellenbosch University

Supervisor: Prof JS Schoonees

December 2017

Declaration

By submitting this thesis electronically, I declare that the entirety of the work contained therein is my own, original work, that I am the sole author thereof (save to the extent explicitly otherwise stated), that reproduction and publication thereof by Stellenbosch University will not infringe any third party rights and that I have not previously in its entirety or in part submitted it for obtaining any qualification.

Signed: ……

Date: December 2017

Abstract

Coastal areas around the world are experiencing a rise in sea level due to the effects of global warming. As a large percentage of the world's population resides within the coastal zone, the rise in sea level is placing evermore developments and people at risk, consequently increasing the demand for more effective coastal defence structures.

One of the most common types of coastal defence structures are seawalls, which reduce or prevent wave overtopping and flooding of the landward side of the structure. These structures are often designed as vertical impermeable walls with high crests to ensure protection against overtopping. However, these designs are not always favourable as the high crest levels often obstruct the view of the sea. Recurve seawalls provide the solution, as they reduce wave overtopping without excessively compromising the sea view. However, existing guidelines for the design and research on the effectiveness of different recurve seawalls are very limited.

This project aims to determine the effectiveness of different overhang forms of recurve seawalls on reducing wave overtopping. In order to achieve the objective of this study, the performance of different recurve forms in reducing wave overtopping was evaluated by conducting overtopping tests in a physical model. The model was constructed in a glass wave flume equipped with a piston-type wave paddle. A total number of 147 tests with varying water levels and wave periods were conducted for five different overhang forms, providing a comprehensive set of results which were analysed to determine the most effective overhang form.

Analysis of the findings clearly indicated that the shape of the overhang has a strong influence on the overtopping reduction capabilities of a recurve seawall. It was found that the concave shape with a squared overhanging edge offered the most reduction in overtopping, when compared with the performances of the remaining forms. For the high relative freeboard cases (large difference between crest level and water level), small amounts of overtopping were observed as a result of colliding incident and reflected waves. These overtopping events constituted mainly of white water spray which were negligibly small but should be treated with caution as the presence of an onshore wind, which was not modelled in this study, could have a significant influence on the amount of overtopping.

In addition, it was found that overtopping generally increases with an increase in the wave return angle of the recurve. When comparing the two different concave recurves tested, the

recurve with the rounded overhanging edge produced up to fifty percent more overtopping, due to the adhesion of water along the rounded edge. This finding led to the conclusion that apart from the overhang length, the shape of the overhanging edge also significantly influences the reduction of overtopping. As opposed to the findings of a previous study, increasing the wave period up to 14 seconds consistently led to an increase in overtopping.

It is recommended that further model tests should be conducted on concaved recurves, including variations in the vertical dimension of the recurve. The effects of different beach slopes and wave heights on overtopping of recurve seawalls should also be investigated, as these remained constant throughout this study.

Opsomming

Kusgebiede regoor die wêreld is besig om ‘n styging in seevlak te ervaar as gevolg van aardverwarming. Aangesien 'n groot persentasie van die wêreld se bevolking binne die kusgebied woon, stel die stygende seevlak al hoe meer ontwikkelings en mense in gevaar, wat gevolglik die vraag na meer doeltreffende kusverdediging strukture verhoog.

Een van die algemeenste tipes strukture vir kusverdediging is seemure, wat golfoorslag en oorstroming van die landwaartse kant van die struktuur verminder of voorkom. Hierdie strukture word dikwels as vertikale ondeurdringbare mure ontwerp met hoë kruine om beskerming teen golfoorslag te verseker. Hierdie ontwerpe is egter nie altyd gunstig nie, aangesien die hoë kruinvlakke dikwels die see-uitsig belemmer. Die gebruik van terugkaatsmure voorsien die oplossing, aangesien die golfoorslag verminder word sonder om die see-uitsig so erg te benadeel. Bestaande riglyne vir die ontwerp en navorsing oor die doeltreffendheid van verskillende terugkaatsmure is egter baie beperk.

Die doelwit van hierdie projek is om die effektiwiteit van verskillende oorhangvorms van terugkaatsmure op die vermindering van golfoorslag te bepaal. Ten einde die doel van hierdie studie te bereik, is die werking van verskillende terugkaatsvorms in die vermindering van golfoorslag geëvalueer deur oorslagtoetse in 'n fisiese model uit te voer. Die fisiese model was in 'n golfkanaal, toegerus met ‘n suiertipe-golfopwekker, gebou. 'n Totaal van 147 toetse met verskillende watervlakke en golfperiodes is vir vyf verskillende oorhangvorms uitgevoer, wat sodoende 'n omvattende stel resultate verskaf het wat ontleed is om die effektiefste oorhangvorm te bepaal.

Ontleding van die bevindings het duidelik aangedui dat die vorm van die oorhang ‘n sterk invloed het op die vermoë van ‘n terugkaatsmuur om oorslag te verminder. Daar is bevind dat die konkawe vorm met 'n vierkantige oorhangrand die grootste vermindering in oorslag bied, in vergelyking met die werking van die oorblywende vorms. Vir die gevalle met relatiewe hoë vryboorde (groot verskil tussen kruinvlak en watervlak), is klein hoeveelhede oorslag waargeneem as gevolg van botsende inkomende en weerkaatste golwe. Hierdie tipes oorslag het hoofsaaklik uit witwaterspatsels bestaan wat weglaatbaar klein was, maar dit moet versigtig geïnterpreteer word, aangesien die teenwoordigheid van 'n aanlandige wind, wat nie in hierdie studie gemodelleer is nie, 'n beduidende invloed op die hoeveelheid oorslag kan hê.

Daarbenewens is gevind dat oorslag oor die algemeen toeneem met 'n toename in die golfterugkaatshoek van die terugkaatsvorm. By die vergelyking van die twee verskillende konkawe terugkaatsvorms, het die terugkaatsvorm met die geronde oorhangrand tot vyftig persent meer oorslag veroorsaak as gevolg van die adhesie van water teen die ronde rand. Hierdie bevinding het tot die gevolgtrekking gelei dat behalwe vir die oorhanglengte, die vorm van die oorhangende rand ook ‘n beduidende invloed op die vermindering van oorslag het. In teenstelling met die bevindings van 'n vorige studie, het die verhoging van die golfperiode tot 14 sekondes geleidelik tot 'n toename in oorslag gelei.

Daar word aanbeveel dat verdere toetse op konkawe terugkaatsmure uitgevoer moet word, met wisselende afmetings van die terugkaatsvorm se hoogte. Die invloed van verskillende strandhellings en golfhoogtes op die oorslag van terugkaatsmure moet ook ondersoek word, aangesien hierdie veranderlikes konstant deur die studie gebly het.

Acknowledgements

I would like to express my gratitude and acknowledge the contribution of a number of people, without whom this would not have been possible.

- My study leader, Prof Koos Schoonees, for your enthusiasm, knowledge and continued guidance throughout this study;
- Estelle Swart, for your guidance and willingness to give advice during the time-consuming setup of the physical model;
- Johann Nieuwoudt, Iliyaaz Williams and Marvin Lindoor, for your time, enthusiasm and unwavering support throughout my time in the Hydraulics Laboratory;
- Lastly, I would like to thank my girlfriend and family for their never-ending support and understanding throughout my post graduate studies.

Table of Contents

List of Figures

List of Tables

List of Abbreviations and Symbols

2D	-	Two dimensional
Capex	-	Capital expenditure
CoV	-	Coefficient of variation
CLASH	-	Crest Level Assessment of coastal Structures and Hazard analysis on permissible wave overtopping
JONSWAP	-	Joint North Sea Wave Project
Opex	-	Operating expenses
PM	-	Pierson Moskowitz
PVC	-	Polyvinyl chloride
SWL	-	Still water level
α	-	Angle of recurve (°)
γ	-	JONSWAP peak enhancement factor
σ	-	Standard deviation of overtopping rates
μ	-	Average of overtopping rates
Ø	-	Wave return angle (°)
B_r	-	Horizontal extension of recurve overhang (m)
g	-	Gravitational acceleration (m/s^2)
h_*	-	Wave breaking parameter
H_i	-	Incident wave height (m)
H_{mo}	-	Incident spectral significant wave height (m)
h_r	-	Vertical dimension of recurve (m)
H_r	-	Reflected wave height (m)
h_s	-	Water depth at toe of wall (m)
H_s	-	Significant wave height at toe of seawall (m)

k-factor	-	Reduction factor of wave overtopping
K_r	-	Bulk reflection coefficient
N_X	-	Scale ratio between prototype and model values
P_c	-	Height of vertical part of wall above SWL (m)
q	-	Mean overtopping discharge per meter of seawall (l/s/m)
R_c	-	Freeboard (m)
T	-	Wave period (s)
T_m	-	Nominal mean wave period of the JONSWAP spectrum (s)
$T_{m-1,0}$	-	Spectral wave period (s)
T_p	-	Peak wave period (s)
WL_{toe}	-	Water level at toe of wall (m)
X_m	-	Dimensional value in model
X_p	-	Dimensional value in prototype

Chapter 1: Introduction

1.1 Background

Wave overtopping occurs when wave action causes water to rush up the face of a seawall and pass over the crest of the structure. Seawalls are coastal defence structures used to reduce or prevent wave overtopping or flooding of the landward side of the structure. Overtopping discharges can jeopardize the safety of pedestrians, vehicles, and infrastructure. Due to the potential negative impacts of overtopping, these structures are often designed as vertical impermeable walls with high crests to ensure protection against overtopping. However, these designs are not always favourable to all parties as high crest levels reduce the view of the ocean which is of importance when considering aspects such as potential coastal developments or the negative effect it will have on beach tourism.

Fortunately, the reduction of overtopping can be achieved by another method, other than increasing the wall height. This method includes the use of a recurve at the top of the seawall. The design of recurve seawalls incorporates an overhang pointing seawards at the top of a vertical/near vertical wall. The advantage of using a recurve seawall is that it offers a reduced overtopping rate to that of a vertical wall, but with a lower crest height. Therefore, by using recurve seawalls, a better view of the ocean can be maintained.

The seaward overhang of a recurve seawall, see Figure 1, deflects uprushing water from impacting waves back towards the sea, which would otherwise, without the presence of a recurve, rise into the air and pass over the wall due to momentum. Onshore blowing winds also contribute to overtopping volumes by carrying spray over the wall. However, wind usually only has a significant effect on low overtopping rates when small amounts of spray are generated which can easily be carried over the wall and little or no effect on large overtopping rates with heavy volumes of overtopping water. In addition, the generation and control of wind in an empirical study is a financially-intensive exercise. Therefore, studying the effect of wind on overtopping is economically unjustifiable and not considered in this project.

There exists a number of design types commonly known as a recurve, parapet, wave return wall, or bullnose. Even though there are certain distinctions between the different types, they all still serve the same purpose of reducing wave overtopping by deflecting back seaward uprushing water (Pearson et al., 2004).

Figure 1: Recurve seawall at Exmouth, Devon, Great Britain (Cox, 2008)

The main focus of this study is on determining and comparing the effects which different overhang forms have on reducing wave overtopping of vertical recurve seawalls.

The current design guidance for recurve seawalls is based upon limited research. A popular form of guidance on the analysis of wave overtopping of recurve seawalls can be found in the EurOtop Wave Overtopping of Sea Defences and Related Structures: Assessment Manual (EurOtop, 2007).

According to literature findings, the mechanisms describing the effectiveness of a recurve are not yet fully described, and even though previous studies have been done on the effects of recurve walls on reducing wave overtopping, it is suggested that no systematic study has been undertaken on the effects of different recurve shapes on reducing overtopping (EurOtop, 2007).

1.2 Objective

This project aims to determine and provide a comparison of the effectiveness of different overhang forms of recurve seawalls on reducing wave overtopping through physical modelling.

1.3 Definitions and Methodology

A recurve seawall can be defined as a vertical, impermeable wall combined with a curved overhang structure atop the wall pointing seawards. For the purpose of this empirical study, the environment in which the recurve seawall is tested represents that of a coastal beach with a gradual beach slope and relatively shallow water depths.

The objective of this study was to determine the effectiveness of different overhang shapes on the reduction of wave overtopping. To achieve this objective, overtopping tests with different recurve seawalls were conducted in a physical model. The dimensions of the recurve overhang length and height were kept constant, with only the recurve profile shape changing between tests. The beach slope, seawall crest level and wave height were kept constant throughout the study, with only two varying hydraulic parameters, namely, water level and wave period. The investigation of wave forces against recurve walls was excluded from this study.

1.4 Brief outline of project structure

This report is made up of 7 chapters, including the introductory chapter.

Chapter 2 consists of a literature review on the topics of wave overtopping, wave processes at vertical walls and types of recurve seawalls. In addition, the chapter includes reviews on existing design methods and guidelines, as well as previous studies of recurve seawalls. Furthermore, research on hydraulic physical modelling is included to provide a thorough understanding of the procedure required to achieve valuable empirical results.

Chapter 3 describes the setup of the physical model, based on the literature findings, and provides the test execution followed. In addition, the model scaling, controlled hydraulic parameters, measurement technique and validation of test accuracy are discussed.

Chapter 4 provides the physical model test results obtained together with performance overviews of the recurves tested. The results from Chapter 4 are represented in varying graphical formats, which are analysed and discussed in Chapter 5.

Chapters 6 and 7 discuss the conclusions of the project and the recommendations for further studies.

Chapter 2: Literature review

2.1 Overtopping

In general, overtopping is defined as water which runs up the face and passes over the crest of a structure due to wave action. According to EurOtop (2007), there exists several types of overtopping. The first of these can be described as 'green water' overtopping which takes place when a large solid volume of water runs up and passes over the crest of the structure. This type of overtopping could be expected in cases where the crest of the structure is relatively low or in extreme circumstances of high inshore seawater levels due to a combination of factors such as spring high tide, wind setup, barometric setup, and high wave run-up (USACE, 2006).

The second type of wave overtopping is described as 'white water' or spray overtopping which occurs when incident waves break either before they reach the structure or as they impact the structure, generating large amounts of spray (Figure 2). This aerated volume of water is then carried over the wall either by its own momentum or by the forces of an onshore blowing wind (EurOtop, 2007).

Figure 2: Wave overtopping on a vertical seawall without recurve
(van der Meer et al., n.d.)

The last type of overtopping can only take place in the presence of a strong onshore wind. Water in the form of spray is carried from the crests of incident waves or from turbulent action between incoming and reflected waves over the crest of the seawall. The amount of overtopping caused by this type is negligibly small when compared with the first two types (EurOtop, 2007).

Therefore, and as the facility to be used for testing is unable to model the effects of wind, only the first two types of overtopping will be examined in this study.

Guidance on tolerable mean overtopping discharges and individual maximum overtopping volumes exists for pedestrians, vehicles, and buildings/infrastructure on the landward side of sea defence structures. These overtopping safety limits are a result of previous guidance and empirical results from the CLASH database and other researchers and can be seen in Table 1 (EurOtop, 2007; CIRIA et al., 2007).

It is important to note that individual maximum discharge volumes are better indicators of safety than average discharges for people. However, individual maximum volumes of overtopping will not be modelled in this study as only average discharges over an entire test duration will be available. Therefore, caution will be taken when interpreting the overtopping results with regard to the safety of pedestrians.

Table 1: Tolerable overtopping discharge (EurOtop, 2007); (CIRIA et al., 2007)

Pedestrians	Mean discharge q (l/s/m)
Unsafe for unaware pedestrians, no clear view of the sea, relatively easily upset or frightened, narrow walkway or proximity to fall hazard	q > 0.03
Unsafe for aware pedestrians, clear view of the sea, not easily upset or frightened, able to tolerate getting wet, wider walkway	q > 0.1
Unsafe for trained staff, well shod and protected, expecting to get wet, overtopping flows at lower levels only, no falling jet, low danger of fall from walkway	q > 1 - 10
Vehicles	
Unsafe for driving at moderate or high speed, impulsive overtopping giving falling or high velocity jets	q > 0.01 - 0.05
Unsafe for driving at low speed, overtopping by pulsating flows at low flow depths, no falling jets, vehicle not immersed	q > 10 - 50
Buildings and Infrastructure	
No damage	q < 0.001
Minor damage to fittings	0.001 < q < 0.03
Structural damage	q > 0.03
Damage to grassed or lightly protected promenade behind seawall	q > 50
Damage to paved or armoured promenade behind seawall	q > 200

2.2 Wave regimes at vertical walls

In order to assess overtopping at vertical structures such as plain vertical walls, EurOtop (2007) suggests that the regime of the wave/structure interaction must first be identified. This is important, as each regime offers a specific indication of the type of overtopping, as discussed in Section 2.1, that can be expected.

When considering the type of wave action which occurs at vertical structures, EurOtop (2007) refers to either a "non-impulsive" or "pulsating" wave condition and an "impulsive" wave action. "Non-impulsive" conditions occur when the height of the incident significant wave is relatively small compared to the local water depth, i.e. the wave has a lower wave steepness (wave height divided by wavelength). Waves which do overtop the structure in this condition, illustrated in Figure 3 (A), are considered as non-turbulent "green water" overtopping, as mentioned earlier. Conversely, "impulsive" conditions take place when the incident wave height is large compared to the local water depth or has a higher wave steepness. Violent wave breaking can occur at the vertical wall under these conditions which leads to previously mentioned “white water” or spray overtopping, Figure 3 (B).

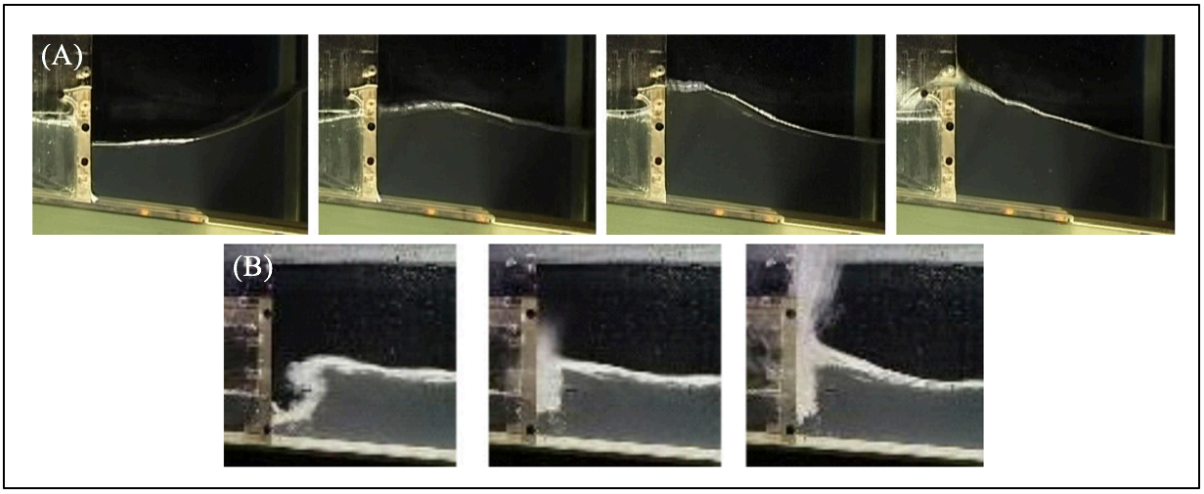

Figure 3: Non-impulsive (A) and impulsive (B) wave conditions at a vertical wall (EurOtop, 2007)

In order to determine the wave regime which governs at a vertical wall, EurOtop (2007) provides a wave breaking or "impulsiveness" parameter, h_*, which is defined based on the depth at the submerged toe of the wall ($h_s > 0$):

$$h_* = 1.35 \frac{h_s}{H_{mo}} \frac{2\pi h_s}{g T_{m-1,0}}$$

Non-impulsive: $h_* > 0.3$
Impulsive: $h_* < 0.2$

where

H_{mo} incident spectral significant wave height

$T_{m-1,0}$ spectral period, ($T_{m-1,0} = T_p/1.1$)

Therefore, this equation can be used to validate and identify the type of wave action encountered in the empirical analysis of this study.

2.3 Recurve-type seawalls

Various types of overhang forms have often been incorporated into the design of seawalls worldwide. The more common forms are known as parapets and recurves. Parapets have a straight seaward extension or overhang with an angle larger than zero with a vertical wall, while recurves dominate either the upper part of the wall as a curved parapet or the entire wall as a seaward curving wall-face (Kortenhaus et al., 2003).

Figures 4 – 10 illustrate different recurve types used around the world.

Figure 4: Recurved seawall on stepped slope at Burnham on Sea, Somerset, United Kingdom (Grainger, 2009)

Figure 5: High seawall with recurve at the Sandbank Sand Spit, Southwest of Bournemouth, Dorset, United Kingdom

(West, 2007)

Figure 6: Recurve sea defence wall at Cheyne beach, Devon, United Kingdom

(McAuley, 2015)

Figure 7: Flaring seawall at Kunigami, Okinawa
(Kobelco, 2012)

Figure 8: Seawall with parapet at Kailua-Kona, Hawaii
(Hawaii Real Estate, n.d.)

Figure 9: Seawall with recurve section at Three Anchor Bay, Cape Town, South Africa

(CMA, 2012)

Figure 10: Recurve seawall at the Sea Point Promenade, Cape Town, South Africa

2.4 Existing design methods and previous studies

This section provides a literature review on current design methods and previous studies on recurve type seawalls carried out by other researchers which will serve as a basis for compiling the methodology of this study.

As mentioned in Section 1.1, current guidance on analysis of wave overtopping of recurved seawalls follows that as stipulated in the EurOtop Manual. The EurOtop Manual is a result of a collaboration between various researchers. However, for the purpose of this study, focus will be placed only upon the contributions by researchers such as Kortenhaus et al. (2003) and Pearson et al. (2004), as they offer the most relevant information on this subject.

According to the findings of Kortenhaus et al. (2003), sufficient data exists from results of case studies and systematic studies on mean overtopping discharges of vertical seawalls. However, research on wave overtopping of vertical seawalls with recurves or parapets are based only on a few studies. Therefore, Kortenhaus et al. (2003) focused on establishing a possible reduction factor approach for recurve/parapet walls based on their geometry, size, and form.
During the experiments, it was found that for the case of a recurve seawall with a relatively high freeboard (R_c/H_s = 1.5), no overtopping took place and that the impacting wave was completely deflected. For lower crest freeboards, the overhang could no longer capture and deflect all the wave energy, resulting in overtopping of the structure.

In order to determine wave overtopping rate reduction factors, Kortenhaus et al. (2003) conducted overtopping tests of vertical walls with recurves present ($q_{recurve}$) and then repeated the same test but with no recurve installed ($q_{no\ recurve}$), i.e. just a plain vertical wall with the same dimensions and input conditions. The reduction factor k, was defined as:

$$k = \frac{q_{recurve}}{q_{no\ recurve}}$$

A detailed analysis of the data obtained from the experiments led to the derivation of a new approach for predicting a reduction k-factor for wave overtopping of parapets or recurves. The governing parameters influencing the k-factor were identified as the non-dimensional freeboard, parapet width and angle as illustrated in Figure 11 (Kortenhaus et al., 2003).

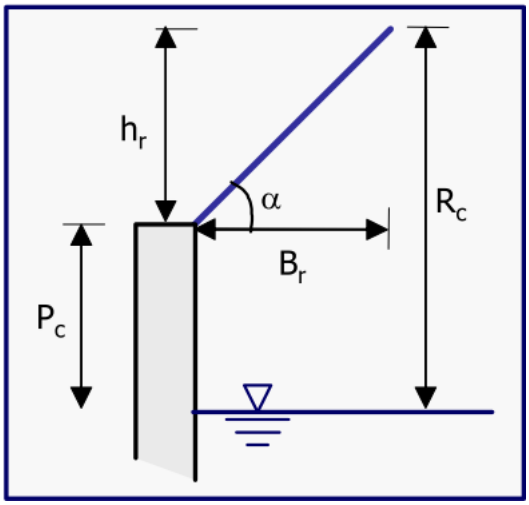

Figure 11: Relative parameter sketch and definitions (Kortenhaus et al., 2003)

Freeboard R_c/H_s; Width B_r/P_c; Angle B_r/h_r

With:

R_c = Freeboard (m)

H_s = Significant wave height (m)

α = Angle of recurve (°)

B_r = Width of parapet overhang (m)

h_r = Height of parapet (m)

P_c = Relative elevation (m)

The final equations for determining the k-factor for three different regimes depending on the structural and hydrodynamic parameters involved and ranging from little or no effect (k-value close to 1.0) to large reductions (very small k-values), as per the new approach developed by Kortenhaus et al. (2003), are provided in the top half of Figure 12. However, implementation of the calculated k-factors still led to significant scatter in the data points, especially for large reductions in overtopping rates, i.e. small k-values (Kortenhaus et al., 2003).

In an attempt to produce a generic guidance for the design of recurve type structures, another method was introduced by Pearson et al. (2004) which built upon the approach developed by Kortenhaus et al. (2003). Pearson et al. (2004) introduced the use of an adjusted k'-factor and decision chart to determine the appropriate k-value to be used in calculating the predicted discharge for a parapet or recurve seawall. During the study conducted by Kortenhaus et al. (2003), one of the most influential parameters on the k-value were identified as the relative crest freeboard (R_c/H_s). However, further research revealed that the k-value also strongly depended on the relative water depth at the base of the wall (h_s/H_s). Both of these structural and wave parameters, respectively, tended to cause significant scatter in the test results. In an attempt to reduce the scatter, it was decided to combine these two parameters which would result in k being dependent on a new dimensionless parameter of R_c/H_s x $H_s/h_s = R_c/h_s$. The adjusted k'-factor used for large reductions in wave overtopping was then sub-divided into three regimes dependent on R_c/h_s, similar to the Kortenhaus et al. (2003) method (Pearson et al., 2004).

The design guidance formulated by Pearson et al. (2004) as described above was summarized in a decision chart as illustrated in Figure 12. Significant scatter was still present at very small discharges, i.e. large overtopping reductions. It is therefore important to note that it would be deemed impractical to design for k-values smaller than about 0.05, as it is very difficult to accurately predict reductions in mean discharges with a factor greater than 20 without the use of a detailed physical model study (Pearson et al., 2004).

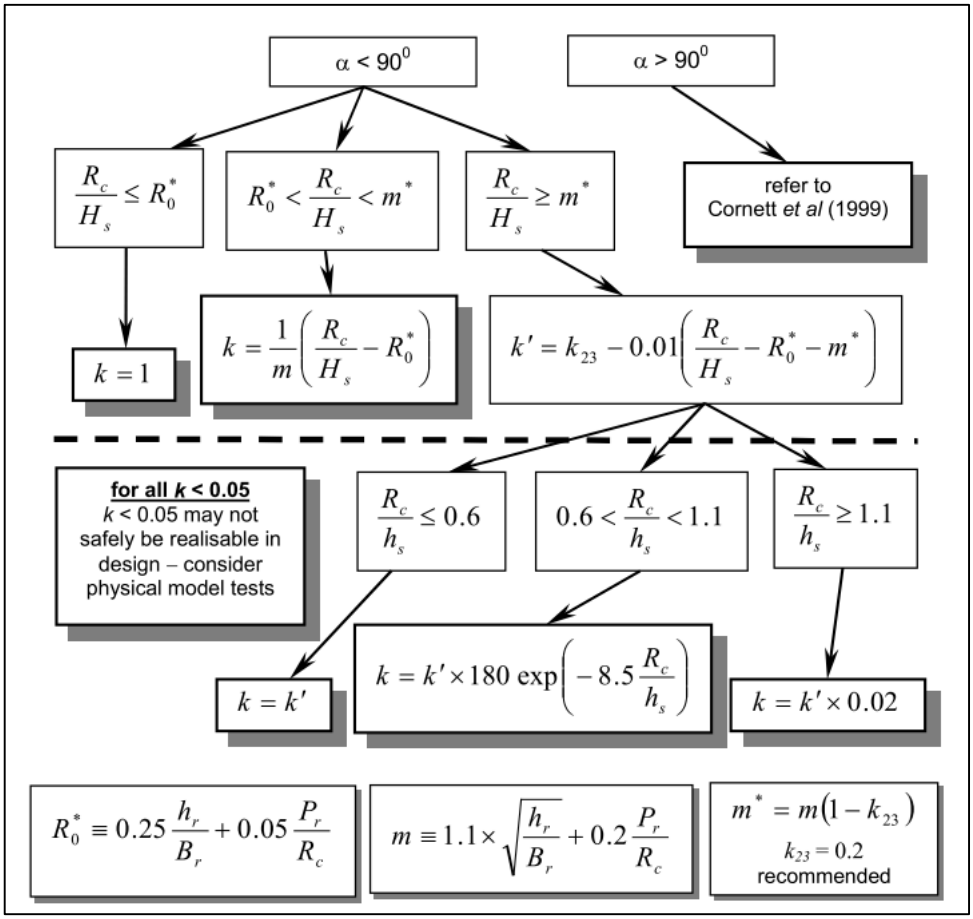

Figure 12: Decision chart for design guidance of recurve wall (Pearson et al., 2004)

The EurOtop Overtopping Manual includes an overall calculation tool for the prediction of wave overtopping discharges for a variety of structures. The calculation tool is available online and provides a simplified method for applying the empirical equations defined within the manual.

The calculation tool provides good first estimates of overtopping discharges for basic structures, although use of the Neural Network prediction tool is recommended for more complex designs (HR Wallingford, n.d.). For a vertical wall with a wave return, the input parameters required in the calculation tool for calculating average overtopping discharge are illustrated in Figure 13

and described in Table 2.

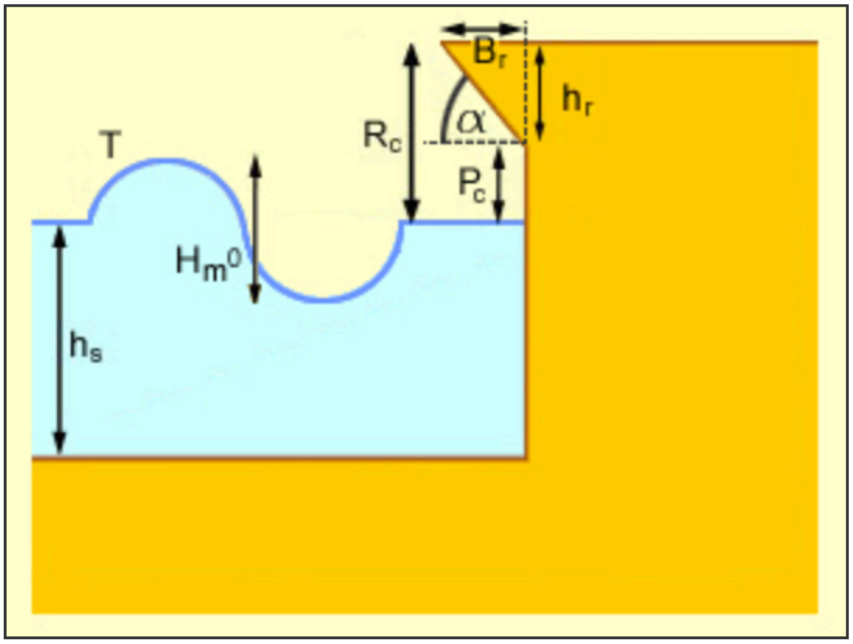

Figure 13: Schematization of wave return wall in EurOtop Calculation Tool (HR Wallingford, n.d.)

Table 2: Description of input parameters used in Calculation Tool

Symbol	Description	Unit
h_s	Water depth at toe of structure (SWL)	m
H_{mo}	Wave height at toe of structure	m
T	Wave period	sec
R_c	Height of wall crest above SWL	m
P_c	Height of vertical part of wall above SWL	m
h_r	Height of wave return	m
B_r	Horizontal extension of wave return	m
α	Angle of recurve	°

As the equations used within the calculation tool are based on empirical models which contain uncertainties in their predictions, the calculation tool includes the option of two methods to address this uncertainty, namely probabilistic and deterministic methods. The probabilistic method suggests that, for collected data points with a normal distribution, around 50% of the data points are larger than the prediction by the model, and 50% are smaller than the predicted model value (EurOtop, 2007).

The deterministic method produces a mean overtopping value plus one standard deviation, which is derived from comparing the model data with the predicted model value. The deterministic method therefore produces a larger/more conservative overtopping value and is safer to use as it takes model uncertainty into account (EurOtop, 2007).

Another prediction method for average overtopping discharges is the use of Neural Network tools, as described in the EurOtop Manual (EurOtop, 2007). Neural networks can be described as a combination of various layers, with each layer containing one or more processing elements which are called 'neurons'. A neural network is typically divided into three layers: the first layer contains the input parameters, such as structural and hydraulic parameters, the second layer is known as the hidden layer and contains neurons configured to the specifications of the task which receive information from the preceding input layer and carries out operations to produce the third and final, output layer (EurOtop, 2007).

In order for a neural network tool to be effective, it requires a large amount of data. This is why neural networks are effective in wave overtopping calculations, as there exists an overwhelming amount of test data on the subject. This led to the inception of the European CLASH project (EurOtop, 2007).

The European CLASH project (Crest Level Assessment of coastal Structures by full scale monitoring, neural network prediction and Hazard analysis on permissible wave overtopping) was undertaken with the objective of solving possible scale/model effects for wave overtopping and to produce a generic prediction method for seawall crest height design (De Rouck et al., 2009). In an attempt to solve the problem of scale/model effects, wave overtopping field measurements of different structures were taken at three locations in Europe. The prototype sites were then modelled and the laboratory results compared with the field measurements to obtain conclusions on overtopping-related scale/model effects.

In order to develop a generic prediction method, a large amount of worldwide data on wave overtopping as well as the data obtained from the prototype field measurements and corresponding model results were gathered into one database. The final database consisted of over 10 000 overtopping tests from 163 independent test structures, with each test described by 31 parameters, such as structural and hydraulic parameters (De Rouck et al., 2009).

The database was used to train the neural network tool developed within the CLASH project and the configuration consisted of 15 parameters in the input layer describing structural geometry and wave characteristics and a single average overtopping discharge, q, in the output layer, as illustrated in Figure 14. The neural network tool can be used to provide a first estimation of overtopping discharge for a given structure.

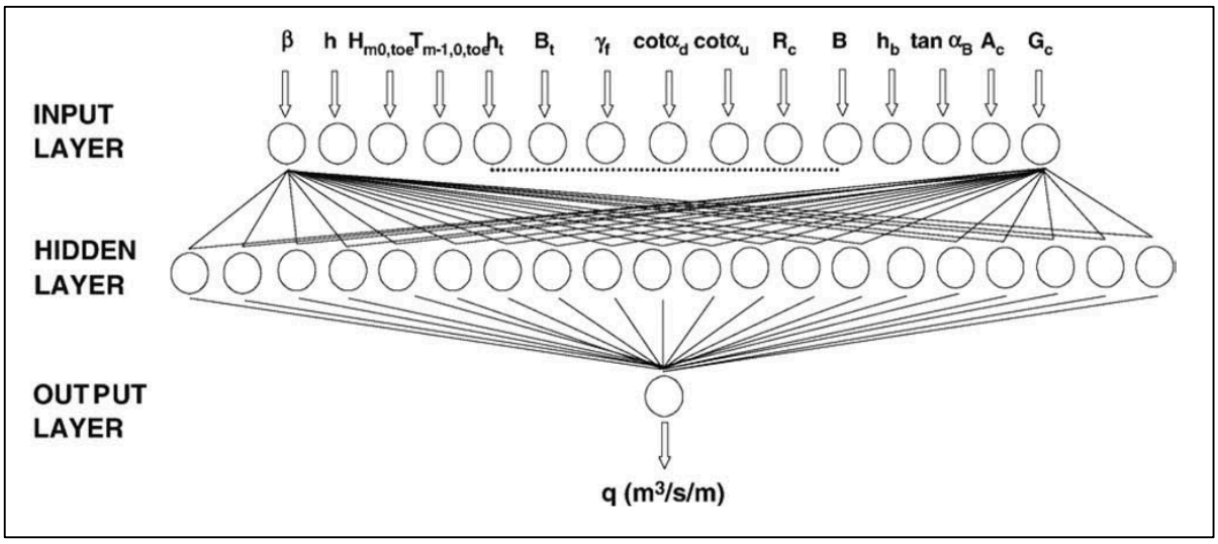

Figure 14: Neural Network Configuration **(De Rouck et al., 2009)**

The only disadvantage of the CLASH neural network is that it was configured to only consider overtopping data, so even in a range where no overtopping would be expected, the tool would still produce some prediction of overtopping which would obviously be false.

In addition to guidance provided by the likes of Kortenhaus et al. (2003) and Pearson et al. (2004), more recent studies were carried out by Schoonees (2014), Schoonees & Toms (2016), and Swart (2016). Schoonees (2014) focused on the effects of impermeable recurve seawalls in reducing wave overtopping, specifically investigating the difference in effectiveness of a plain vertical wall versus recurve walls in reducing wave overtopping as well as the influence of two different overhang lengths of the recurve on wave overtopping.

The results from the physical model study concluded that the wave return walls were overall more effective in reducing overtopping than the vertical seawall. The recurve seawall with the longer overhang length proved to be the most efficient, although no significant difference between the two overhang lengths was observed for low water levels at the toe of the structure.

Schoonees (2014) and Schoonees & Toms (2016) produced a graph (Figure 15) indicating the influence of the recurve overhang length on overtopping, which could assist in the design of recurve seawalls to maintain a lower crest height and still achieve low overtopping rates.

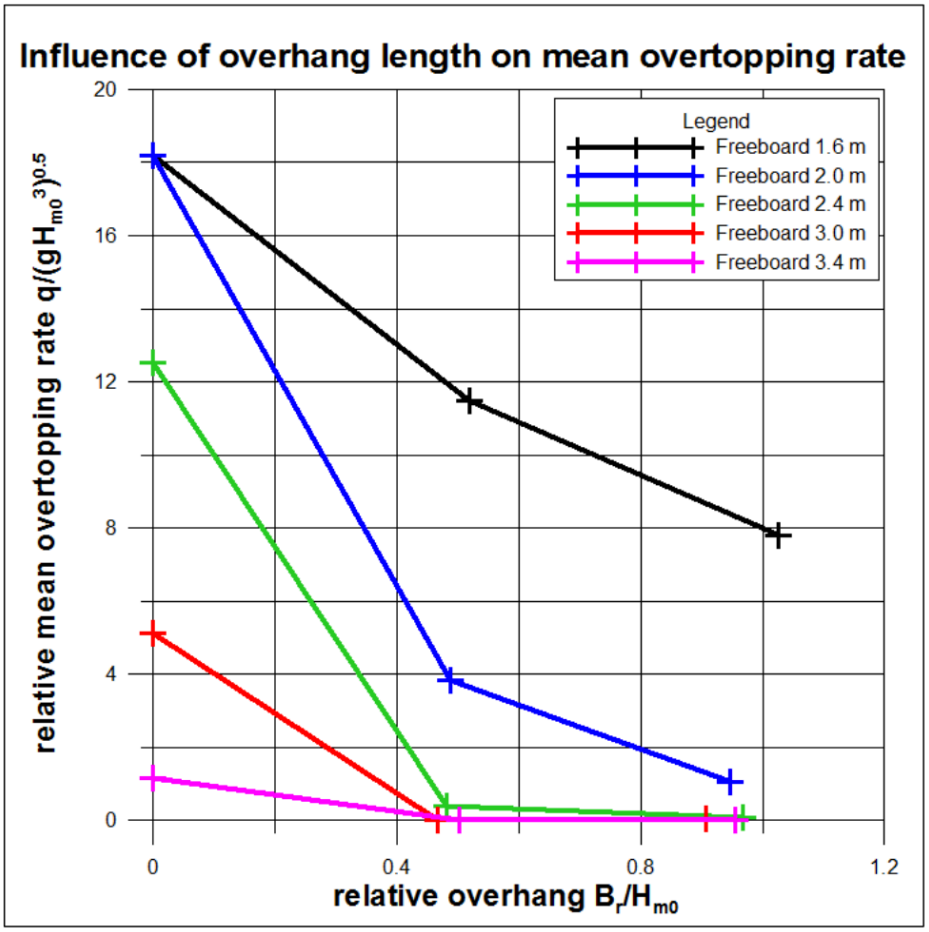

Figure 15: Influence of the recurve overhang length on mean overtopping rate (Schoonees, 2014) & (Schoonees & Toms, 2016)

The study carried out by Swart (2016) also focused on determining the effects of recurve seawalls in reducing wave overtopping. The specific objectives of the study were to determine the effectiveness of recurve walls in reducing overtopping in terms of various geometrical properties of the recurve, such as the overhang length and freeboard height (Swart, 2016).

Figure 16 provides the complete dataset produced by Swart (2016), showing a comparison of the overall performance of the different recurve overhang lengths on a plot of dimensionless overtopping discharge ($q/(gH_{mo}^3)^{0,5}$) versus relative crest freeboard (R_c/H_{mo}). Note that the overtopping rate, q, is in $m^3/s/m$.

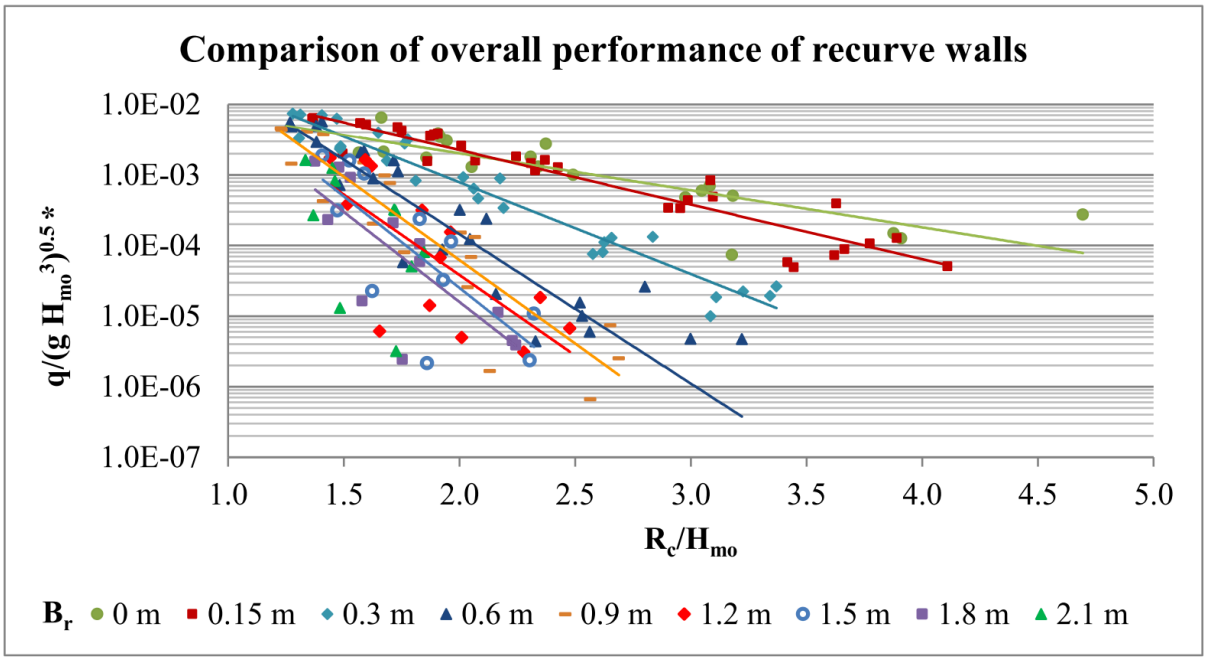

Figure 16: Comparison of overall performance of recurve walls (Swart, 2016)

The results of the study indicated that an increase in overhang length does increase reduction in overtopping and that the freeboard level is a critical parameter in determining overtopping. However, the study also found that after a certain point, an increase in the overhang length would no longer have a significant effect on reducing the overtopping and that the 0.15 m overhang length, under certain conditions, produced less reduction in overtopping than the vertical wall. As the angle of the recurve is a function of the overhang length, the results indirectly indicated that a recurve wall with a recurve angle, α, greater than 50° would not increase a reduction in wave overtopping, compared to a vertical wall under the same conditions.

In addition to the studies conducted by Schoonees (2014), Schoonees & Toms (2016), and Swart (2016), another study including wave overtopping was conducted by Muller (2016). Although an analysis of wave overtopping also formed part of the study conducted by Muller (2016), the primary objective of the study was to determine the adequate size of the toe rock required to ensure stability of the armour layer of the rubble foundation at the base of a vertical seawall for a variety of transitional water depths.

The overtopping results obtained by Muller (2016) were not comparable with the results of this study, and are therefore not included in this literature review, due to a number of reasons:

- The incident wave energy was affected by the rock toe, influencing wave overtopping volumes
- The test conditions of Muller (2016) such as wave height, water depth and freeboard levels differed from those used in this study
- The design of the recurve seawall used in Muller (2016) did not correspond with any recurves used in this study

A profile of the recurve seawall and model setup used in the study by Muller (2016) are illustrated in Figure 17.

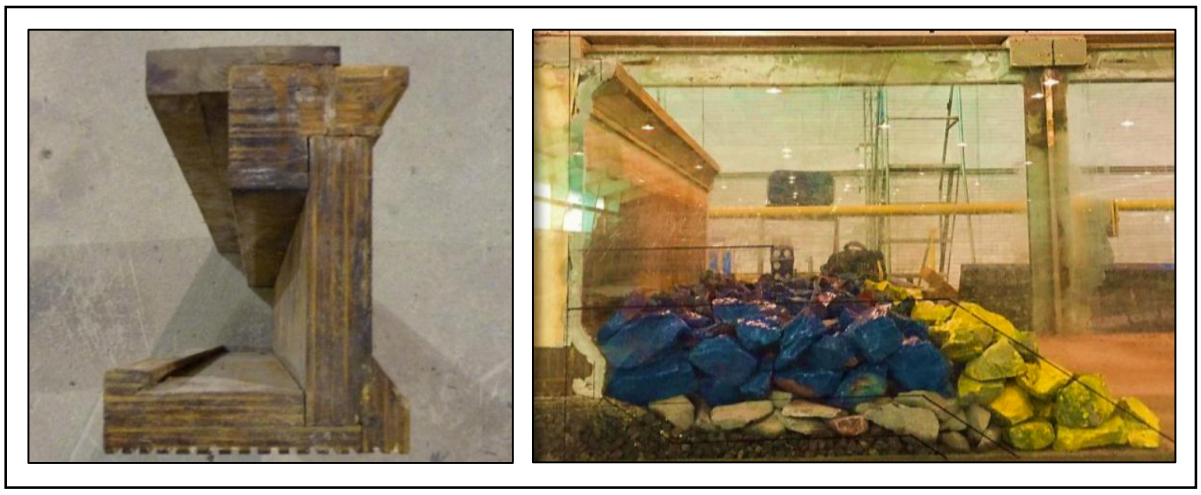

Figure 17: Profile of recurve seawall and model test setup (Muller, 2016)

However, it must be mentioned that the overtopping results obtained by Muller (2016) showed significant scatter when compared with the predicted values obtained from the EurOtop online calculation tool, under identical conditions, indicating that there are still uncertainties in the EurOtop formula used for the prediction of wave overtopping of vertical seawalls with recurves.

2.5 Physical modelling

2.5.1 Laboratory and Scale effects

There are generally three approaches used by coastal engineers to deal with the complexities of fluid flow regimes: field measurements and observations, laboratory measurements/physical modelling and observations, and mathematical/numerical modelling calculations. Although field measurements and observational studies are considered to provide the best data, they are often very expensive and difficult to interpret due to the presence of uncontrollable natural variables. Physical models offer a very convenient alternative to large scale field measurements, also referred to as prototype models, as they are smaller, easier to interpret, less expensive, and still incorporate the most important factors needed for a successful prediction (Hughes, 1993). However, certain factors prohibit a physical model from exactly replicating a field study.

These limiting factors include scale and laboratory effects. Scale effects relate to problems that arise from the inability of physical models to simulate all important variables in correct relationship to the larger prototype variables. Laboratory effects include problems associated with the physical modelling environment, such as the effect of boundaries in a physical model or the inability to simulate the effect of wind (Hughes, 1993).

There are two terms used often in describing scaling relationships, namely similitude and similarity. Similitude criteria, also known as scale laws, are mathematical requirements that need to be satisfied by the scale ratios between prototype and model values, while similarity describes the way in which two models react in the same way regardless of their adherence to similitude criteria (Hughes, 1993).

Scale laws such as the Froude criterion of similitude and Reynolds model law exist to address scaling relationships in hydraulic physical modelling. The Reynolds model law is applied in cases where dynamic similarity of inertia and viscous forces are required. These pertain to studies of fluid flow where viscous forces dominate, surface tension is negligible, and gravity has no influence on the flow (Hudson et al., 1979). As gravitational forces predominate in a wave overtopping study, use of the Froude similitude law will be sufficient.

The scale ratio can be defined as the ratio of a parameter's value in the prototype, X_p, to the same parameter in the model, X_m, and is symbolically presented by Hughes (1993) as,

$$N_X = \frac{X_p}{X_m} = \frac{Value\ of\ X\ in\ Prototype}{Value\ of\ X\ in\ Model}$$

This scale ratio definition is not universally accepted, and in some cases is defined as the reciprocal of the above. However, this definition is preferred as it usually results in scale ratios larger than unity (Hughes, 1993).

Scale ratios according to the Froude and Reynolds laws can be seen in Table 3.

Table 3: Scale ratios of Froude and Reynolds laws (Hughes, 1993)

Characteristic	Dimension	Froude	Reynolds
Geometric			
Length	$[L]$	N_L	N_L
Area	$[L^2]$	$N_L{}^2$	$N_L{}^2$
Volume	$[L^3]$	$N_L{}^3$	N_L^3
Kinematic			
Time	$[T]$	$N_L^{1/2}N_\rho^{1/2}N_\gamma^{-1/2}$	$N_L^2 N_\rho N_\mu^{-1}$
Velocity	$[LT^{-1}]$	$N_L^{1/2}N_\rho^{-1/2}N_\gamma^{1/2}$	$N_L^{-1}N_\rho^{-1}N_\mu$
Acceleration	$[LT^{-2}]$	$N_\gamma N_\rho^{-1}$	$N_L^{-3}N_\rho^{-2}N_\mu^2$
Discharge	$[L^3T^{-1}]$	$N_L^{5/2}N_\rho^{-1/2}N_\gamma^{1/2}$	$N_L N_\rho^{-1} N_\mu$
Kinematic Viscosity	$[L^2T^{-1}]$	$N_L^{3/2}N_\rho^{-1/2}N_\gamma^{1/2}$	$N_\rho^{-1}N_\mu$
Dynamic			
Mass	$[M]$	$N_L^3 N_\rho$	$N_L^3 N_\rho$
Force	$[MLT^{-2}]$	$N_L^3 N_\gamma$	$N_\rho^{-1}N_\mu^2$
Mass Density	$[ML^{-3}]$	N_ρ	N_ρ
Specific Weight	$[ML^{-2}T^{-2}]$	N_γ	$N_L^{-3}N_\rho^{-1}N_\mu^2$
Dynamic Viscosity	$[ML^{-1}T^{-1}]$	$N_L^{3/2}N_\rho^{1/2}N_\gamma^{1/2}$	N_μ
Surface Tension	$[MT^{-2}]$	$N_L^2 N_\gamma$	$N_L^{-1}N_\rho^{-1}N_\mu^2$
Volume Elasticity	$[ML^{-1}T^{-2}]$	$N_L N_\gamma$	$N_L^{-2}N_\rho^{-1}N_\mu^2$
Pressure and Stress	$[ML^{-1}T^{-2}]$	$N_L N_\gamma$	$N_L^{-2}N_\rho^{-1}N_\mu^2$
Momentum, Impulse	$[MLT^{-1}]$	$N_L^{7/2}N_\rho^{1/2}N_\gamma^{1/2}$	$N_L^2 N_\mu$
Energy, Work	$[ML^2T^{-2}]$	$N_L^4 N_\gamma$	$N_L N_\rho^{-1} N_\mu^2$
Power	$[ML^2T^{-3}]$	$N_L^{7/2}N_\rho^{-1/2}N_\gamma^{3/2}$	$N_L^{-1}N_\rho^{-2}N_\mu^3$

According to Hughes (1993), the primary laboratory effects in short-wave modelling are: the physical restrictions that boundaries have on fluid flow, the unintentional nonlinear effects

caused by the application of mechanical wave generators, and the simplification of prototype force conditions, such as representing prototype wave directions as unidirectional.

Wave generation in a two-dimensional wave tank can lead to the development of cross waves or unwanted nonlinear effects, such as higher harmonics in finite-amplitude regular waves, and unintended long-waves that occur due to the use of a wave paddle motion based on linear theory transformation for creating irregular waves (Hughes, 1993).

Another laboratory effect sometimes overlooked by experimenters is the re-reflection of waves by the wave paddle (Hughes, 1993). Under normal circumstances, waves propagating towards a beach or structure would reflect off the structure and travel seawards indefinitely. However, with the presence of a wave paddle in a wave tank, the reflected "seaward" waves get re-reflected off the paddle and travel back towards the structure. The best way in dealing with this effect is by utilizing a wave paddle with active wave absorption which detects and absorbs any reflected waves (Hughes, 1993).

Pearson et al. (2002) conducted a study on violent wave overtopping of large- and small-scale models. Overtopping measurements were taken from large- and small-scale physical models of battered seawall structures under various wave conditions. It was found that the influence of scale effects on peak and mean overtopping volumes were insignificant under impulsive wave conditions, i.e. violent overtopping. In addition, the results also indicated that scale effects are expected to be negligible for pulsating wave conditions (Pearson et al., 2002).

Pearson et al. (2002) also found that the most obvious laboratory effects in physical models were the absence of wind and the use of fresh water instead of sea water. It is suggested that the presence of wind would have very little influence on large overtopping volumes, but could be significant for small discharges, especially when violent breaking occurs. With regard to the use of fresh water in a physical model instead of seawater, no evidence exists to suggest that this laboratory effect would have an influence on wave overtopping (Pearson et al., 2002).

It is also important to note that fixed-bed models, such as the two-dimensional wave tank being used in this study, provide in general very satisfactory results owing to the fact that scaling effects in fixed-bed models are relatively well understood (Hughes, 1993).

2.5.2 Wave generation and overtopping measurement methods

When dealing with wave overtopping studies, various methods exist to empirically determine the volume of overtopping water in a physical model study. One of these methods is described in a study conducted by Owen and Steele (1991).

Extensive research findings exist on the overtopping discharges of embankment-type seawalls as a result of a research programme conducted by the Hydraulics Research Station in the 1970s. However, almost no information is available on the effectiveness of wave return walls in reducing wave overtopping discharges (Owen and Steele, 1991). Owing to this fact, Owen and Steele (1991) contributed to the findings of the Hydraulics Research programme by conducting a series of physical model tests to measure the overtopping discharges of a range of recurved wave return walls for different overtopping conditions.

In the physical model studies conducted by Owen and Steele (1991), overtopping measurements were obtained by collecting all the overtopped water in calibrated tanks behind the seawall. In order to improve accuracy of results, the discharge mean and standard deviation were calculated for each test by using the results of five overtopping intervals for the same test condition.
Each overtopping interval's duration was taken as $100T_m$ seconds, where T_m is the nominal mean wave period of the JONSWAP spectrum.

The overtopping volume was calculated by using a float which monitored the difference in water level in the tank. After each overtopping interval, the measurement of the higher water level was taken after allowing the water in the tank to settle. Thereafter, water from the collecting tank would then be pumped back into the flume to re-establish the desired water level condition (Owen and Steel, 1991).

In the study conducted by Pearson et al. (2002) overtopping measurements were taken by directing discharges via a chute into a container suspended from a load cell. In addition to measuring total discharge volumes, individual overtopping events could be identified by two parallel metal strips along the width of the structure crest which acted as a switch closed by the overflowing water. These individual wave-by-wave overtopping volumes could be measured by calculating the incremental water mass in the container after each overtopping event (Pearson et al., 2002).

The measurement system was calibrated by simulating overtopping events where known volumes of water would be thrown into the collecting container, followed by passing the results from the load cell through an algorithm to identify individual overtopping events. This measurement method was found to be very accurate, as differences between derived and actual total volumes were found to be less than 0.7% (Pearson et al., 2002).

Waves were generated by using a flap-type wave maker with active wave absorption, which reduced the effect of reflected waves from the structure on incident wave height measurements. Pearson et al. (2002) also reduced uncertainties and calibrated incident and inshore wave conditions by repeating the test sequence with wave gauges at the location where the structure would have been.

2.5.3 Test duration

When dealing with wave overtopping in empirical model studies, the test duration and number of waves are crucial parameters that need to be taken into account. The number and duration of incident random waves are usually determined by the specific requirements of a particular study. Therefore, in order to optimize the test duration, it is very important to obtain a correct balance between the total number of tests and the required accuracy of the measurements (Reis et al., 2008).

Reis et al. (2008) investigated lengths of scale model tests with the aim of identifying a minimum test duration and number of runs required to accurately measure mean overtopping discharges.

The study included 87 physical model tests with varying test durations. The results indicated that measured mean discharge values did generally decrease with increasing number of waves, but only up to about 1100 to 1400 waves, whereafter only very small reductions were identified. However, no convergence of the mean overtopping discharge to a constant value for increasing test durations was found (Reis et al., 2008).

The information obtained from a single test with a very long duration still gives limited guidance on the mean discharge, as overtopping measurements vary even for identical test conditions. Therefore, it is suggested by Reis et al. (2008) to rather conduct several tests of a similar shorter duration than one test with a long duration. This method is also recommended

when an active wave absorption system is either not available or inefficient in its purpose, as shorter durations would minimize the chances for unwanted energy build up from re-reflecting waves off the wave paddle (Reis et al., 2008).

2.5.4 Wave spectra

The elevation of the sea surface for a given sea state can be described with the use of empirical expressions which closely fit the spectrum of the sea surface. These expressions are called parametric spectrum models (USACE, 2006). One of the first spectrum models was that of the single-parameter Pierson-Moskowitz PM spectrum. The JONSWAP (Joint North Sea Wave Project) spectrum is an extension of the PM spectrum, usually including three constant - and two varying parameters, making it a widely applied spectrum model (USACE, 2006).

The type of waves generated in most of the studies on wave overtopping followed that of the JONSWAP spectrum. In addition, the spectrum of waves along the Southern African coastline indicate a close fit to the JONSWAP spectrum (Rossouw, 1989). The JONSWAP spectrum is applicable to sea states which are fetch-limited or in other words, a sea state with a given windspeed that cannot become fully developed due to a fetch distance limitation.

The empirical expression of the JONSWAP spectrum and the relationship between the PM and JONSWAP spectra can be seen in Figures 18 and 19, respectively.

$$E(f) = \frac{\alpha g^2}{(2\pi)^4 f^5} \exp\left[-1.25\left(\frac{f}{f_p}\right)^{-4}\right] \gamma^{\exp\left[-\frac{\left(\frac{f}{f_p}-1\right)^2}{2\sigma^2}\right]}$$

$$f_p = 3.5\left[\frac{g^2 F}{U_{10}^3}\right]^{-0.33} \quad ; \quad \alpha = 0.076\left[\frac{gF}{U_{10}^2}\right]^{-0.22} \quad ; \quad 1 \le \gamma \le 7$$

$$\sigma = 0.07 \quad for\ f \le f_p \quad and \quad \sigma = 0.09 \quad for \quad f > f_p$$

Figure 18: JONSWAP spectrum expression

(USACE, 2006)

where

α = equilibrium coefficient

γ = peak enhancement factor

σ = dimensionless spectral width parameter

F = fetch length

f_p = frequency at the spectral peak

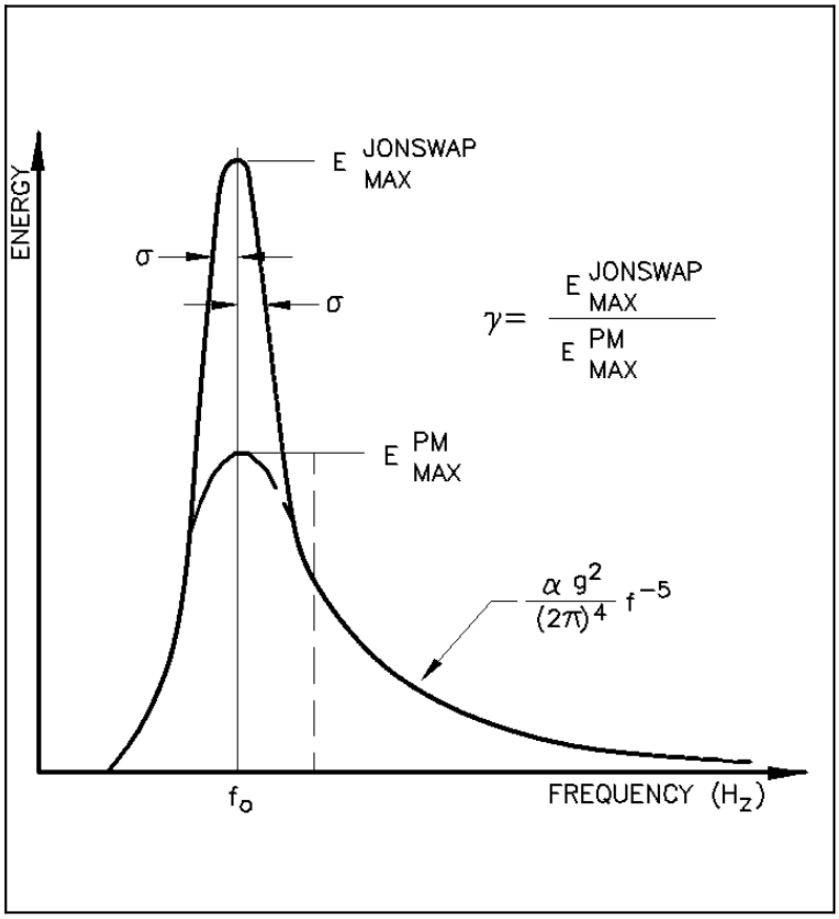

Figure 19: Comparison of PM and JONSWAP spectra

(USACE, 2006)

The type of wave generated in this study was chosen to follow a JONSWAP spectrum, which is further discussed in Section 3.7.

2.6 Conclusions

Although Kortenhaus et al. (2003) found that a sufficient amount of data on mean overtopping discharges of vertical seawalls exists, research on wave overtopping of vertical walls with recurves or parapets were based on less comprehensive studies. Therefore, Kortenhaus et al. (2003) produced a reduction factor (k-factor) approach by conducting overtopping tests of

vertical walls with recurves and then repeating the same test with no recurve present. It was found that the most influential parameters on the k-factor were the freeboard, parapet width and recurve angle. However, as large reductions in overtopping led to very small k-factors, implementation of the calculated k-factors in wave overtopping predictions led to significant scatter in the data points.

Pearson et al. (2004) improved upon the approach developed by Kortenhaus et al. (2003) by introducing the use of an adjusted k'-factor and comprehensive decision chart as design guidance to determine the appropriate k-value to be used in the prediction of wave overtopping of a parapet or recurve seawall. Although the adjusted k'-factor introduced more accurate predictions of large reductions in overtopping, significant scatter was still present, leading to the conclusion that detailed physical model studies should be considered when designing for reduction k-factors smaller than 0.05.

The European CLASH project (Crest Level Assessment of coastal Structures and Hazard analysis on permissible wave overtopping) produced a database consisting of over 10 000 overtopping tests. This comprehensive database was used to develop a neural network tool, which included the input of 15 variables, providing a reliable first prediction of overtopping discharge for a given structure.

Schoonees (2014) conducted a study on the effects of impermeable recurve seawalls in reducing wave overtopping, with an emphasis on investigating the difference in effectiveness of a plain vertical wall versus recurve walls in reducing wave overtopping as well as the influence of two different overhang lengths of the recurve on overtopping. It was found that the recurve walls were overall more effective in reducing overtopping than the vertical seawall and that the recurve with the longer overhang length proved to be the most efficient (Schoonees, 2014). However, for cases with relatively high freeboards or low water levels, no significant difference between the performances of the two recurves in reducing overtopping was observed.

Swart (2016) also researched the effects of recurve seawalls in reducing wave overtopping, specifically with the objectives of determining the effectiveness of recurve walls in reducing overtopping in terms of the recurve's various geometrical properties, such as the overhang length and freeboard height. Swart (2016) found that an increase in overhang length does increase the reduction in overtopping and that the amount of freeboard is a critical parameter in

determining overtopping. However, it was also found that after a certain point, increasing the overhang length would no longer have a significant effect on reducing overtopping and that under certain conditions, the 0.15 m overhang length would produce more overtopping than the vertical wall. In addition, Swart (2016) observed that a recurve seawall with a recurve angle greater than 50° would provide a lower reduction in overtopping than a vertical wall under the same conditions.

Chapter 3: Physical model tests

3.1 Overview

3.1.1 Objective

In order to empirically analyse the effects that different overhang forms of a recurve seawall have on reducing wave overtopping, experiments were carried out in a physical model.

The physical model tests for this study were conducted in the same Hydraulic Laboratory as used in the study conducted by Schoonees (2014), Schoonees & Toms (2016), and Swart (2016). Therefore, the methodology applied in this study was, in many instances, based upon the methods used by Schoonees (2014), Schoonees & Toms (2016), and Swart (2016) in order to achieve comparable results and for the purpose of validation.

3.1.2 Testing facility and overhang forms

The physical model was constructed in a 2D glass wave flume equipped with a piston-type wave paddle in the Hydraulic Laboratory of the Civil Engineering Department at the University of Stellenbosch, illustrated in Figures 20 and 21. The wave flume is 30 m long, 1 m wide and a maximum operational depth of 0.8 m can be achieved. The piston-type wave paddle can be used to generate both regular and irregular waves and is equipped with active wave absorption, which reduces the unwanted effects of reflected waves off the seawall (HR Wallingford, n.d.).

Figure 20: 2D wave flume (Swart, 2016)

Figure 21: Wave paddle in 2D wave flume
(Swart, 2016)

The heights of the generated waves were measured by using resistance probes which record voltage signals and then store the data in a connected computer. The voltage signals are analysed by a data acquisition and analysis software package, HR DAQ, developed by HR Wallingford and then converted to water-level readings in metres. Calibration of the resistance probes before every subsequent test was carried out, as the probes are particularly sensitive to differences in water temperature which occurred in the form of stratified water layers whenever the water body in the flume was left stagnant for too long.

The recurve forms were designed according to the Froude scale law. The overhang forms were constructed as individual pieces separated from the seawall, making installation and replacement of the forms uncomplicated and saving time between experiments.

Schematizations (in mm) of the five recurve forms can be seen in Figure 22. The three base points marked a, b, and c on Recurve A in Figure 22 will have the same coordinates on each recurve shape, with only the shape between those points changing for the different forms. This is done in order to maintain a constant model overhang length, B_r = 60 mm, and height of recurve, h_r = 50 mm, for all the recurves. The height and thickness of the vertical seawall used in this model study are 200 mm and 18 mm, respectively. With the applied scale of 1:20, the thickness of the model overhang edge was chosen as 20 mm, corresponding to a 0.4 m prototype thickness, which would provide adequate concrete cover for reinforcement.

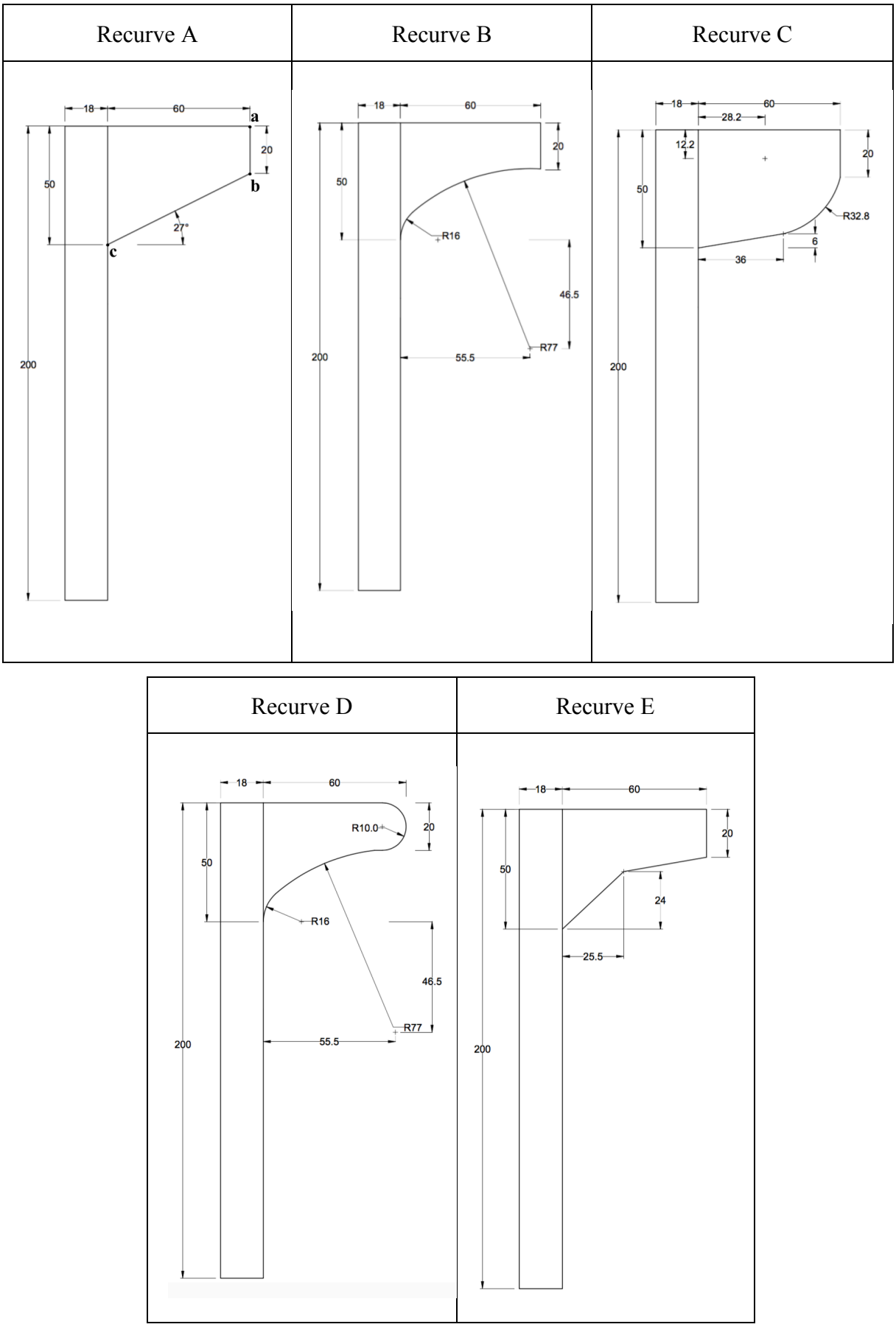

Figure 22: Model recurve shapes (in mm)

3.2 Model set-up

The approach slope in the wave flume, the seawall height, the overhang length, as well as the height of the recurve were kept constant throughout all the physical model tests. Swart (2016) optimised the overhang length and thus the dimensions of these parameters were based on the conclusions found in empirical studies conducted by Schoonees (2014) and Swart (2016).

The wave flume had a nearshore slope of 1:50 and an additional built-in upper beach slope directly in front of the seawall of 1:18.6 resembling a typical South African beach. The slope of 1:18.6, which was obtained by taking the average of numerous beach slopes along the South African coast, was determined by Schoonees (2014). The two slopes are illustrated in Figure 23.

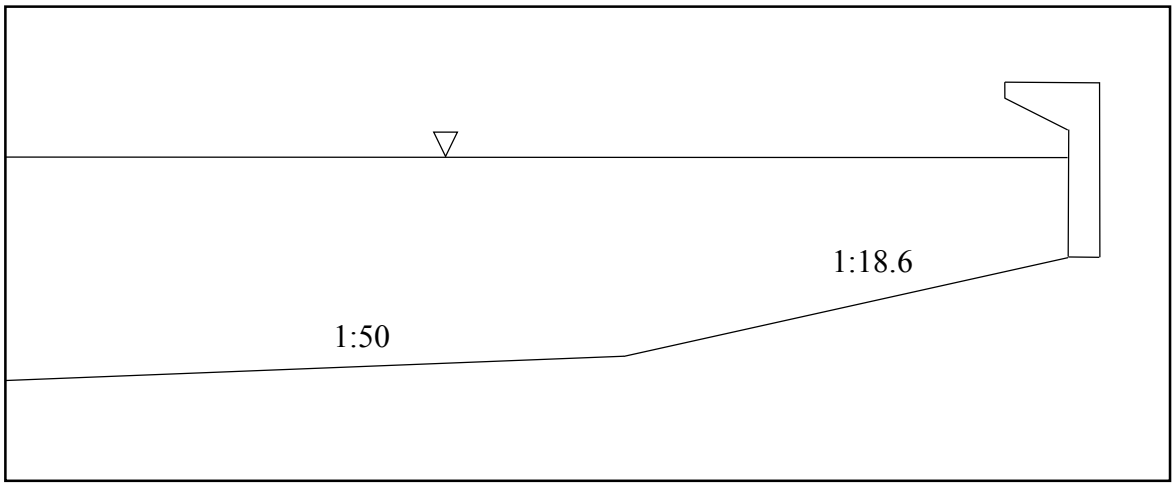

Figure 23: Schematic of slopes in wave flume

The recurved seawall extends across the entire 1 m width of the flume and is located 28 m from the wave paddle, as can be seen by referring to the detailed long-section, including dimensions, of the wave flume provided in Appendix A.

As mentioned previously, the recurve forms were constructed as separate pieces apart from the vertical seawall, which served as the base structure. The forms were bolted to the vertical seawall, which consisted of an 18 mm thick PVC panel, in order to simplify the process of exchanging recurve forms. The material used to construct the forms was Meranti hardwood which was painted with a water-proof paint in order to protect the wood from swelling. In order to prevent any water leaking around the structure, a silicon-based material was applied as a sealant between the structure and flume wall contact points.

The overtopped water was collected in a pre-calibrated container or overtopping bin situated behind the seawall in the wave flume, Figure 24. The pump used in the experiment to extract the water out of the bin was unable to completely empty the overtopping bin, so a starting or "zero" water level along with the calibrated water levels were marked on the bin.

Figure 24: Overtopping bin and pre-calibrated water levels

After completion of a test, the overtopped water volume was determined by measuring the water level in the pre-calibrated overtopping bin, accurate to 0.25 litres, followed by emptying the bin to the starting water level for the next test. Otherwise, if the test sequence allowed for overtopping exceeding the capacity of the overtopping bin of 100 litres, the water was pumped out of the overtopping bin during the test into drums on the outside of the flume where they were weighed on a scale, accurate to 20 grams, to determine the volume of overtopping. Figure 25 shows the pump used to extract the overtopped water and weighing station for the drums.

The overtopped water was directed into the overtopping bin by a plastic sail which sloped downwards into the bin from the flume walls and backside of the recurve seawall. In addition to the plastic sail sloping towards the bin, a wooden framed structure spanning up to 4 m from the recurve wall towards the wave maker was built atop the flume walls covered with plastic sheets to mitigate any loss of water over the flume walls due to violent overtopping. The plastic sail sloping into the overtopping bin and wooden frame with plastic sheets atop the flume walls are shown in Figure 26.

Figure 25: Pump in overtopping bin and weighing station

Figure 26: Plastic sail and sheets to guide overtopped water

The water level in the flume was maintained during a test by monitoring the overtopped water in the pre-calibrated overtopping bin, followed by adding the same volume of water into the flume behind the wave paddle in order to mitigate any effects on wave generation.
It is important to note that the physical model tests were conducted with fresh water, so a density of 1000 kg/m^3 was assumed.

The resistance probes used to measure incident wave heights were spaced accordingly along the length of the flume. The incident wave heights directly in front of the structure are the most

important to consider. Therefore, the resistance probes were located as close as possible to the structure, but also far enough so that breaking waves did not influence the probe readings.

The use of four resistance probes was required in order for the HR DAQ software tool to perform a reflection analysis, which is further discussed in Section 3.6. The first three wave probes were spaced according to a method established by Mansard and Funke (1980). The positioning of the fourth wave probe (closest to the seawall) was initially determined as one average wavelength away from the structure. However, this positioned the fourth probe on the 1:18.6 slope leading up to the structure. In order to minimize the effects of reflected and amplified waves on the probes and to ensure that waves did not break in the vicinity of the probes, the fourth probe was positioned at the 1:50 and 1:18.6 slope intersection, slightly further than the one average wavelength. The probes used in the physical model and a schematic showing the spacing of the probes can be seen in Figures 27 and 28, respectively.

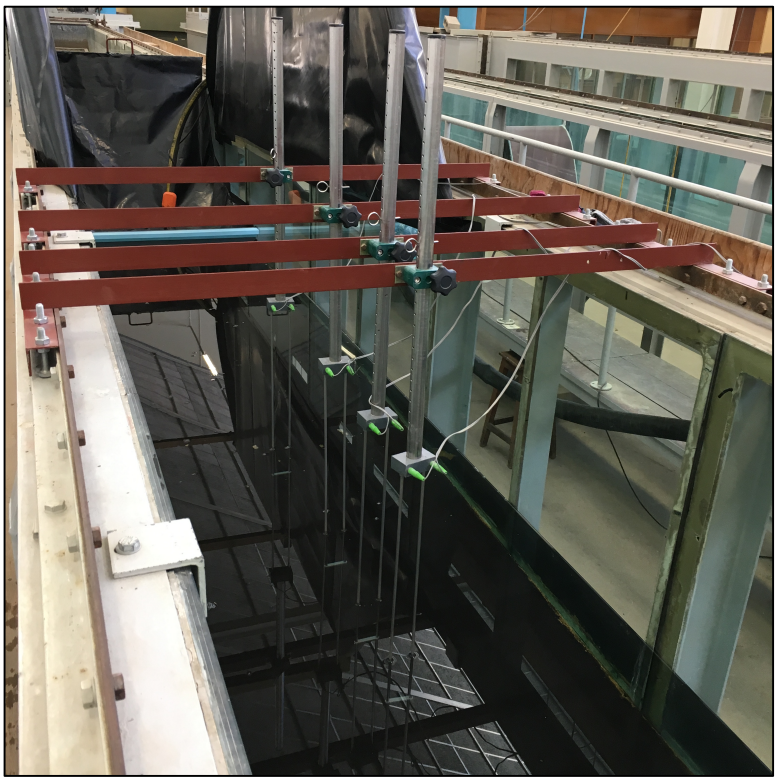

Figure 27: Resistance probes in physical model

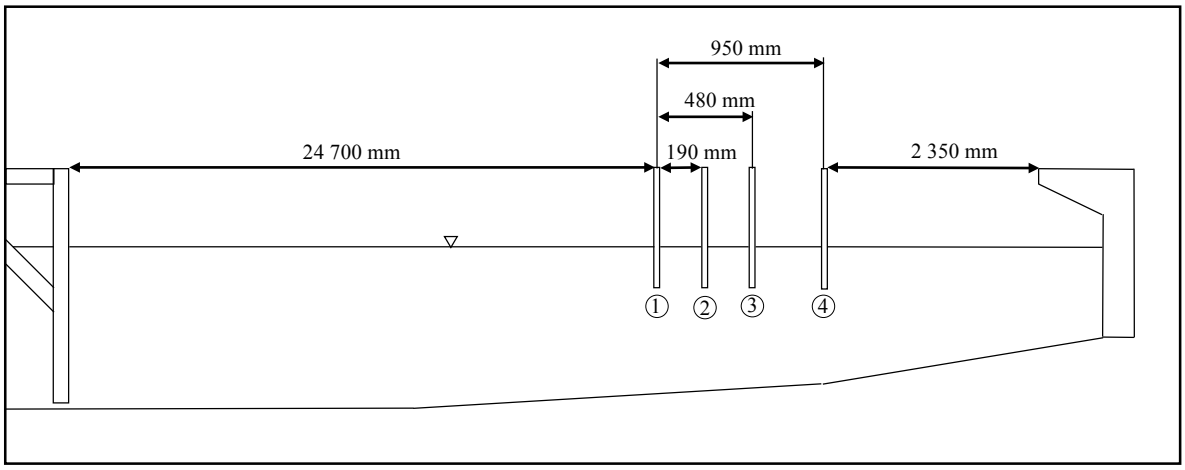

Figure 28: Probe spacing schematic

3.3 Parameter scaling

In designing a physical model, it is always important to scale as large as possible in order to mitigate scale effects. Therefore, it was chosen to use a 1:20 scale and apply the Froude similitude scale law as described in Section 2.5.1. This scale was also chosen based on the existing vertical seawall height in the flume and the wave generating capacity of the wave paddle (Schoonees, 2014 & Swart, 2016). A summary of the scales used in this study can be seen in Table 4.

Table 4: Summary of scales used

Scale Type	Parameter	Froude Scale
Linear scale	Water depth, wavelength, wave height, wall dimensions	1:20
Time scale	Wave period, test duration	1: $\sqrt{20}$ = 1:4.472…
Mass scale	Mass of overtopped water	$1:20^3$ = 1:8000

3.4 Controlled hydraulic parameters

In order to test various conditions, parameters such as water level, wave height and wave period were controlled. Five different water levels were tested for each recurve shape. These levels were chosen so as to compare the results obtained with those of previous studies conducted by Schoonees (2014) and Swart (2016). In addition, the chosen levels included two cases of breaking waves (waves break when $H_{mo}/h_s > 0.78$), 1.0 m and 0.6 m, and three cases of non-

breaking waves, 2.4 m, 2.0 m, and 1.6 m. The design wave height chosen represented a prototype wave height of 1.0 m and remained constant throughout all the tests.

During a study conducted by Roux (2013) it was found that increasing the wave period caused an increase in wave overtopping, but only up to 12 seconds, after which point overtopping started to decrease. According to Roux (2013) this was due to increasing wave height as a result of shoaling, as longer wave periods cause longer wavelengths which in turn cause waves to start shoaling in deeper water and break, dissipating wave energy and decreasing overtopping. Due to the results found by Roux (2013), five different wave periods were selected, ranging from 6 seconds to 14 seconds, with 2 second increments. Wave periods of 6, 10, and 14 seconds were tested first in order to get an initial indication of the sensitivity of overtopping to wave period. Thereafter, the 8 second and 12 second period tests were conducted and with the initial overtopping volumes already obtained for the other three wave periods, an estimation of the overtopping for the 8 second and 12 second cases could be made, which also served as an indication of the validity of the results obtained.

3.5 Test execution

The process followed when executing a test is described as follows:

1. Set up the overtopping bin and flume water levels to starting water level and required water depth, respectively;
2. Mix the water in the flume by generating a sequence of waves for 100 seconds in order to eliminate temperature differences due to stratified water layers;
3. Wait for the water surface in the flume to even out;
4. After a still water level has been achieved, calibrate the wave probes;
5. Ensure that the water depth in the flume and water level in the overtopping bin are at the required levels;
6. The wave condition for a specific wave period and water depth are initiated and the corresponding absorption value is set;
7. The wave data is recorded by the data acquisition software for a duration of $1000T_p$;
8. During the test:
   8.1. Monitor the water level in the overtopping bin; if 20 *l* overtops the structure, add 20 *l* back into the flume behind the wave paddle in 5 *l* increments.

8.2. If the overtopping bin is close to reaching its capacity, water is pumped out of the bin into a drum at the weighing station until the starting water level in the overtopping bin is reached.

9. After test completion, measure the water volume in the overtopping bin and weigh the drum on the scale at the weighing station; record both values;
10. Check that water level in flume is within 2 mm of required water depth; if not, disregard test results and repeat.

3.6 Relevant wave height measurements

Wave height readings taken by the wave probes during a test sequence were recorded and then analysed with the HR DAQ software package. However, both the incident (H_i) and reflected (H_r) wave heights were included in the probe readings. For the purpose of this study, only the incident wave height was of significance.

The least squares method, found by Mansard and Funke (1980), is applied to separate the incident and reflected wave heights and, when further developed, becomes a function of the bulk reflection coefficient (K_r) and the significant wave height (H_{mo}).

A Reflection Analysis tool within HR DAQ, which requires a constant water depth and probe spacing as input parameters, was used to calculate the range of allowable reflection frequency and the bulk reflection coefficient K_r for each test sequence. Figures 29 and 30 provide examples of the Reflection Analysis interface.
Post processing of the recorded data in HR DAQ also provided the significant wave height H_{mo} by spectral analysis and important wave statistics, such as the number of waves, by applying the zero upward-crossing method. The H_{mo} used in the calculation of the incident wave height was taken as the average of the four significant wave heights recorded by the four wave probes.

The following process shows how the least squares method (Mansard and Funke, 1980) was developed to obtain an equation for calculating the incident wave height H_i:

$$H_{mo}{}^2 = H_i{}^2 + H_r{}^2$$

$$H_{mo} = \sqrt{(H_i{}^2 + H_r{}^2)}$$

with $H_r = K_r H_i$:

$$H_{mo} = \sqrt{(H_i{}^2 + K_r{}^2 H_i{}^2)}$$

$$H_{mo} = H_i \sqrt{(1 + K_r{}^2)}$$

$$H_i = \frac{H_{mo}}{\sqrt{(1 + K_r{}^2)}}$$

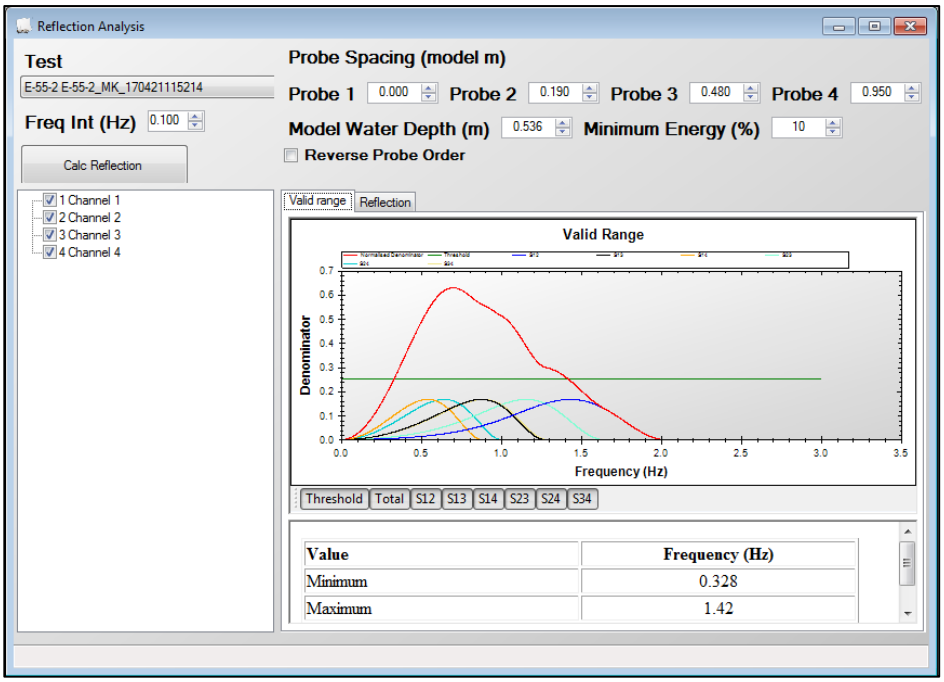

Figure 29: Reflection Analysis providing valid frequency range

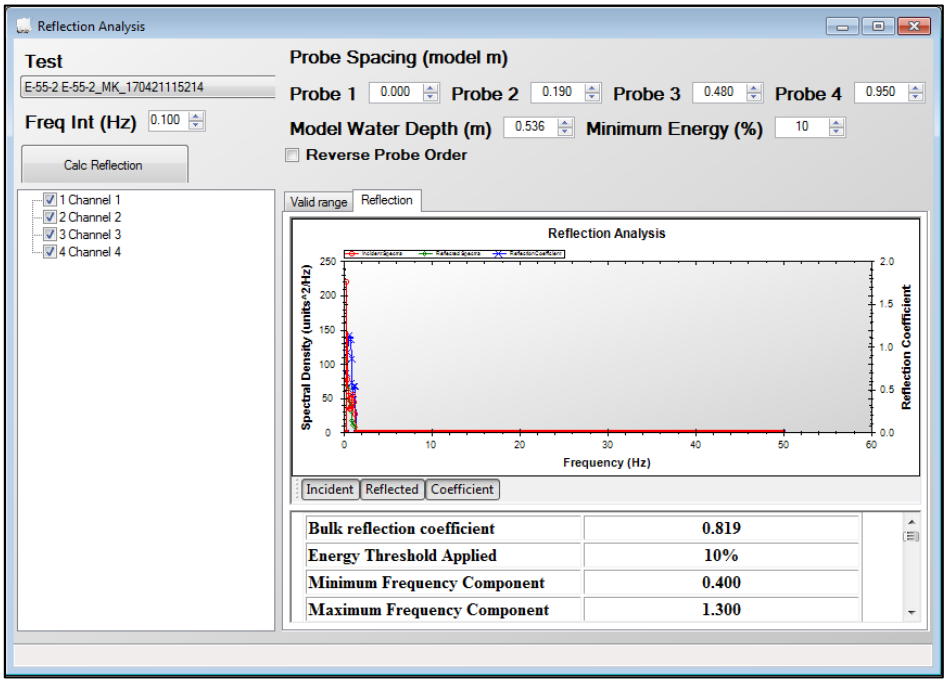

Figure 30: Reflection Analysis providing bulk reflection coefficient

3.7 Test conditions and summary

The test conditions selected were based on a combination of typical wave – and nearshore conditions along the South African coastline and studies conducted by previous researchers in order to compare results.

In order to create a specific wave condition, a wave generation software package developed by HR Wallingford, HR Wavemaker, was used to create a wave generation signal file for each individual test condition, i.e. for each water level and wave period. These signal files consist of wave train signals which specify the conditions of waves to be generated by the wave paddle.

Due to the findings of Reis et al. (2008), and to attain statistically accurate but not overwhelming amounts of data, it was decided that each test would have a duration of 1000 waves, defined by $1000T_p$, where T_p is the peak wave period.

The type of wave generated in this study was chosen to be irregular and following a JONSWAP spectrum, as it is the most commonly used spectrum in overtopping studies and also very similar to the spectrum found along the South African coastline (Rossouw, 1989). According to Rossouw (1989), the value of the peak enhancement factor along the South African coastline varies from 1 to 6 with an average value of $\gamma = 2.2$ and standard deviation of 1.0. However, an average enhancement factor of $\gamma = 3.3$ is used in most overtopping studies. Therefore, in order to compare results of this study with those of previous studies and as it lies well within the range of peak enhancement factors along the South African coastline, the peak enhancement factor for this study was chosen as $\gamma = 3.3$.

A summary of all the conditions tested as described in Section 3.4, for each recurve form, is given in Table 5.

Table 5: Summary of test conditions (prototype values)

Recurve form	Water level at toe (m)	Freeboard R_c (m)	Wave Height H_s (m)	Wave period T_p (s)
Recurve A	2.4, 2, 1.6, 1, 0.6	1.6, 2, 2.4, 3, 3.4	1.0	14, 12, 10, 8, 6
Recurve B	2.4, 2, 1.6, 1, 0.6	1.6, 2, 2.4, 3, 3.4	1.0	14, 12, 10, 8, 6
Recurve C	2.4, 2, 1.6, 1, 0.6	1.6, 2, 2.4, 3, 3.4	1.0	14, 12, 10, 8, 6
Recurve D	2.4, 2, 1.6, 1, 0.6	1.6, 2, 2.4, 3, 3.4	1.0	14, 12, 10, 8, 6
Recurve E	2.4, 2, 1.6, 1, 0.6	1.6, 2, 2.4, 3, 3.4	1.0	14, 12, 10, 8, 6

3.8 Test validation and accuracy

In order to increase the accuracy of test results and to rectify unwanted occurrences during test executions due to uncontrollable circumstances, certain tests were repeated.

As an additional measure of calibration, it was decided that one of the recurve forms tested in this study would replicate a recurve tested by both Schoonees (2014) and Swart (2016), providing the possibility to compare results from exactly the same test conditions. It was found that overtopping measurements tend to change invariably, even for the exact same test conditions. These differences in results are attributed to various influential factors such as: complexity of the measuring technique used, especially for small overtopping rates, limitations due to equipment available, underestimation of the input wave height relative to generated and required wave heights. Therefore, it was necessary to repeat certain tests. However, as it is not feasible to repeat each and every condition, careful analysis throughout the first initial round of tests was done to identify important conditions which needed to be repeated. An analysis of repeated tests as well as test accuracy achieved is provided and discussed in Section 5.4.

Chapter 4: Results

4.1 General

A total number of 147 physical model tests were executed throughout this study. A minimum amount of 125 tests were required due to the prerequisite conditions of testing five different recurve forms for five varying water depths and five different wave periods. However, due to necessary modifications made to the input wave height signal file early in the study as well as repetitions in order to improve the accuracy of test results, an additional 22 tests were conducted.

This chapter provides individual performance overviews of each of the recurve forms tested, a complete set of the overall test results, and results obtained from the EurOtop online calculation tool. Dimensions are given in prototype values except where stated otherwise.

4.2 Physical model test results

4.2.1 Performance overview

The general performance of each recurve form, including a comparison of the effectivity in reducing wave overtopping with other forms, is provided below, ordered from Recurve A to E. Detailed analysis and interpretation of the results are presented in Chapter 5.

Recurve A

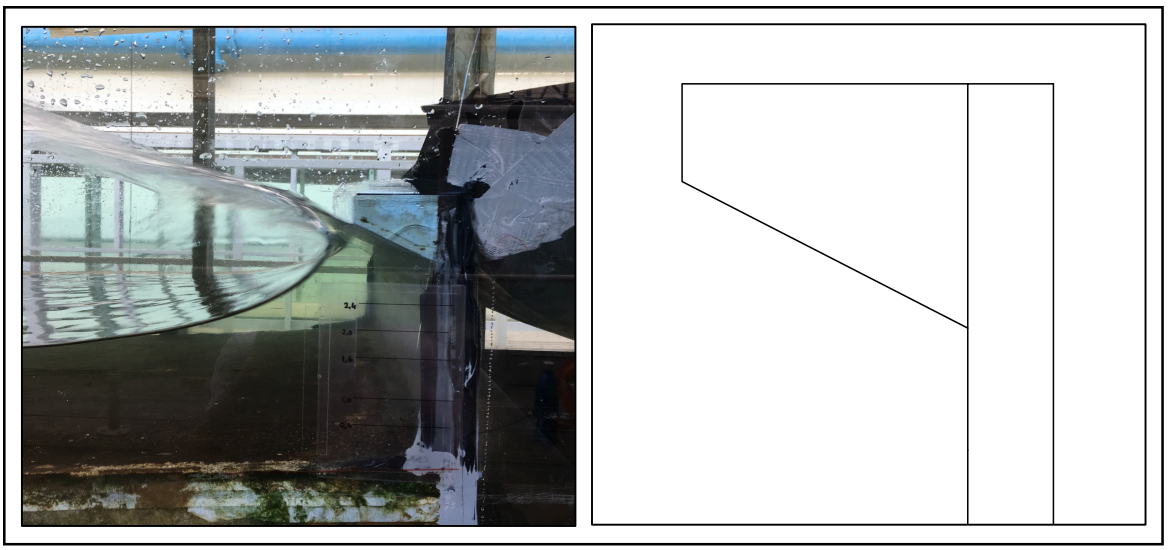

Figure 31: Recurve A

The shape of the overhang in Recurve A was chosen as the first form to be tested, as the initial results could be compared with the results obtained from an identical recurve shape tested in previous studies, therefore validating the experimental procedure followed.
The performance of Recurve A was also used as the initial basis against which to compare the performance of other recurves. The sequence of test conditions per recurve ranged from the lowest to highest water levels, with increasing the wave period per water level from 6 seconds to 14 seconds.

The performance of Recurve A allowed little or zero overtopping of the recurve wall for the two lowest water levels tested. The overtopping which did occur, however, only took place with the shorter (6 second and 8 second) wave periods. As the reflected wave travelled back towards the wave paddle, it would collide with the closely following incident wave causing some amount of spray which, if the collision was large and close enough to the wall, would splash over the crest of the wall. Although reflected and incident waves also collided under the longer period wave conditions, it was observed that the collisions occurred too far away from the wall for the spray to reach and overtop the crest of the wall.

The intended functionality of Recurve A performed well in effectively reflecting waves during the test condition with a water depth of 1.6 m. Due to the relatively low water level and high freeboard, the incident wave would first strike the vertical part of the wall, then travel upwards along the shape of the recurve, finally to be projected seawards as a jet of water at an angle similar to the recurve angle. This occurrence can be seen in Figure 31, illustrating a test condition with a 10 second wave period and 1.6 m water depth.

The recurve shape was very inefficient at successfully reflecting incident waves at the highest water level for wave periods of 10 seconds and longer. During a test with a 10 second wave period, the incident wave would strike the vertical part of the wall, recurve face, and square overhang edge just below the crest of the structure simultaneously, projecting the water straight up into the air instead of reflecting it away from the wall, as can be seen by referring to Figure 46. At this point, the effect of the recurve was almost negligible and the momentum of the wave would simply push the vertically projected column of water onto and over the crest.

The most significant overtopping witnessed occurred during the 14 second period wave, when the wave would completely submerge the recurve wall. During this submerged or "drowned" state, the recurve appeared to be completely ineffective in reflecting any wave energy, allowing large amounts of water to breach the crest.

Recurve B

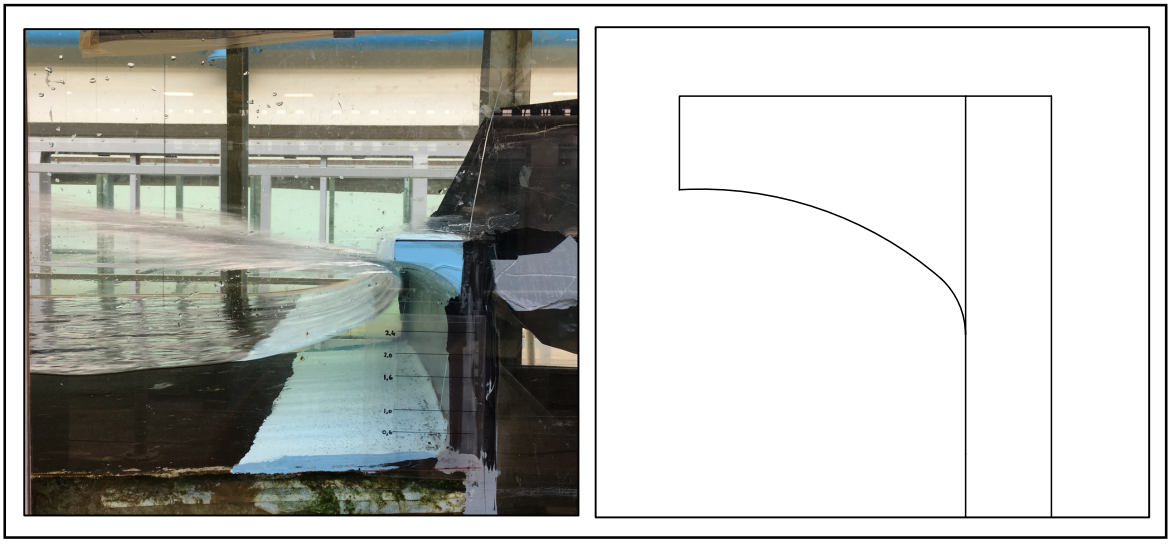

Figure 32: Recurve B

When compared with all the other recurve forms tested, Recurve B provided overall the highest reduction in wave overtopping of the seawall.

Very similar overtopping rates occurred at the two lowest water levels for Recurve B, when compared with Recurve A, as a result of splash overtopping from reflected and incident wave collisions. This observation confirms the finding that the shape of the recurve is irrelevant for shorter period waves at lower water levels.

A clear reduction in overtopping started to occur at the second highest water level. At the highest water level, when compared with Recurve A, Recurve B provided up to 100% reduction in overtopping rates for the shorter period waves (6 seconds and 8 seconds) and up to two times smaller rates for the longer period waves.

It was observed that overall, when compared with Recurve A, the shape of Recurve B was much more effective in successfully reflecting incident waves which led to higher dissipation of wave energy and less overtopping. The successful reflection of an incident wave, projecting the jet

of reflected water seawards at an almost zero degree angle relative to the horizontal plane, can be seen in Figure 32.

Recurve C

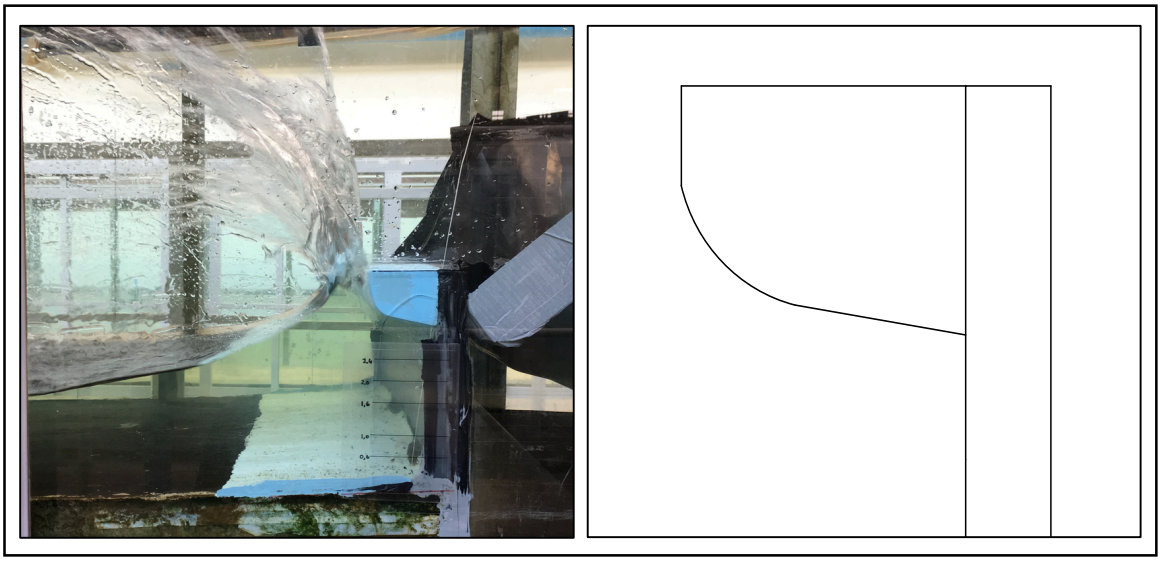

Figure 33: Recurve C

Recurve C provided overall the least reduction in overtopping, when compared with the other recurves. Due to its shape, the recurve acted more as an obstruction to overtopping waves than a reflective structure, as can be seen by its deflection performance in Figure 33.

Recurve C also produced similar overtopping rates at the two lowest water levels, when compared with Recurves A and B, due to splash overtopping, as discussed above.

The first signs of significantly higher overtopping rates for Recurve C, compared with the performance of other forms, occurred at the third water level tested (depth of 1.6 m at the toe). In certain cases, the reflected waves would amplify the incident waves, causing them to break due to increased wave steepness and create an impulsive wave breaking condition in front of the wall. This caused the face of the broken wave to become very aerated. As the aerated wave struck the recurve wall, the air content in the wave formed a pressurized air pocket or bubble at the base of the recurve. This air bubble would then burst, creating additional lift, which pushed the already ineffectively reflected wave further into the air to be carried over the crest of the wall due to momentum.

Due to the ineffectiveness of the shape in reflecting wave energy, Recurve C became submerged by waves at the highest water level much more regularly, when compared with the other recurves, allowing more frequent large volumes of green water overtopping, which is further discussed in Section 5.2.5.

Recurve D

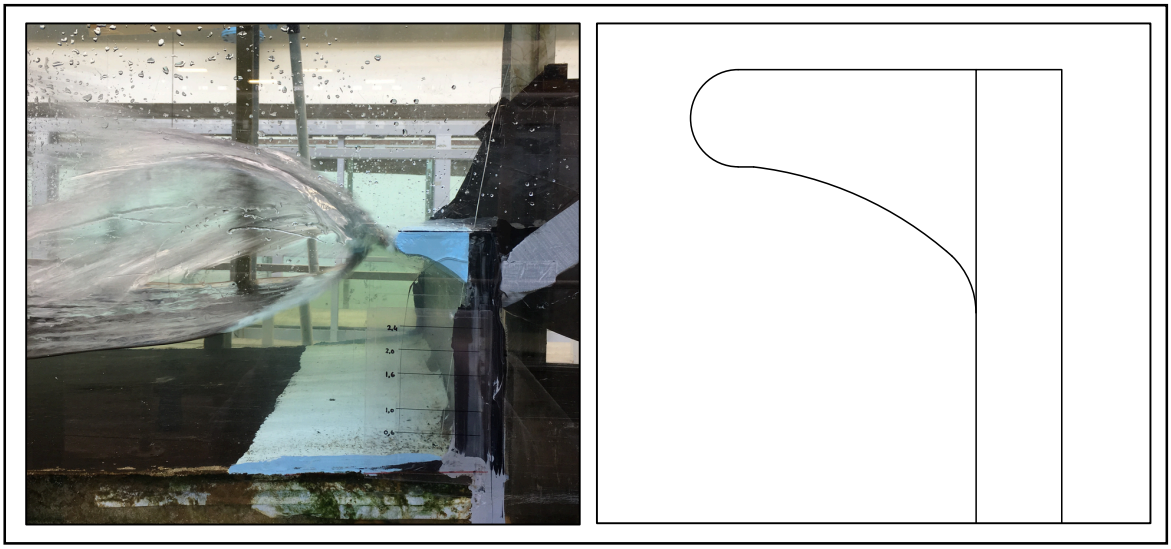

Figure 34: Recurve D

The shape of Recurve D is quite common among existing recurve seawalls, due to the generally applied concave form and aesthetically pleasing rounded overhang edge.

The performance of Recurve D in reducing overtopping was initially expected to be similar, if not better, than that of Recurve B. However, modification of the overhang edge from a squared to a rounded edge actually led to an increase in wave overtopping.

The hypothetical cause of this increase in overtopping was identified during a test at the second water level, with a wave period of 10 seconds. It is postulated that adhesive forces between the water molecules and the surface of the recurve combined with the rounded overhang edge allowed the water travelling along the face of the recurve to remain adhered to the surface and continue its path around and over the crest. This type of "adhesion" overtopping generally increased with an increase in wave period and is further discussed in Section 5.2.7.

When observing the wave reflections resulting from Recurve D, the reflected jet of water was not projected seawards at an almost zero-degree angle as was the case with Recurve B, but

rather as an arc of water similar to the arc of the concave shape, as can be seen in Figure 34. This type of wave reflection was due to the adhesion effect along the rounded edge, as described above, which pulled the reflected water jet upwards, creating an arc of reflected water. In turn, this type of reflection led to a decrease in dissipating incident wave energy and in so doing, an increase in overtopping.

Recurve E

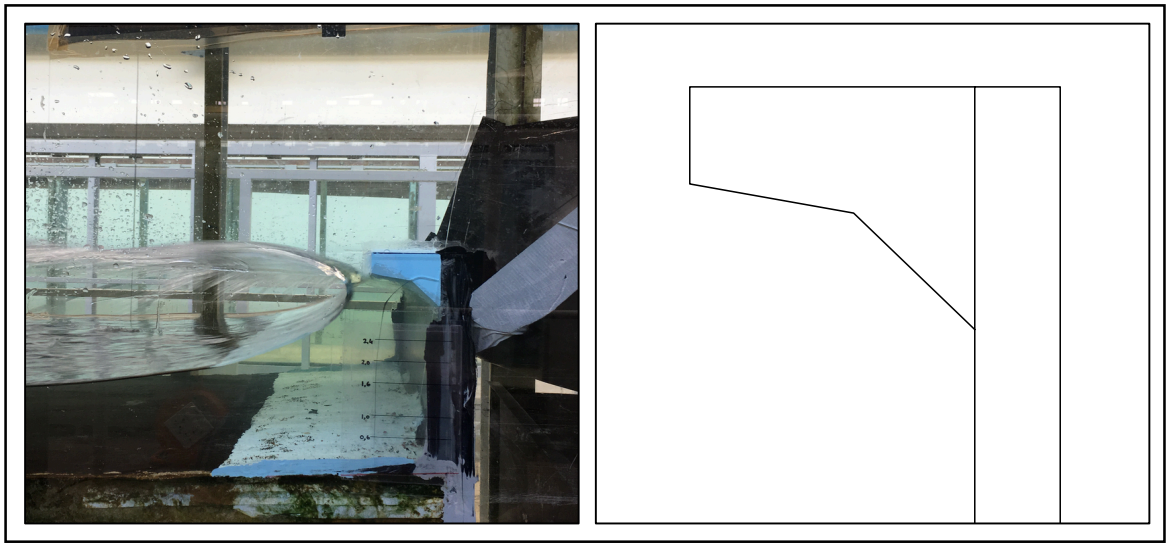

Figure 35: Recurve E

Recurve E was the second-most effective in reducing wave overtopping, after Recurve B, when compared with the performance of the other recurves.

It was initially predicted that this shape would perform similarly to that of Recurve A, owing to its linear shaped recurve. However, the slight modification to the design of Recurve A proved to provide a significant reduction in overtopping for Recurve E.

The recurve was very efficient in preventing wave overtopping at the first three water levels, with little or zero overtopping, and produced very small, consistent amounts of splash overtopping at the lowest water level, as discussed above. At the two highest water levels, Recurve E allowed only moderately more overtopping than Recurve B.

The significant reduction in overtopping, when compared with Recurve A, seemed to be attributed to the smaller angle at which the reflected water jet would be projected away from the wall, as can be seen in Figure 35. With the wave face being reflected more efficiently away

from the wall, greater dissipation of the wave energy took place which led to fewer overtopping events.

4.2.2 Overall test results

The physical model test results together with their prototype values are provided in tabular form in Appendix B per water depth, as the wave period increases. The cells highlighted in green represent the physical model values and the cells in blue the prototype values.

All the relevant test results obtained from this study are presented in Figure 36 on a plot of dimensionless overtopping discharge ($q/(gH_{mo}^3)^{0,5}$) versus relative crest freeboard (R_c/H_{mo}). Repetitions are also included in the graph, although Recurve A results obtained from using the incorrect input wave height signal file are excluded, as comparison of those results are only relevant when comparing with other input wave heights and not the complete data set.

It should be noted that zero overtopping results are not included, as these cannot be plotted on a semi-log graph. It is also important to note that the discharge parameter, q, is in $m^3/s/m$.

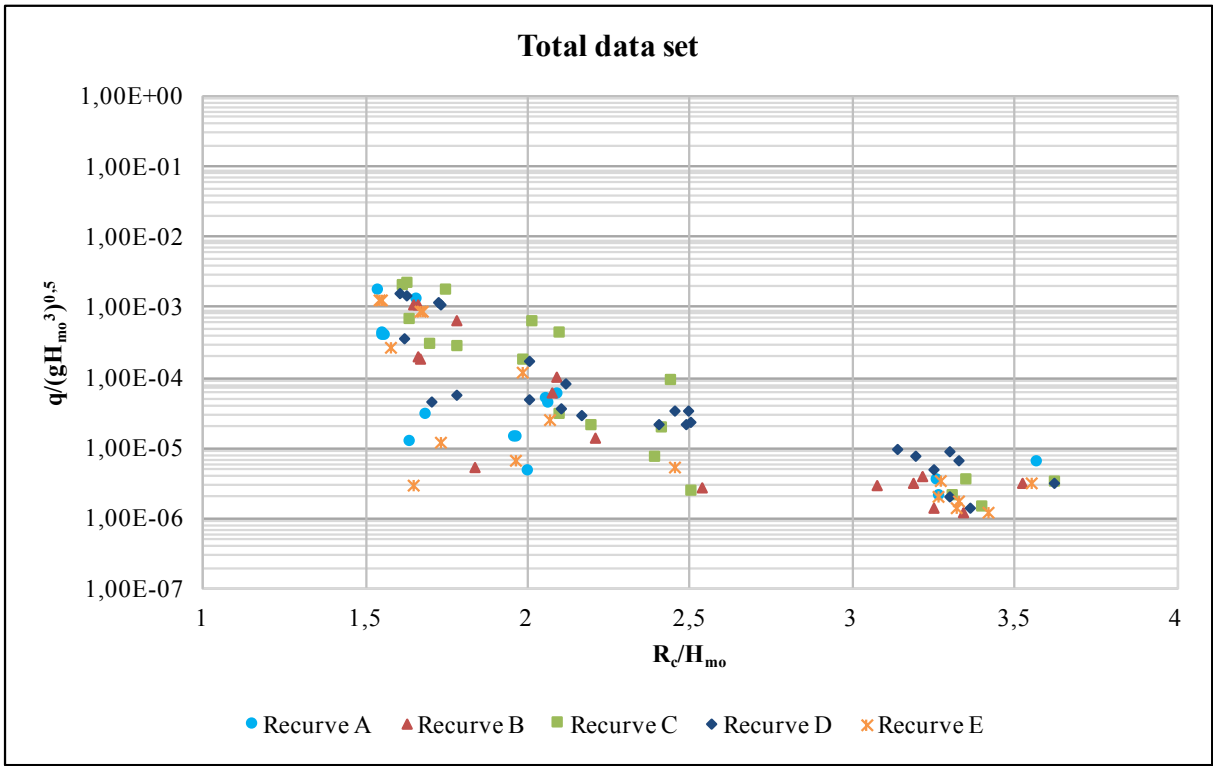

Figure 36: Total data set

4.3 Results from EurOtop online calculation tool

The EurOtop online calculation tool can be used to predict overtopping discharges of simple structures such as a parapet recurve seawall and provides the option of predicting the discharge with the use of the probabilistic (mean value approach) or deterministic method (design approach).

Figures 37 and 38 provide examples of the online tool used to calculate the discharge for specific structural and hydraulic parameters applying both the probabilistic (mean value approach) and deterministic (design approach) methods, respectively. The hydraulic conditions of the discharges calculated in Figures 37 and 38 relate to the largest overtopping event observed in the physical model study, that is, a prototype water depth at the toe of 2.4 m with a wave period of 14 seconds.

A set of comparable predicted overtopping results obtained from the calculation tool for both the probabilistic and deterministic methods are provided, analysed and discussed in Section 5.3.2.

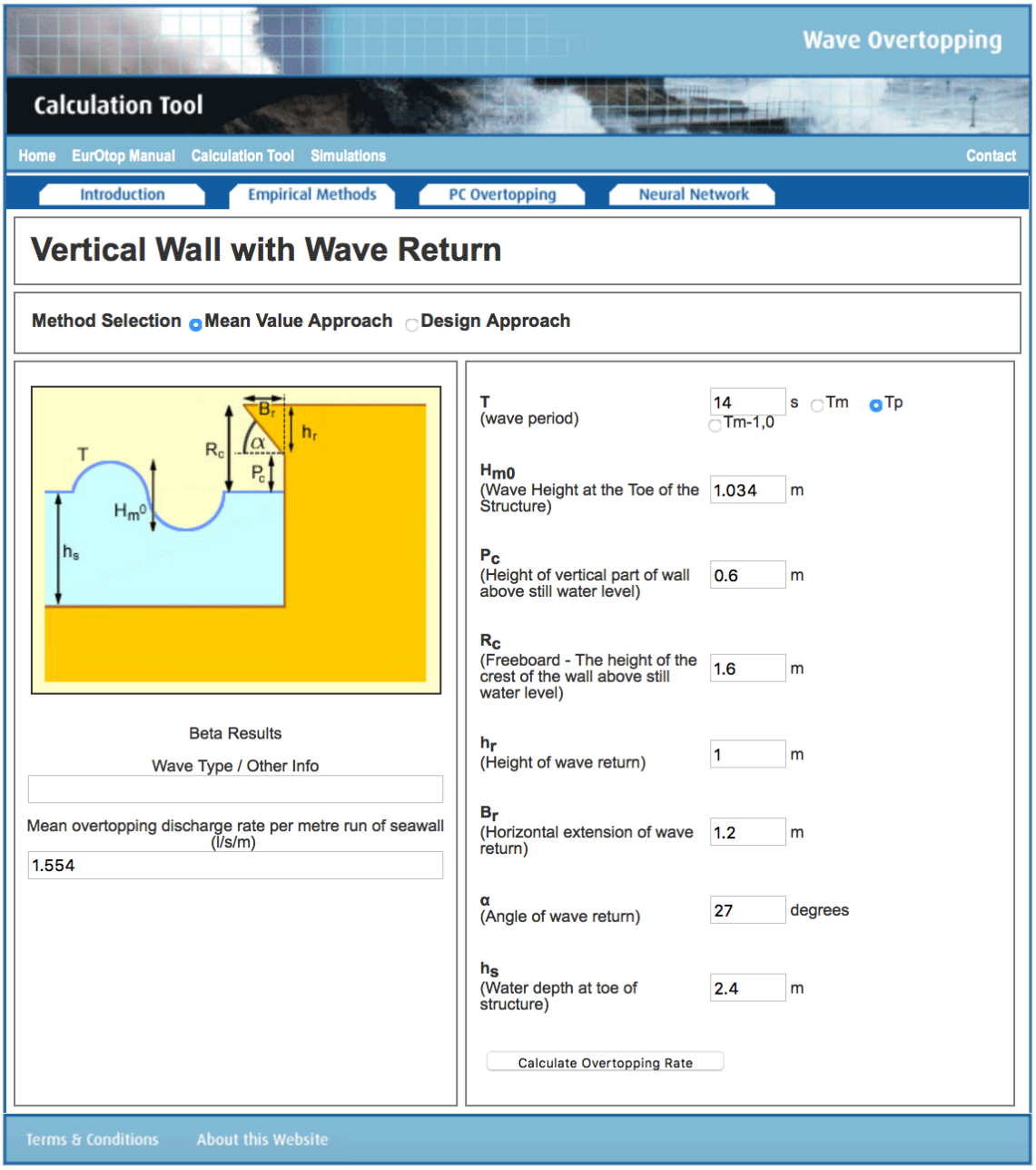

Figure 37: EurOtop online calculation tool applying probabilistic method (HR Wallingford, n.d.)

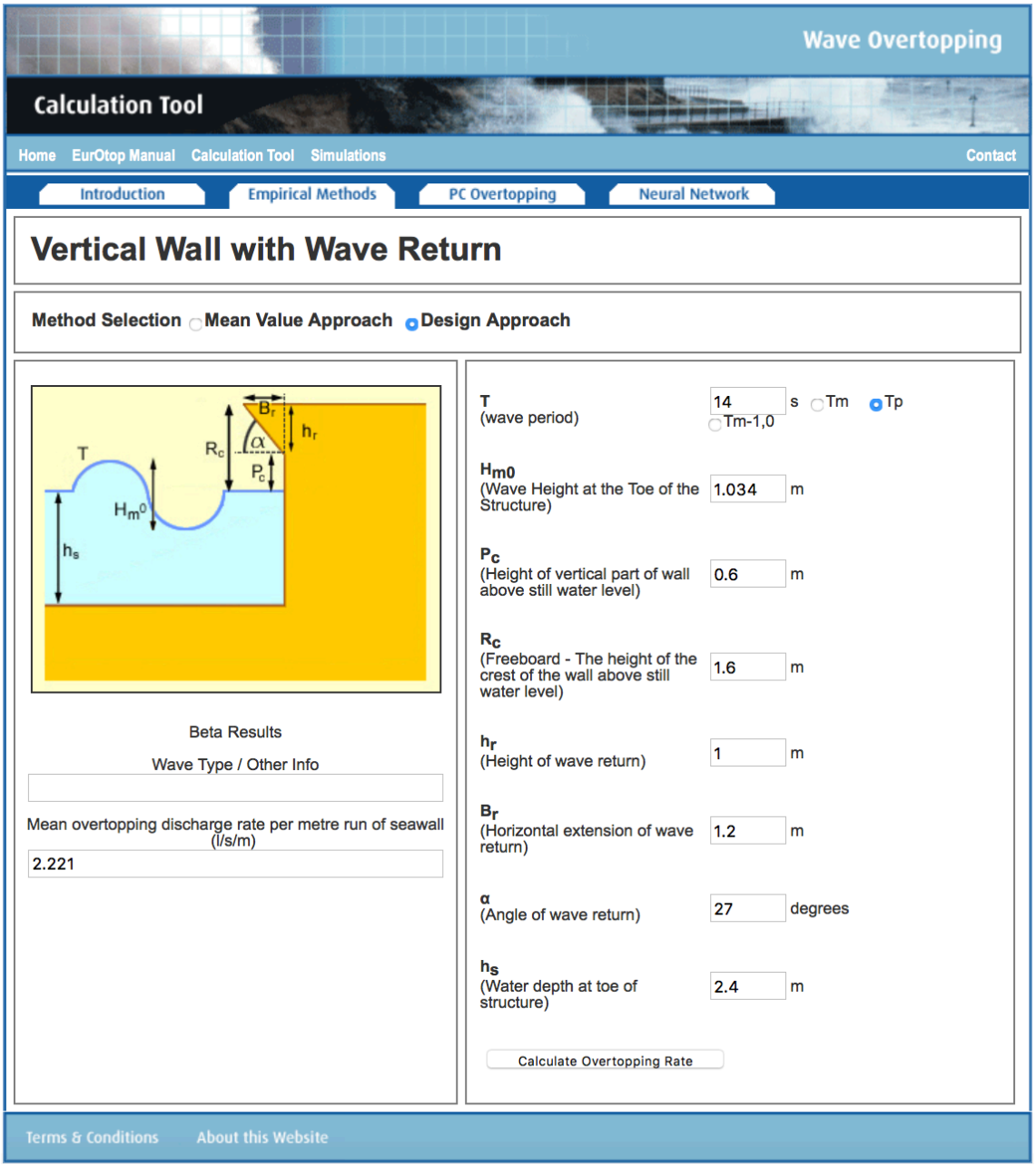

Figure 38: EurOtop online calculation tool applying deterministic method (HR Wallingford, n.d.)

Chapter 5: Analysis and Discussion

5.1 General

The objectives of this study have been accomplished and are demonstrated in this chapter by providing an in-depth analysis and discussion of the results given in the previous chapter. The performance of each recurve in reducing overtopping is compared under the influence of a variety of significant hydraulic parameters and the effect of the wave return angle, shape of the overhang edge, and collision of incident and reflected waves on overtopping is evaluated. In order to validate the study's findings, the measured results obtained in this study are compared with those predicted with the use of the EurOtop online calculation tool as well as with the results obtained from previous studies. In addition, the process followed to ensure accuracy of the tests performed, as well as additional aspects considered, are provided.

5.2 Physical Model Tests

5.2.1 Comparison of overall test results

A comparison of the overall test results for each recurve form is made by analysing the complete data set provided in Figure 39.

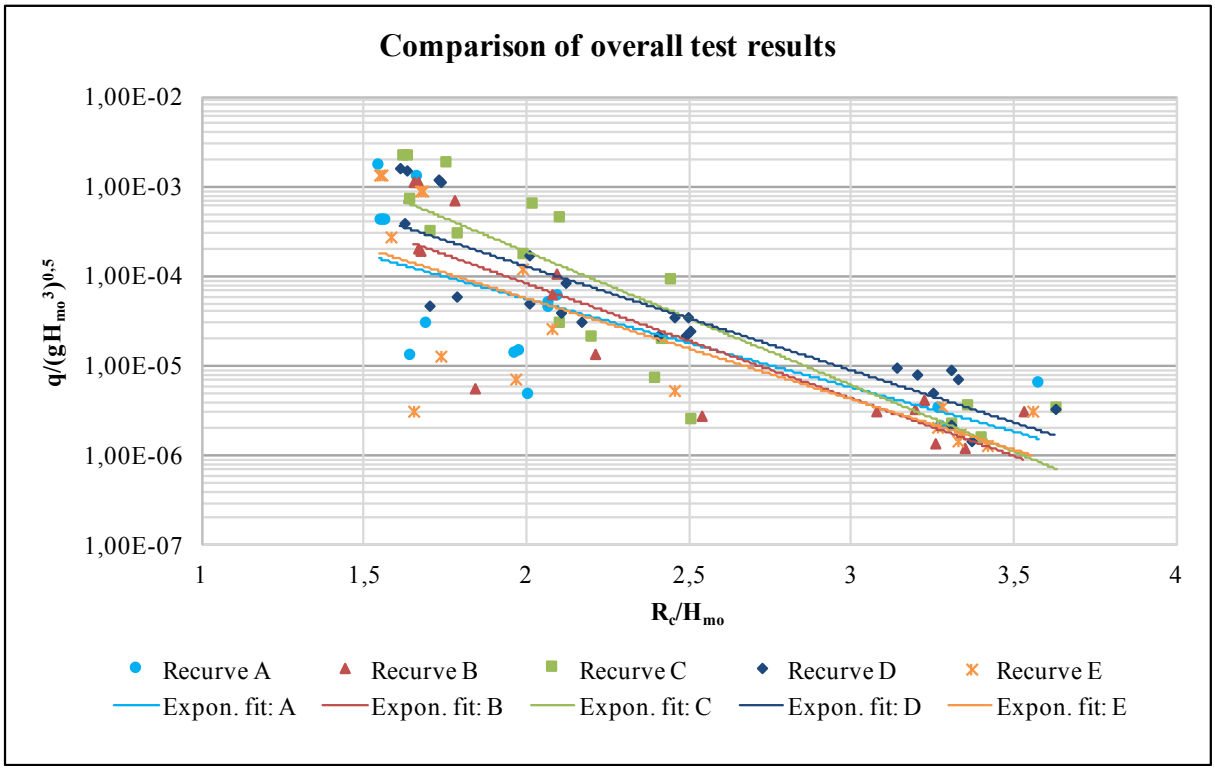

Figure 39: Comparison of overall test results

By comparing the performances of the different recurves, it is clear from Figure 39 that Recurve C provides the least reduction in overtopping for $R_c/H_{mo} < 2.5$, validating the observation made in Section 4.2.1 that Recurve C is overall the least effective in reducing wave overtopping. However, for $R_c/H_{mo} > 3$, Recurve D exhibits the worst performance in reducing overtopping. This is as a result of the combination of overtopping caused by collisions of incident and reflected waves and adhesion overtopping of the rounded overhang edge, which only occurred with Recurve D.

The initial assumption that very little or zero overtopping would occur across all the recurves for the highest freeboard case of $R_c/H_{mo} = 3.4$ m was discredited due to the unexpected contribution of overtopping due to colliding incident and reflected waves in front of the recurve wall. This is part of the reason why the trend lines shown exhibit similar gradients and paths as opposed to the expectation of an increase in gradient for recurves more effective in reducing overtopping.

All the recurves produced similar overtopping rates for the higher freeboard cases, as can be seen by the cluster of data points for $R_c/H_{mo} > 3.0$, which strongly influenced the gradient of the trend lines, making them unreliable indicators of the recurve's performance. Another reason is the presence of fewer data points from the more effective recurve forms, as they produced more zero overtopping results than the other forms, which are not displayed on the plot, as only positive values can be displayed on a semi-log graph, and therefore cannot influence the gradient of the trend line. This is evident when analysing the performance and lack of data points of Recurves B and E for $R_c/H_{mo} = 2.4$, as these recurves provided the highest reduction in overtopping and therefore produced the most zero overtopping results. However, despite the unreliability of the trend lines due to the distribution of data points for $R_c/H_{mo} > 3$, the trend line of Recurve C for $R_c/H_{mo} < 2.5$ clearly lies above those of the other recurves due to its substantial overtopping rates for the lowest freeboard case, therefore supplementing the finding that Recurve C is the least effective in reducing overtopping.

5.2.2 Performance of all recurves relative to optimum recurve

The plot in Figure 40 below represents the overall performance, during the largest overtopping event, of each of the recurves tested relative to the performance of the most optimum recurve. The largest overtopping event was chosen because it is important that the overtopping during these events must be reduced as much as possible. Recurve B was found to be the most effective

in reducing overtopping of a recurved seawall, as indicated in Figure 40. When comparing the performances of the recurves, it was surprising to find that Recurve E, with a shape never tested before, performed second-best in reducing overtopping. This was a significant finding as the design of Recurve E was based on a combination of Recurves B and A, with the intention of creating a recurve possessing the effectiveness of a concave recurve and a parapet easy to construct. The effectiveness of Recurve D was overpredicted due to the unexpected influence of the rounded overhang edge on overtopping, as discussed further in Section 5.2.7.

It is clear from Figure 40 that the convex-shaped Recurve C produced the least reduction in overtopping, showing an increase in overtopping rate, relative to Recurve B, by a factor of nearly two.

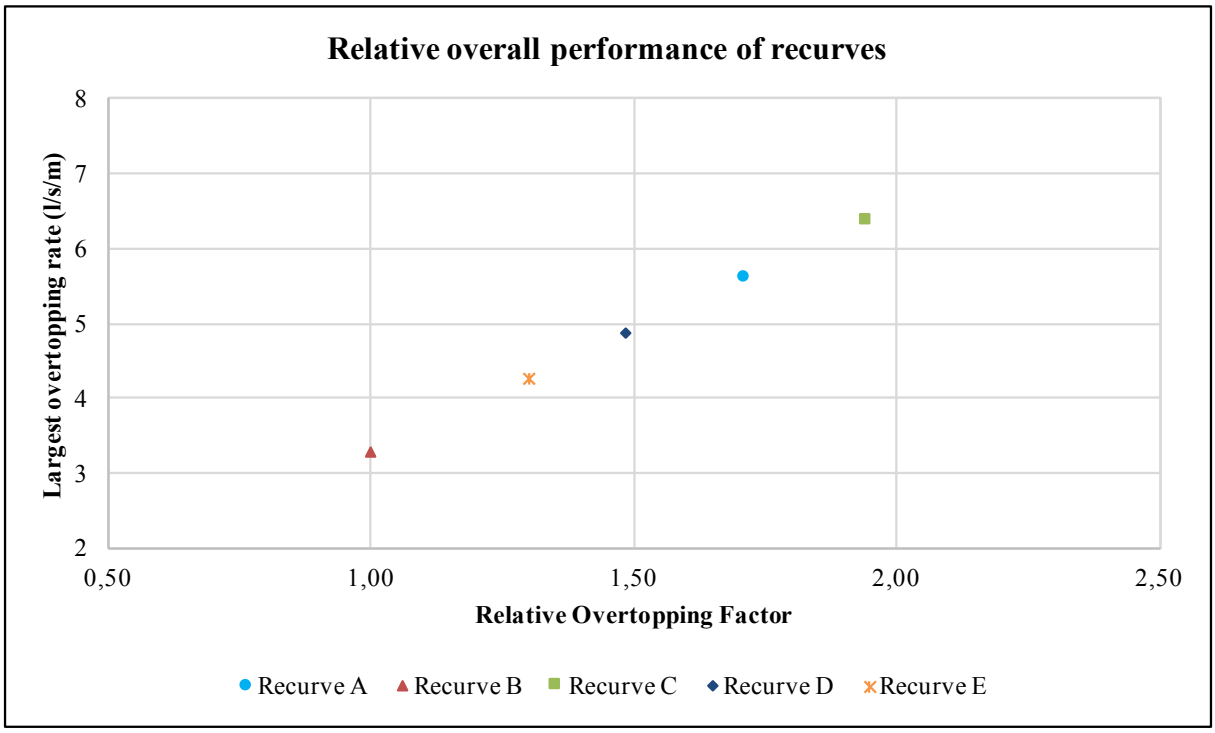

Figure 40: Relative overall performance of recurves

5.2.3 Influence of the wave return angle on overtopping

It was initially expected that the varying shape of the recurve form would not have such a significant influence on overtopping reduction, due to the fact that the overhang length as well as the three base points were kept constant throughout the design of all the different shapes.

Due to their unique design, each recurve form possessed a particular angle at the point where the reflected volume of water, during a successful wave reflection, would leave the surface of

the form. It is important to note that this angle is not defined as the recurve angle (α) of a parapet recurve wall mentioned in Section 2.4 (Figure 11). For simplicity reasons, this angle would from here onwards be referred to as the wave return angle.

The wave return angle was measured counter-clockwise from the horizontal plane starting at base point b, the point at which the reflected water jet leaves the form's surface, as illustrated in Figure 42. Figure 41 provides a plot of the performance of each recurve shape in terms of its wave return angle related to the largest overtopping event recorded.

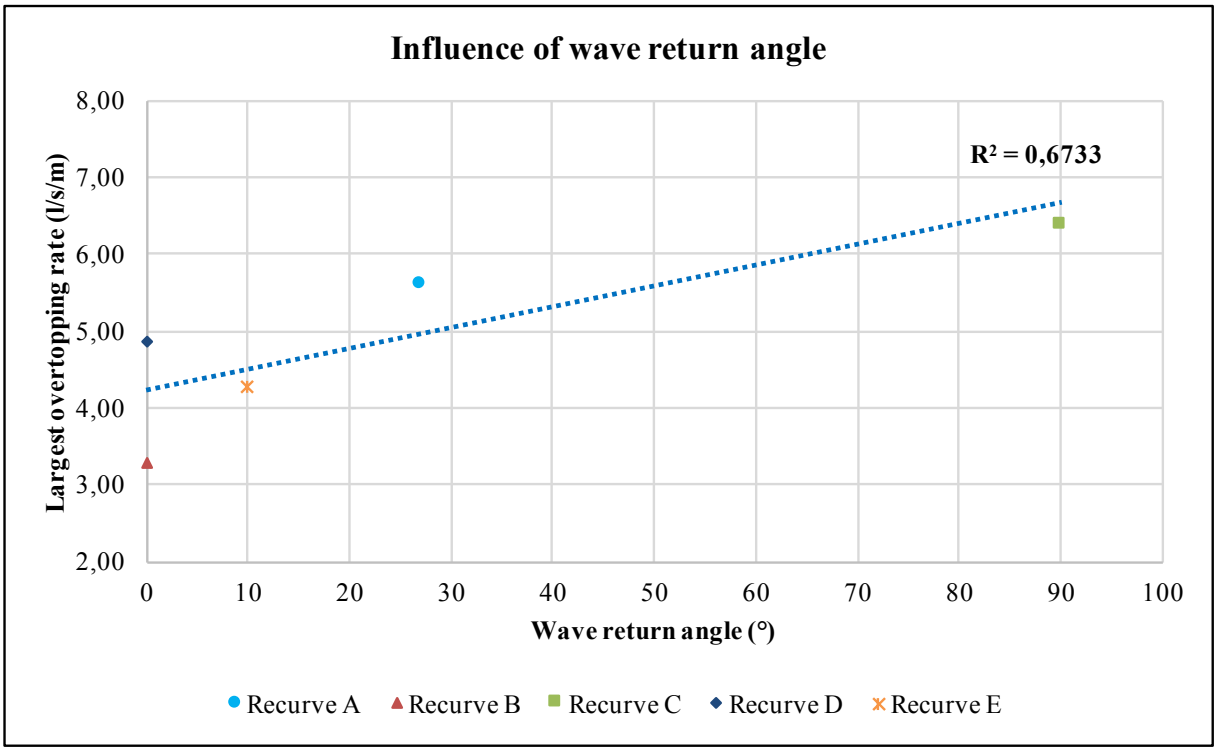

Figure 41: Influence of wave return angle

At a first glance, it is clear from Figure 41 that the most effective recurve shape, as described in the previous section, Recurve B, also possesses the smallest wave return angle, i.e. 0°. The overall distribution of data points together with the trend line in Figure 41 indicate that an increase in the wave return angle leads to an increase in overtopping. This finding is well established when observing the almost linear trend of the performances of Recurves B, E, and A, with wave return angles of 0°, 10°, and 27°, respectively.

However, caution must be taken when analysing the performances of Recurves D and C. Although Recurve D possesses a zero degree angle identical to that of Recurve B, it is still found to be significantly less effective in reducing overtopping. The ineffectiveness of Recurve D is attributed to the rounded "bullnose" overhang edge which allowed for more overtopping compared to the squared overhang edge of Recurve B, as discussed in Section 5.2.7.

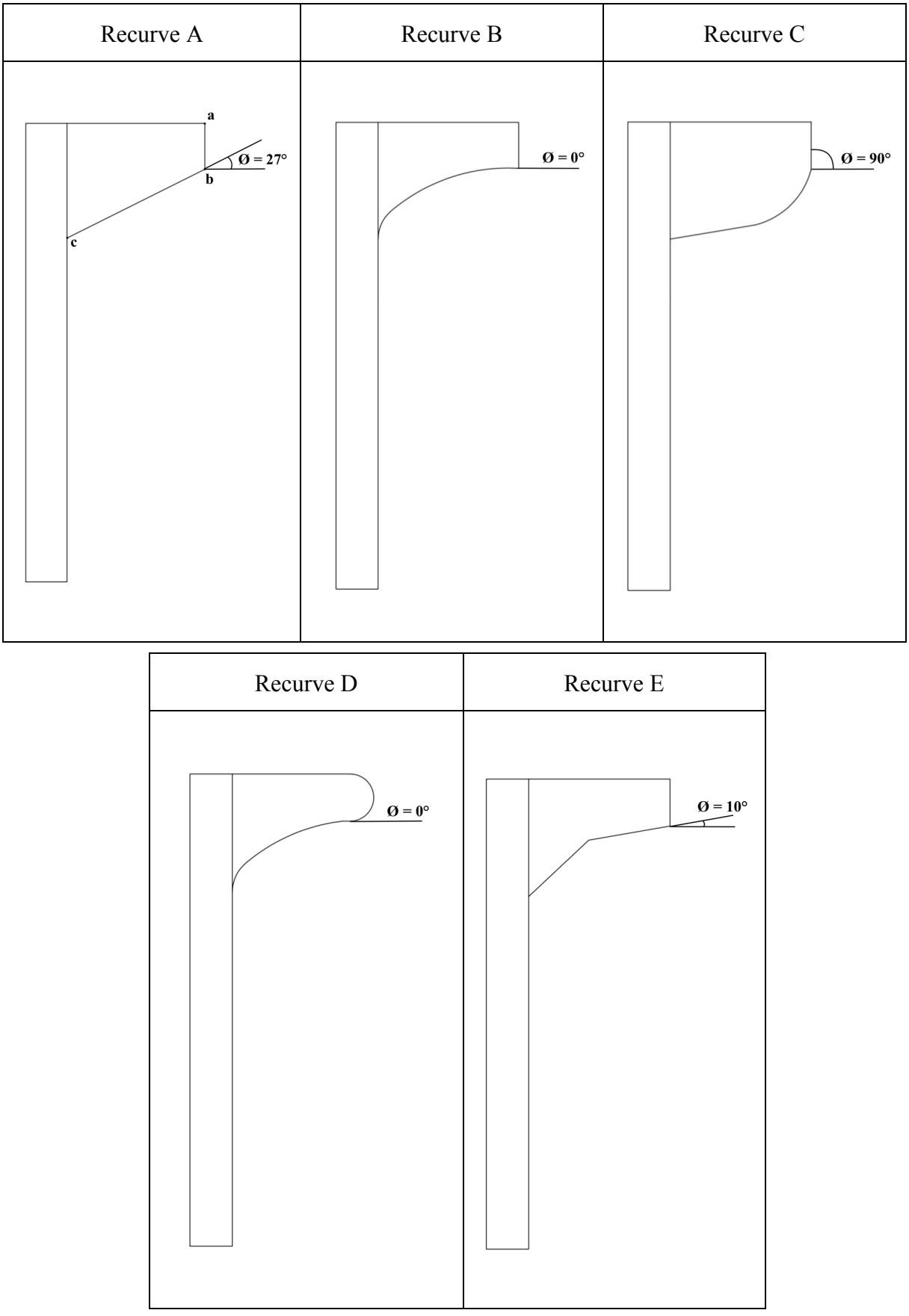

Figure 42: Illustration of wave return angle (Ø)

Due to a lack of guidelines on the design of a convex recurve shape, the shape of Recurve C was in essence based on the inverse of the concave shape of Recurve B. This implies that the wave return angle of Recurve C would follow the inverse path to that of Recurve B, leading to the designation of a 90° wave return angle. However, the reflected water did not always follow the designated angle of 90°.

Nevertheless, it is clear from the results that Recurve C was the least effective in reducing wave overtopping and that the wave return angle of Recurve C was observed to always be larger than 27°, which supports the finding that increasing the wave return angle generally increases wave overtopping. This finding also correlates well with the finding of Swart (2016), stating that a parapet with a recurve angle greater than 50° provides less reduction in overtopping, compared to a vertical wall under the same conditions.

5.2.4 Influence of wave period

As described in Section 3.4, the wave periods tested in this study ranged from 6 to 14 seconds, in 2 second increments. A previous study on wave overtopping of recurve seawalls by Swart (2016) included a range from 8 to 16 seconds. Although a short wave period of 6 seconds lies outside the swell wave spectrum along the South African coastline and originates more often from wind waves, it was still included in this study due to the lack of previous research on the subject. In addition, the validity of the assumptions made by Roux (2013) stating that wave periods larger than 12 seconds produce less overtopping was tested.

Figure 43 represents the sensitivity of wave period on overtopping rates for all the recurves at a water depth of 2.4 m. The wave period sensitivity at each of the water depths is provided in Appendix C.

It is clear from Figure 43 that, for all but Recurve C, wave periods from 6 to 8 seconds exhibit negligibly small overtopping rates as well as little increase in overtopping for a water depth of 2.4 m at the toe of the recurve wall. However, it is important to note that even though the overtopping rates seem small for this period range when compared to larger periods, there still exists some spray overtopping which in fact is in no way linked to the shape of the recurve form. This phenomenon was observed due to colliding incident and reflected waves, which is further discussed in Section 5.2.8.

A significant increase in overtopping of all recurve forms appears at the wave period increases from 8 to 10 seconds. For the 2.4 m water depth case, which corresponds to a freeboard of 1.6 m, the performance of all the recurve forms exhibit an almost linear increase in overtopping rate from the 10 to 14 second wave periods. It can be noted that a slight decrease from the linear trend in the overtopping rate trend for Recurve C is observed from 12 to 14 seconds, although this should be considered with caution due to the irregular and ineffective shape of Recurve C.

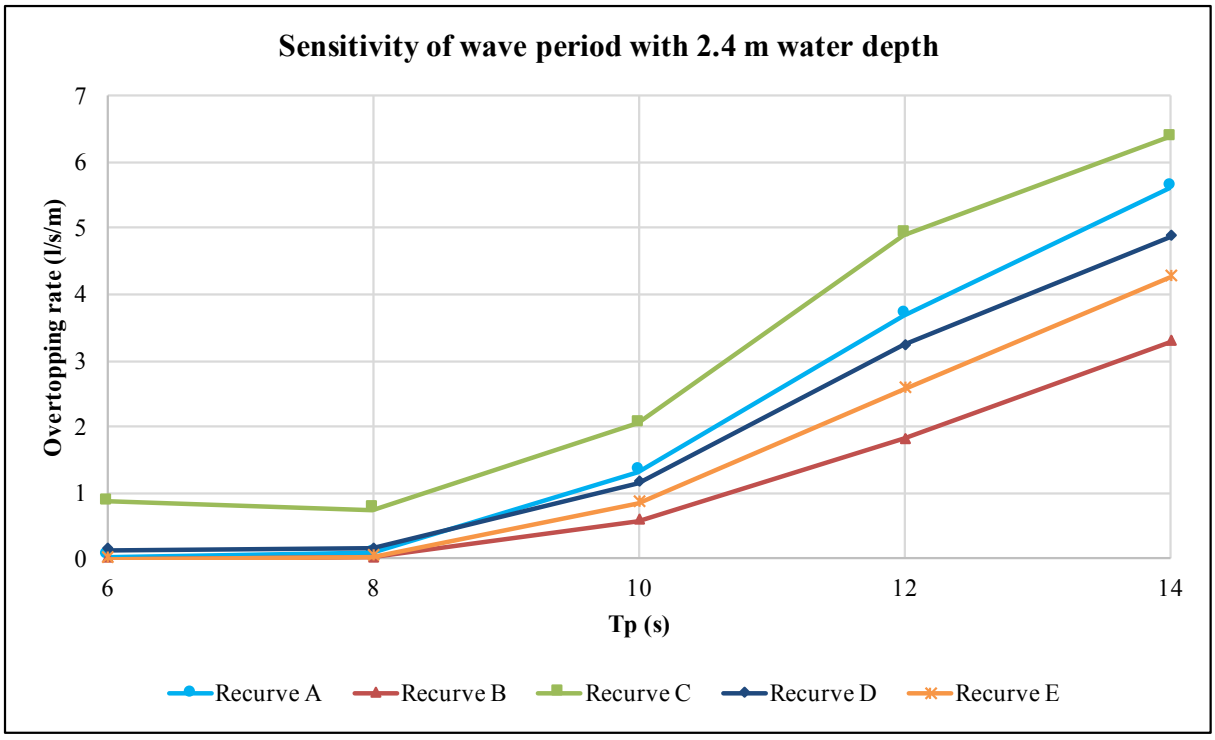

Figure 43: Sensitivity of wave period with 2.4 m water depth on overtopping

It can be concluded that the results obtained from this study do not correlate with the findings of Roux (2013), due to the findings that overtopping generally increased with an increase in wave period and that shoaling of longer period waves did not occur in deeper water, but rather at the shallower water depths, at which point the freeboard becomes high enough to prevent any wave overtopping whatsoever. In addition, short period waves of 6 seconds should not be disregarded as they generally originate from wind waves and could therefore be coupled with an onshore wind, leading to an increase of splash overtopping from colliding incident and reflected waves in front of the structure.

5.2.5 Influence of water depth

The range of water depths at the toe of the structure tested for this study were identical to the water depths used by Swart (2016) and Schoonees (2014), in the same wave flume, with a corresponding freeboard range of 3.4 m, 3.0 m, 2.4 m, 2.0 m, and 1.6 m.

Figure 44 represents the sensitivity of water depth on overtopping rates for all the recurves, with a wave period of 14 seconds. The water depth sensitivity at each of the wave periods is provided in Appendix D.

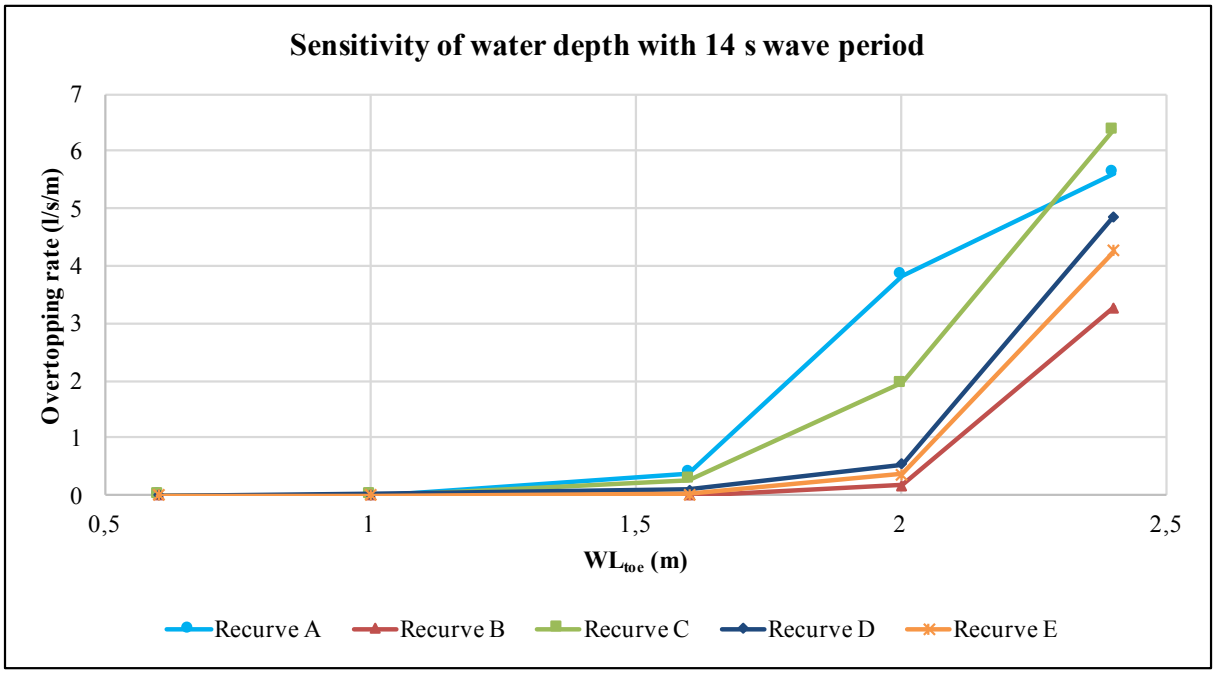

Figure 44: Sensitivity of water depth with 14 s wave period on overtopping

As expected, overtopping rates remained consistently low for the higher freeboard cases of 3.4 m and 3.0 m. For the longest wave period of 14 seconds, the first signs of significant overtopping were observed at a water depth of 1.6 m, corresponding to a freeboard of 2.4 m. A relatively small increase in overtopping occurred for an increase in water depth from 1.6 m to 2.0 m for Recurves B, E, and D, whereas the convex-shaped Recurve C exhibited a significantly larger increase in overtopping. At this point, it became evident that the assumption made of Recurve C's ineffectiveness in reducing overtopping would be validated.

It should be noted that the overtopping rate of Recurve A at a water depth of 2.0 m was not considered relevant in the comparison, as the test was executed with incorrect wave height input parameters. Although certain tests were repeated in order to gain the most accurate results, it was decided that this test did not merit a repetition due to the already existing empirical research findings on this specific recurve shape.

The gradient of the overtopping trend lines for each recurve increased significantly from a water depth of 2.0 m to 2.4 m, indicating that the reduction in overtopping is significantly reduced when decreasing the freeboard from 2.0 m to 1.6 m.

The significantly larger amounts of overtopping at the deepest water depth was due to the recurve wall becoming submerged much more regularly, thereby greatly reducing the effectivity of the recurve in reflecting wave energy and allowing much larger volumes of green water overtopping. Due to its ineffectiveness in reflecting wave energy, Recurve C produced the largest amount of green water overtopping events. Figure 45 shows Recurve C in a drowned state during Test C-53, where the incident wave completely submerged the structure, allowing a large volume of green water to overflow the crest.

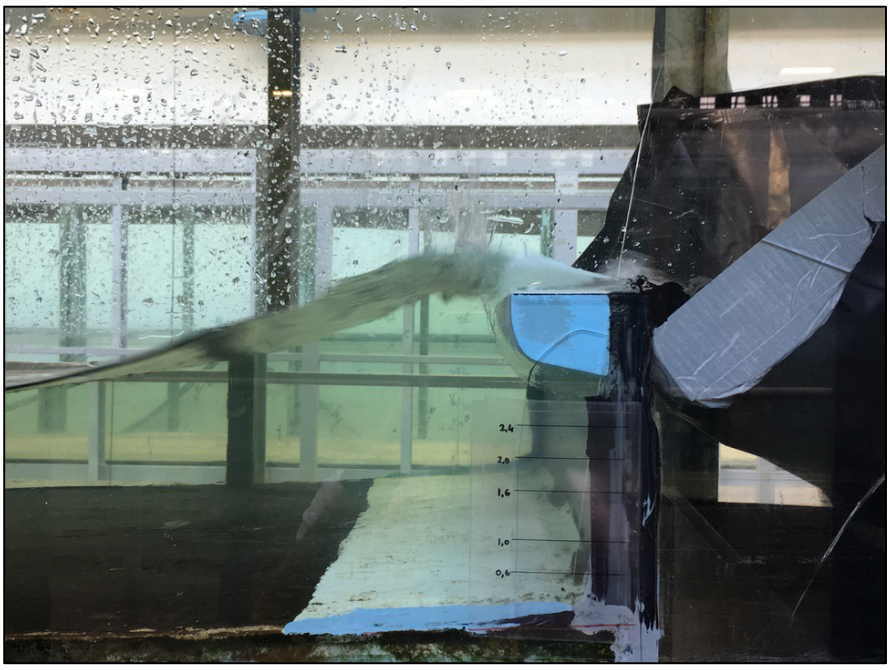

Figure 45: Example of green water overtopping, Test C-53 (WL_{toe} = 2.4 m, T_p = 10 s)

It can be concluded that overtopping increases with increasing water depth and that caution should be taken with regard to crest level design of recurve seawalls, especially if the seawall will become submerged.

5.2.6 Influence of wave height

In order to determine the influence of varying wave heights on overtopping, two separate cases were evaluated:

- Varying input wave heights with Recurve A

- Comparing identical conditions between Recurve A and Recurve B

The first case simply investigated how overtopping volumes and rates would increase relative to a certain increase in input wave height for one specific recurve shape. The second case originated from the observation that overtopping rates for Recurve B were significantly lower than for Recurve A, under identical input conditions but with slightly varying recorded incident wave heights.

Waves were generated by specifying an input wave height into the HR Wavemaker software package, which then transferred the signal file to the wave paddle. It was initially assumed that an input wave height signal file of 1 m (prototype value) would ultimately generate the required design incident wave height of 1 m. However, due to the imperfect performance of the active wave absorption system, the resultant incident wave height would differ quite significantly from the input wave height. To counteract this problem, adjustments were made to the input wave height in order to achieve the required design wave height. This is illustrated in Figure 46, showing the influence of different wave heights for Tests A-53 and A-53-2. Tests A-53 and A-53-2 were specified with input wave heights of 1 m and 0.8 m which corresponded to resultant incident wave heights of 1.27 m and 1.02 m, respectively.

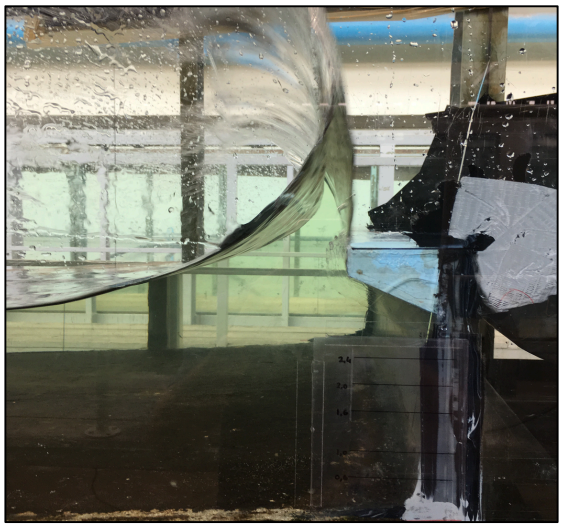

A-53
(H_i = 1.27 m)

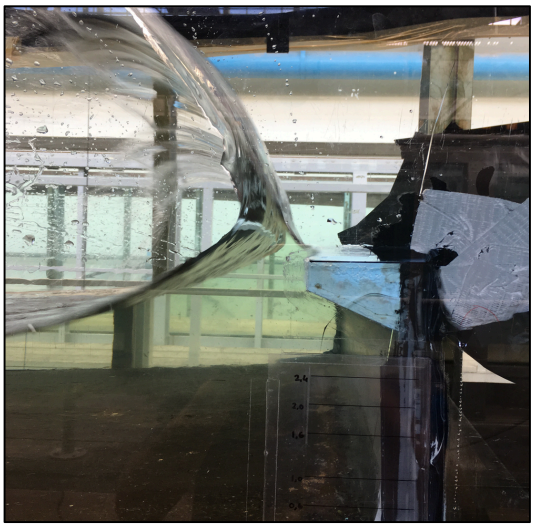

A-53-2
(H_i = 1.02 m)

Figure 46: Influence of wave height adjustment

The overtopping results of Tests A-53 and A-53-2 are provided in Table 6 below, used to determine the effects of varying input wave heights on overtopping.

Table 6: Influence of wave height adjustments on overtopping

Influence of wave height adjustments on overtopping			
Test		**A-53**	**A-53-2**
Water level at toe	**m**	2.4	2.4
Peak wave period	**s**	10	10
Input wave height	**m**	1.0	0.8
Incident wave height	**m**	1.27	1.02
Overtopping volume model	**l**	138.98	33
Overtopping rate prototype	**l/s/m**	5.56	1.32

An analysis of Figure 46 and Table 6 proves that the input wave height has a significant effect on both the incident wave height and on wave overtopping of the seawall. In this case, an increase in the incident wave height, H_i, by a factor of about 1.25 led to an increase in the overtopping rate by a factor of 4.2. This large increase in overtopping is clearly visible in Figure 46, where the H_i of 1.27 m almost completely submerges the recurve, with minimal seaward reflection taking place, whereas the H_i of 1.02 m only slightly submerges the recurve, with most of its energy being reflected away from the wall.

Table 7 provides the overtopping results obtained from tests with identical input parameters from Recurves A and B, used to determine the influence of incident wave height on overtopping.

Table 7: Influence of incident wave height on overtopping

Influence of incident wave height on overtopping					
Test		**A-53-2**	**A-53-3**	**B-53**	**B-53-2**
Water level at toe prototype	**m**	2.4	2.4	2.4	2.4
Peak wave period prototype	**s**	10	10	10	10
Incident wave height model	**mm**	51.05	51.42	48.02	47.92
Overtopping volume model	**l**	33	33.5	14.5	14.25
Overtopping volume Avg	**l**	33.25		14.38	
Incident wave height Avg	**mm**	51.24		47.97	
Overtopping/wave height	**l/mm**	0.649		0.3	

From Table 7 it can be noted that the incident wave heights from Tests A-53-2 and A-53-3 were slightly larger than those recorded in Tests B-53 and B-53-2, under the same input conditions.

However, for this slight increase in wave height, a significant increase in overtopping was observed. This observation was surprising and prompted further investigation into the effect of varying incident wave heights on overtopping.

In order to determine how the overtopping volume of Recurve A would have changed if it was tested under the smaller wave height condition obtained in the test with Recurve B, the average value of overtopping volume per wave height (in l/mm) was calculated (Table 7). By multiplying this average value calculated for Recurve A, 0.649 l/mm, with the average incident wave height of Recurve B, 47.97 mm, a predicted overtopping value for Recurve A of 31.1 litres was found. This value was very close to the average overtopping value calculated for Recurve A, proving that the influence of H_i was negligible and that the large overtopping difference was due to the effectivity of the recurve shape in preventing overtopping.

By taking the first case into account, it is clear that the input wave height can become an influential variable if not accurately adjusted to produce the required design H_i. It should be noted that even after the appropriate input wave height has been achieved, it can still be expected that small differences in H_i will occur under identical wave input conditions for two different recurve shapes. However, analysis of the second case has proved that these small differences in H_i have a negligible effect on wave overtopping and that it is, in fact, the shape of the recurve that has the largest influence on reducing wave overtopping.

5.2.7 Influence of squared versus rounded overhang edge

It was initially predicted that the concaved shape of Recurve D, with a rounded overhang edge or “bullnose” would perform similarly to the strictly concaved Recurve B. However, during Test D-23, with a 3.0 m freeboard and 10 second wave period, it was noted that some water from waves striking the wall would travel along the surface of the recurve and, instead of being reflected seawards, would remain adhered to the surface and continue running along and over the crest of the recurve. This phenomenon led to an increase in overtopping of Recurve D, relative to Recurve B, by a factor of up to 1.49, as can be seen in Figure 40.

It is postulated that this type of overtopping is due to the strong adhesive forces between the water molecules and the surface of the recurve which, when combined with the rounded overhang edge, allowed the water running along the face of the recurve to remain adhered to the surface and traverse around and over the crest. This type of overtopping would and could

not have occurred with Recurve B, as the square overhanging edge of the form would interrupt the adhesion and motion of water along the surface.

The sequence in which this type of overtopping took place is illustrated in Figure 47 as a series of consecutive photographs (marked a - d) taken during Test D-24. The red arrows indicate the flow of adhered water as it travelled along the surface and rounded edge of the recurve.

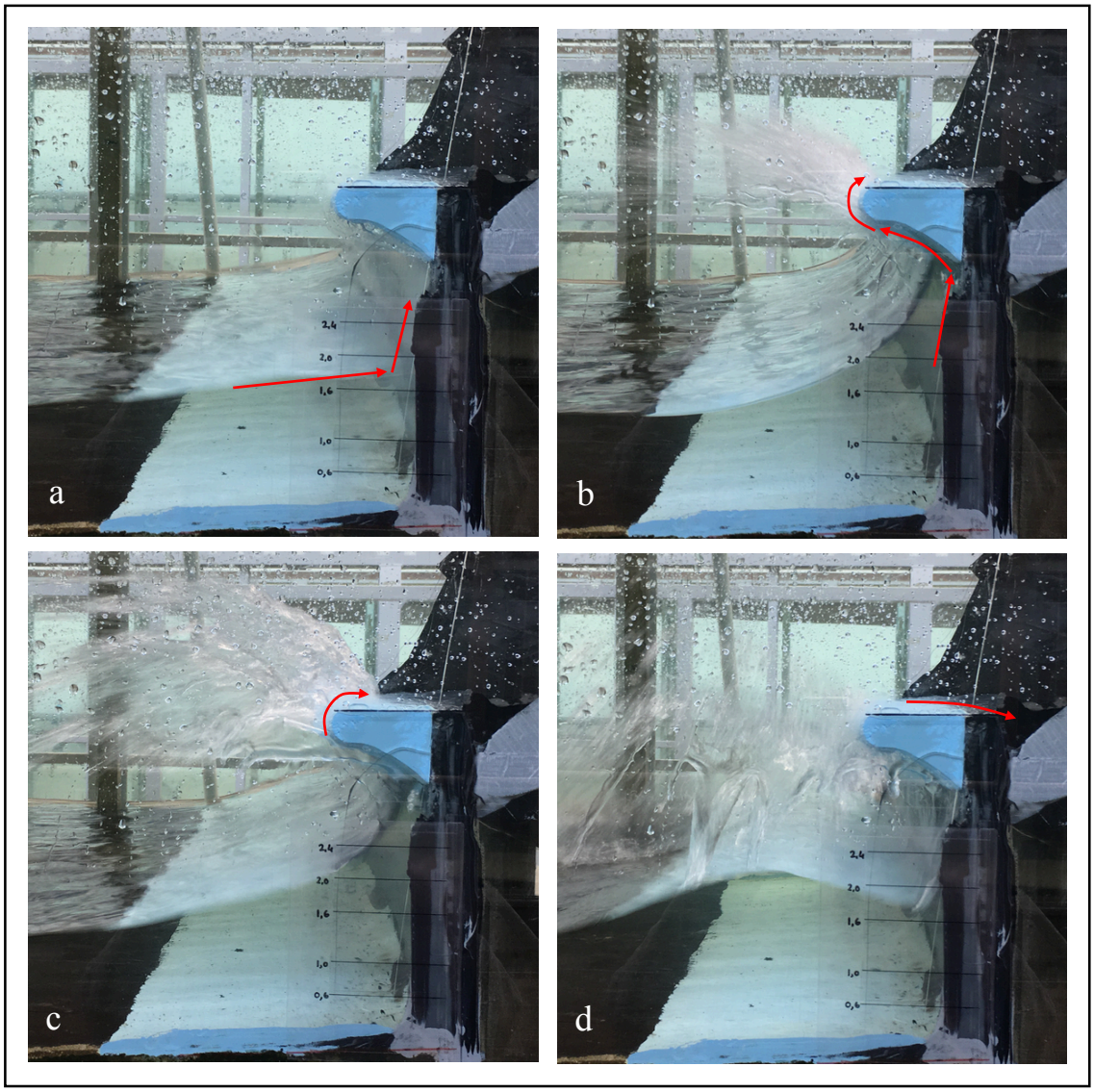

Figure 47: Adhesion overtopping during Test D-24 (WL_{toe} = 1 m; T_p = 12 s)

This phenomenon also occurred regularly during the 2.4 m freeboard scenario, leading to generally higher overtopping rates across the entire wave period range, as can be seen by the performance of Recurve D in Figure 48. Figure 48 provides a plot illustrating the performance of the recurves in reducing wave overtopping in terms of their sensitivity to varying wave periods at a water depth of 1.6 m. This type of plot would normally be included under Section 5.2.4, however, as it provides graphical data which supports the phenomenon of increased overtopping due to a rounded overhang edge, it has been included in this section.

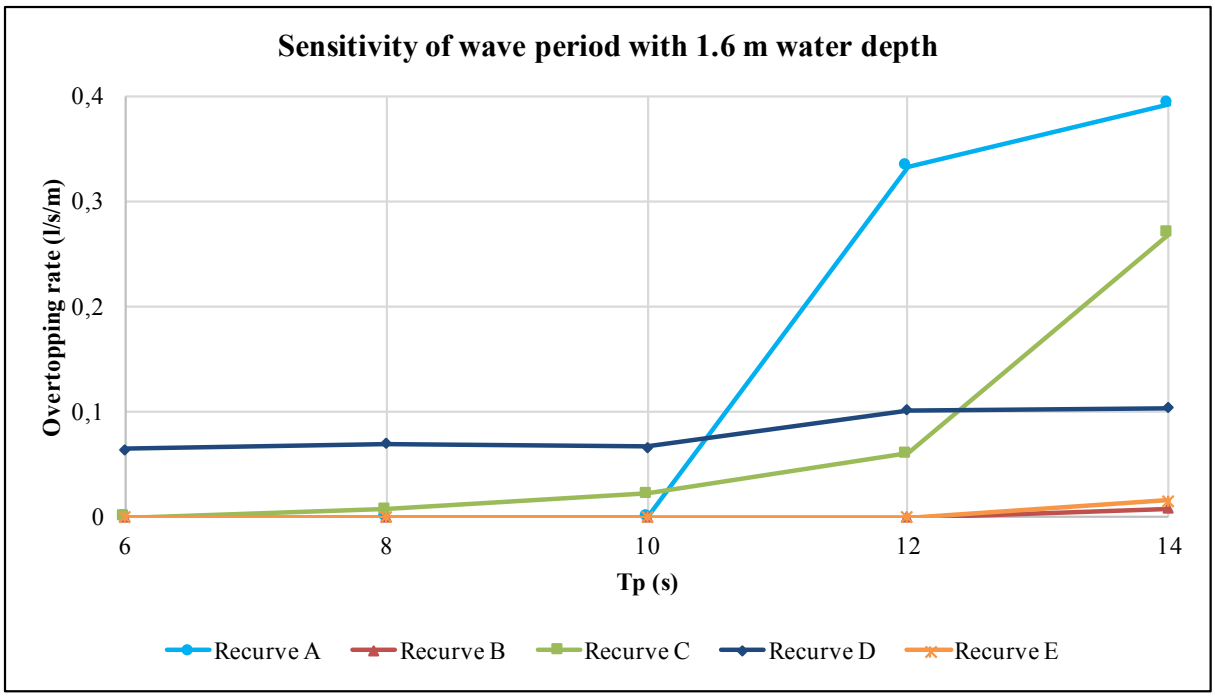

Figure 48: Sensitivity of wave period with 1.6 m water depth on overtopping

It should be noted that the data points of Recurve A for the 12 and 14 second wave periods should be disregarded, as they were recorded during tests with incorrect input wave heights, but are included in order to present a full data set. The effect of the rounded overhang edge on overtopping can clearly be seen in Figure 48.

Although the overtopping rates remain small, it is clear in Figure 48 that Recurve D still consistently produced significantly higher overtopping rates, compared to those of Recurves B and E, across the entire range of wave periods tested, with further increases for the longer period wave conditions.

It was noted that this phenomenon did not occur very regularly at the larger freeboard cases with shorter wave periods. This was naturally due to the higher freeboard which needed to be traversed as well as the effect of shorter period waves on incident wave energy. It was speculated that wave reflections from short period waves would dissipate the energy of closely following incident waves, which in turn dissipated the adhesive forces needed for water to traverse the rounded overhang edge.

Overtopping in this sense increased with an increase in wave period. This can be attributed to the speculation that waves with longer wave periods have more energy than dissipated short period waves, allowing more potential for successful adhesion along the entire face of the rounded recurve edge.

5.2.8 Influence of incident and reflected wave collisions

In general, it has been assumed that as the wave period increases, so does the amount of wave overtopping. However, this assumption was partially discredited during tests with shorter period waves at the two lowest water levels.

After completion of Test B-21, with a wave period of 6 seconds, which was expected to produce zero overtopping, the water level in the overtopping bin had risen slightly and a substantial amount of droplets of overtopped spray was still caught on the overtopping catchment sail. This result was unexpected as zero overtopping was recorded for a case of identical water level, WL_{toe} = 1 m, with a longer wave period of 14 seconds. This strange occurrence is explained by analysing Figure 49, below. The red arrows indicate incident and reflected wave positions.

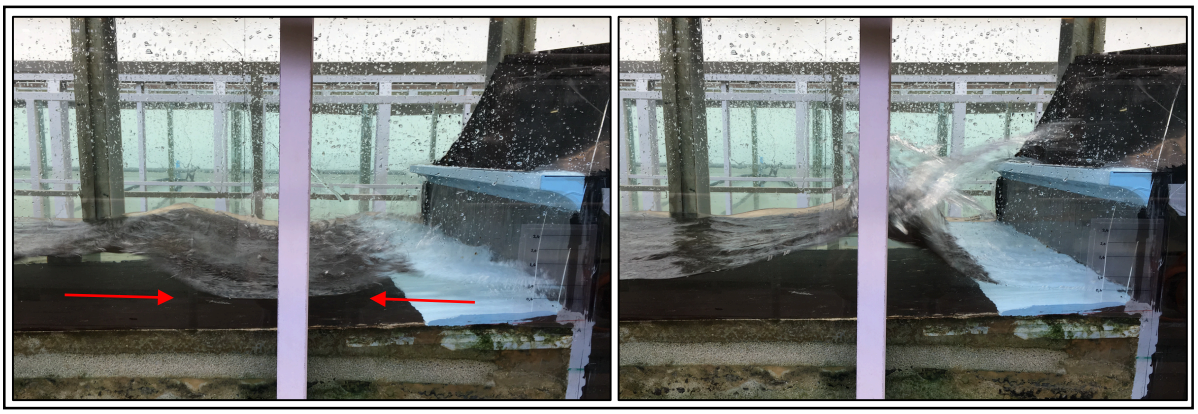

Figure 49: Example of colliding incident and reflected waves, Test B-21 (WL_{toe} = 1 m, T_p = 6 s)

It can be seen that the recurve form was 100% effective in successfully reflecting incident waves. However, the reflected wave would then collide with the closely following incident wave and, as the short period waves have short wavelengths, the collision would occur very close to the wall, generating a fair amount of splash which was carried over the crest of the wall, as can be seen in Figure 49. Collisions between reflected and incident waves with longer periods also occurred. However, it was observed that these collisions occurred too far away from the wall for the spray to reach and overtop the crest of the wall. This observation is

represented in Figure 50, below, comparing the distances from the wall (white arrows) at which wave collisions occurred for 6 and 14 second wave periods.

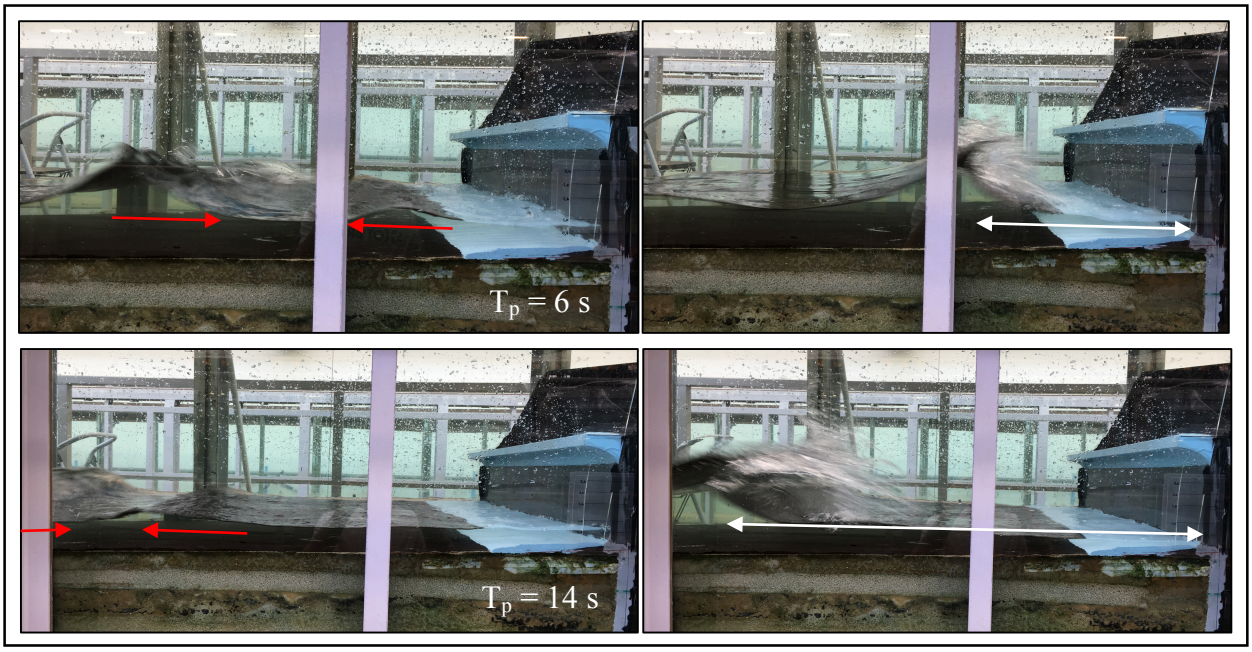

Figure 50: Comparing incident and reflected wave collisions between 6 and 14 second wave periods

In conclusion, it was found that for short period waves in shallow water depths ($WL_{toe} \leq 1$ m), as depth-induced wave breaking amplifies wave collisions, the functionality of the recurve becomes negligible as overtopping would take place in the form of splash from waves colliding in the close proximity of the structure.

This was an interesting finding, as apparently no other researchers have studied the effects of such short wave periods on overtopping. It can be assumed that in reality, with an additional onshore blowing wind, these types of collisions could in fact create larger overtopping values than recorded here.

5.3 Comparison with EurOtop calculation tool and previous studies

5.3.1 General

The physical model results from this study were compared with the results obtained from the EurOtop online calculation tool, as well as with the results obtained by Schoonees (2014) and Swart (2016). However, it is important to note that only the results obtained from Recurve A in this study were applicable for these comparisons, as the EurOtop online calculation tool only allows for overtopping predictions of basic structures such as parapet recurves and as the studies

by Schoonees (2014) and Swart (2016) both included model results of a 1.2 m overhang profile recurve, identical to Recurve A.

5.3.2 EurOtop online calculation tool

Figure 51 provides a graphical representation of the measured results from Recurve A compared with the results obtained from using both the probabilistic (mean value approach) and deterministic (design approach) methods of the EurOtop online calculation tool. The deterministic method includes a factor of safety of one standard deviation and therefore produces more conservative overtopping results than the probabilistic method, as can be seen in Figure 51. The results are plotted on a semi-log graph, implying that zero overtopping results are not displayed on the plot.

When comparing the trend line slopes of the measured overtopping results with the predicted overtopping from the calculation tool in Figure 51, it is clear that the overtopping discharges of the physical model study decreases at a more rapid rate as the freeboard increases. This result could be due to the measuring technique applied, which proved especially difficult when recording low overtopping volumes at high freeboards as a relatively significant amount of overtopping in the form of spray would be caught and trapped on the plastic catchment sail, therefore not contributing to the already minimal overtopping volume.

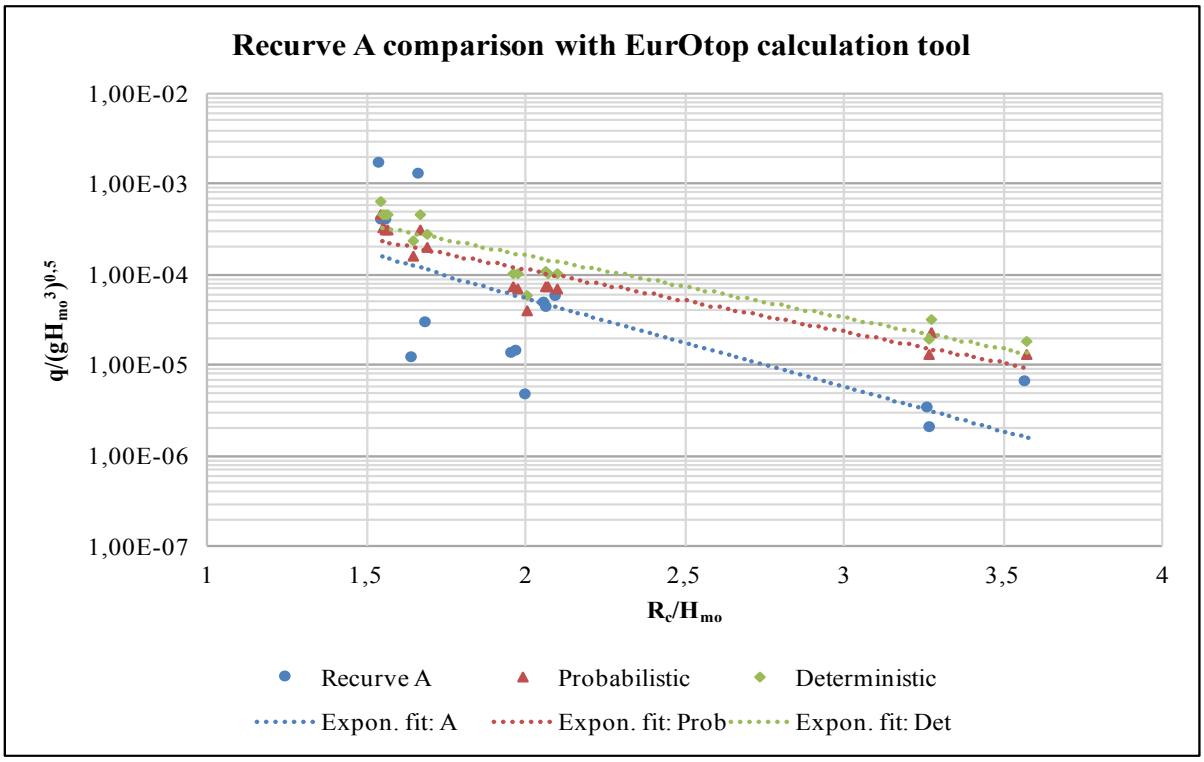

Figure 51: Recurve A comparison with EurOtop calculation tool

Significant scatter of only the measured results can be seen at R_c/H_{mo} = 1,6. This is due to the significant increase in overtopping discharge for wave periods above 8 seconds, as discussed in Section 5.2.4. This result makes it evident that the calculation tool is much less sensitive to changes in wave period than a physical model. The only instance where the physical model study produced larger overtopping results, compared to both the probabilistic and deterministic prediction methods, was at the lowest freeboard case of R_c/H_{mo} = 1,6 combined with wave periods exceeding 10 seconds.

As previously mentioned, the deterministic method used for predicting overtopping discharges produced a mean overtopping value plus one standard deviation, making it the more conservative method and better for design. The probabilistic method follows a mean value approach and does not include an additional standard deviation, making it more suitable for comparisons with measured results from physical model studies. It is for this reason that Figure 52 provides a comparison of overtopping results obtained from the physical model study with predictions from the calculation tool using the probabilistic method.

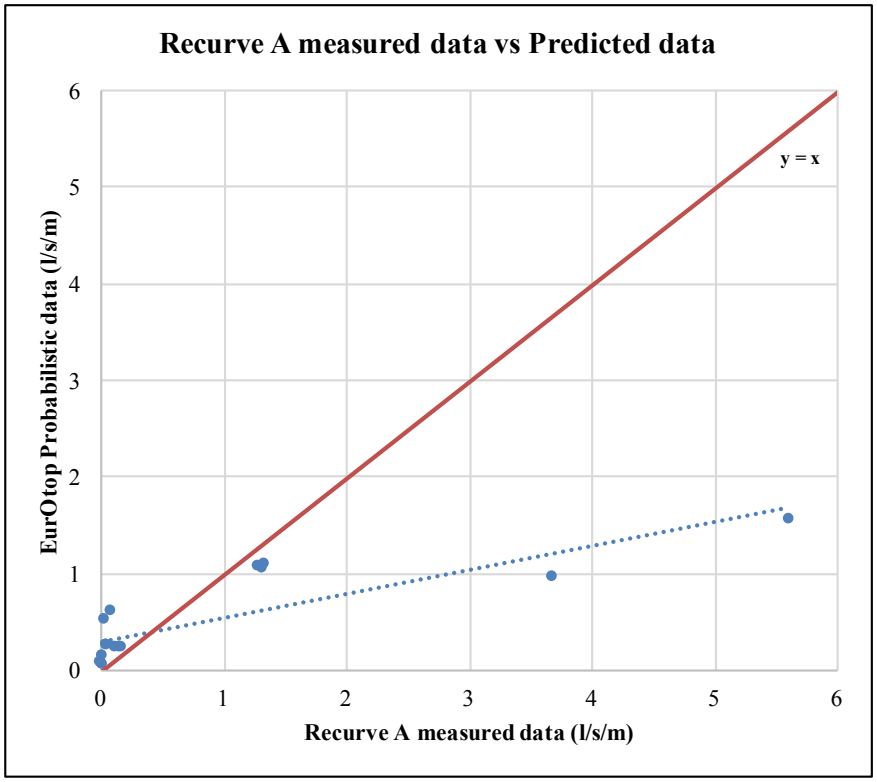

Figure 52: Recurve A measured data versus Predicted data

Figure 52 shows that for smaller overtopping rates due to shorter wave periods and relatively high freeboards, the measured and predicted overtopping values correlate seemingly well with

each other, although mostly over-predicted by the calculation tool, as can be seen by the cluster of data points around the x = y line for q < 1 l/s/m (q = measured discharge). However, for the lowest relative freeboard case with longer wave periods, where q > 3 l/s/m, two values are largely under-predicted by the online calculation tool. This indicates that the online calculation tool is inadequate for predicting comparable overtopping discharges for extreme low freeboard cases and longer wave periods, as is also evident when analysing the slope of the trend line which deviates strongly from the "perfect fit" x = y line due to the significantly higher overtopping values recorded in the study.

After comparing all the results obtained from both the measured and online prediction methods, it was found that the physical model results correlated relatively well with the predicted values only when $1.6 < R_c/H_{mo} < 2.4$ and with wave periods of 10 to 12 seconds. This implies that the online calculation tool does not provide an accurate prediction of comparable overtopping discharges for extreme low - and high freeboard cases and is inadequate in considering the effects of varying wave periods.

This finding is supported by one of the conclusions made in the study by Muller (2016), after observing significant scatter between measured and predicted overtopping discharges, stating that there are still some uncertainties in the formula applied in the EurOtop calculation tool. It should also be noted that the EurOtop tool does not incorporate a beach slope into its calculations and that the dimensions of the schematized seawall do not correspond perfectly with the recurve seawall used in this model study, possibly increasing the deviations from measured results. However, the lack of measured data points in this study due to very small or zero overtopping rates and incorrect wave input parameters must be taken into account, and that a more comprehensive set of comparable data in the future could improve the correlation between measured and predicted overtopping rates.

5.3.3 Schoonees (2014)

As previously mentioned, only the results obtained from Recurve A in this study are comparable with the results obtained in the study conducted by Schoonees (2014), which included an identical recurve shape with an overhang length of 1.2 m.

In an attempt to achieve similar and comparable results, the physical model setup in this study was based on the setup applied by Schoonees (2014), which was also applied by Swart (2016).

With identical seawall dimensions and water levels, the freeboards were also identical, as can be seen in Table 8, which provides a comparison of the physical model overtopping results obtained from Recurve A with those from Schoonees' (2014) 1.2 m recurve.

Table 8: Comparison of Recurve A model results with Schoonees (2014) 1.2 m recurve

Recurve A - 1.2 m overhang recurve						
Test		**A-13**	**A-23**	**A-33-2**	**A-43-3**	**A-53-2**
WL_{toe}	**m**	0.03	0.05	0.08	0.1	0.12
R_c	**m**	0.17	0.15	0.12	0.1	0.08
T_p	**s**	2.236	2.236	2.236	2.236	2.236
H_i	**m**	0.050	0.047	0.050	0.051	0.051
Overtopped Volume	**l**	0.00	0.00	0.00	1.11	33.00

Schoonees (2014) - 1.2 m overhang recurve						
Test		**C-5**	**C-4**	**C-(1-3) $_{Avg}$**	**C-(6-9) $_{Avg}$**	**C-(10-12) $_{Avg}$**
WL_{toe}	**m**	0.03	0.05	0.08	0.1	0.12
R_c	**m**	0.17	0.15	0.12	0.1	0.08
T_p	**s**	2.236	2.236	2.236	2.236	2.236
H_i	**m**	0.063	0.066	0.062	0.063	0.059
Overtopped Volume	**l**	0.00	1.22	2.23	26.16	153.30

It should be noted that only the 10 second wave period cases were compared, as this was the only wave period tested by Schoonees (2014) across the entire range of water levels.

It is clear from Table 8 that the overtopping volumes recorded in this study are significantly lower than those obtained in Schoonees's (2014) study. These large differences in overtopping would normally be attributed to various factors, namely, water level, crest level and wave height. However, as the water - and crest levels are identical in both studies, the overtopping differences are solely due to the differences in wave height.

This is clearly evident when analysing the incident wave heights, H_i, achieved by Schoonees (2014), which are significantly larger than the wave heights achieved in this study and the design wave height of 0.05 m. After careful analysis of the the input wave conditions used by Schoonees (2014), it was noted that no adjustment was made to the input wave height signal file to accommodate for the imperfect performance of active wave absorption by the wave maker. Therefore, it can be stated that the waves generated by Schoonees (2014) did not accurately simulate the chosen design wave height condition, and consequently produced different overtopping volumes.

The overtopping results of Recurve A in this study and the 1.2 m recurve tested by Schoonees (2014) are compared in Figure 53, which provides a plot of dimensionless overtopping discharge versus relative crest freeboard.

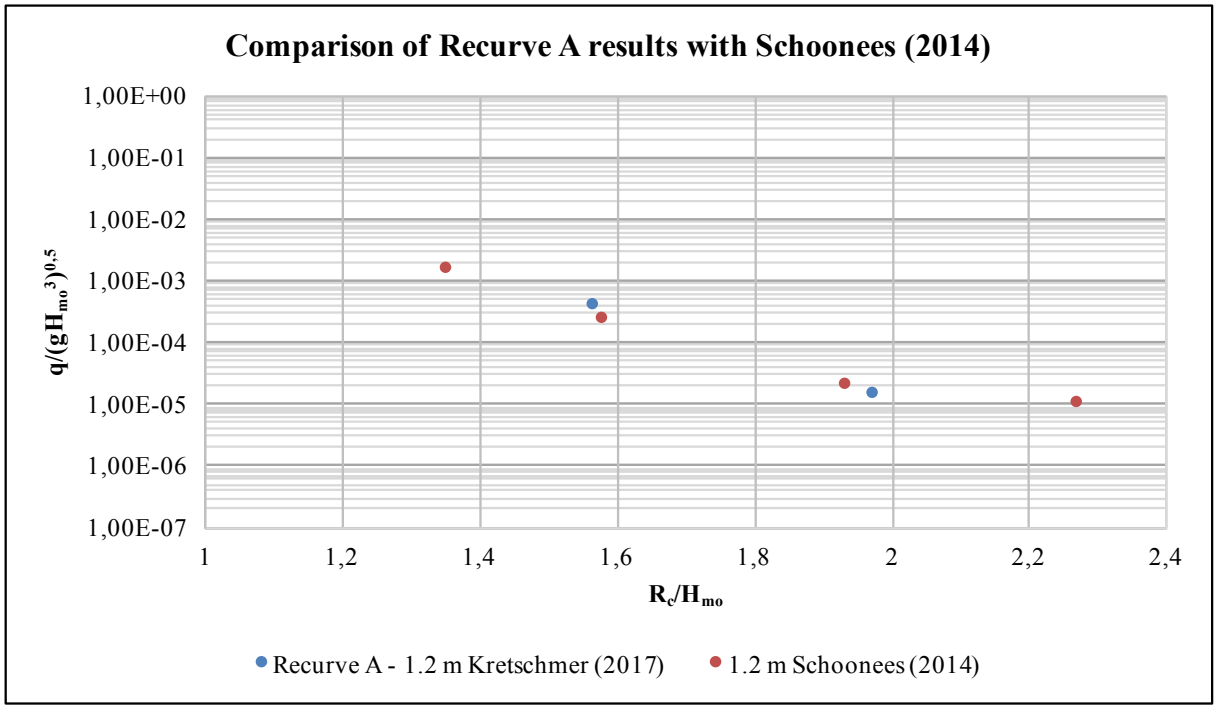

Figure 53: Comparison of Recurve A results with Schoonees (2014)

It should be noted that the results in Figure 53 resemble prototype values and that zero-overtopping results are not included, as these cannot be plotted on a semi-log graph. With this in mind, it can be noted that only two results from Recurve A are displayed, which, under identical input conditions, should have correlated with the two largest values recorded by Schoonees (2014), but which deviated significantly due to the influence of different wave heights.

It can be concluded that the results obtained by Schoonees (2014) do not correlate well with the results from this study, mainly due to the significant difference in generated wave heights which, as mentioned in Section 5.2.6, can have a strong influence on wave overtopping if not accurately adjusted to compensate for the imperfect functionality of active wave absorption by the wave maker.

5.3.4 Swart (2016)

In an attempt to achieve comparable results with previous studies, Swart (2016) also tested a recurve profile with an overhang length of 1.2 m, identical to one of the recurves tested by Schoonees (2014) and Recurve A tested in this study.

Table 9 provides a comparison of the physical model results (model values) of Recurve A obtained in this study with the results from Swart's (2016) 1.2 m overhang recurve.

Table 9: Comparison of Recurve A model results with Swart (2016) 1.2 m recurve

Recurve A - 1.2 m overhang recurve						
Test		**A-13**	**A-23**	**A-33-2**	**A-43-3**	**A-53-2**
WL_{toe}	**m**	0.03	0.05	0.08	0.1	0.12
R_c	**m**	0.17	0.15	0.12	0.1	0.08
T_p	**s**	2.236	2.236	2.236	2.236	2.236
H_i	**m**	0.050	0.047	0.050	0.051	0.051
Overtopped Volume	**l**	0.00	0.00	0.00	1.11	33.00
Swart (2016) - 1.2 m overhang recurve						
Test		**F-2**	**F-7**	**F-12**	**F-17-2**	**F-22**
WL_{toe}	**m**	0.03	0.05	0.08	0.1	0.12
R_c	**m**	0.175	0.155	0.125	0.105	0.085
T_p	**s**	2.236	2.236	2.236	2.236	2.236
H_i	**m**	0.048	0.051	0.054	0.056	0.056
Overtopped Volume	**l**	0.00	0.00	0.00	1.32	35.75

Although Swart's (2016) study included a wider range of wave periods than Schoonees's (2014) study, it was decided that for comparative purposes, Table 9 would only provide results from conditions similar to those compared in Table 8 in Section 5.3.3. A complete set of comparable results of Recurve A and the 1.2 m overhang recurve from Swart's (2016) study is provided in Figure 54.

Although the measured overtopping volumes from Recurve A in Table 9 correlate very well with the results from the 1.2 m overhang recurve from Swart (2016), some important aspects need to be considered. As previously mentioned in Section 5.3.3, the model setup of this study replicated that of the model used by Schoonees (2014) to achieve comparable results. The same was attempted by Swart (2016). However, due to uncontrollable circumstances during installation of the wall into the wave flume, Swart's (2016) vertical wall had a height of 0.205 m as opposed to the design height of 0.2 m, increasing the freeboard levels by 0.005 m as can

be seen in Table 9. By comparing the results from Recurve A with those from Swart's (2016) 1.2 m overhang recurve, it would be expected that the additional freeboard would result in less water overtopping the crest of the recurve wall. However, as can be seen in Table 9, the measured overtopping volumes at the two highest water levels correlated very well with each other, as the effect of the higher freeboard was counteracted by the higher incident wave heights achieved by Swart (2016). In these specific cases, it is interesting to note that the wave heights achieved by Swart (2016) were 0.005 m higher than those achieved in this study, which equal the difference in freeboard. However, this observation could have been purely coincidental and does not imply that the freeboard level has any significant influence on the incident wave height.

Figure 54 provides a plot of dimensionless overtopping discharge versus relative crest freeboard, comparing the results of Recurve A and the 1.2 m overhang recurve from Swart (2016). It should be noted that the results represent prototype values and that zero-overtopping values are not included, as these cannot be plotted on a semi-log graph.

The values plotted in Figure 54 represent results that were obtained from tests conducted at all five water levels and for a range of wave periods from 8 to 14 seconds only, as the 6 second wave period was not included in the study by Swart (2016).

The tests that were repeated for Recurve A are shown in Figure 54 as average values, in order to provide singular data points which are easier to compare with their corresponding results from Swart (2016) and so as to not influence the slope of the trend line.

When analysing the plotted results in Figure 54, the trend lines indicate that there is a significant deviation in results between the two recurves. However, it must be noted that the trend line of Recurve A from this study is strongly influenced by the presence of the data point at $R_c/H_{mo} > 3.0$, which corresponds to an 8 second wave period at the lowest water level tested. This result forms part of the overtopping values recorded due to colliding incident and reflected waves, a type of overtopping which seems to not have been recorded by Swart (2016). Therefore, it is expected that, without the presence of this data point, the trend lines would have possessed very similar slopes. It should be noted that this expectation was validated, as the removal of the data point in a simple graphical test did in fact result in very similar trend line slopes.

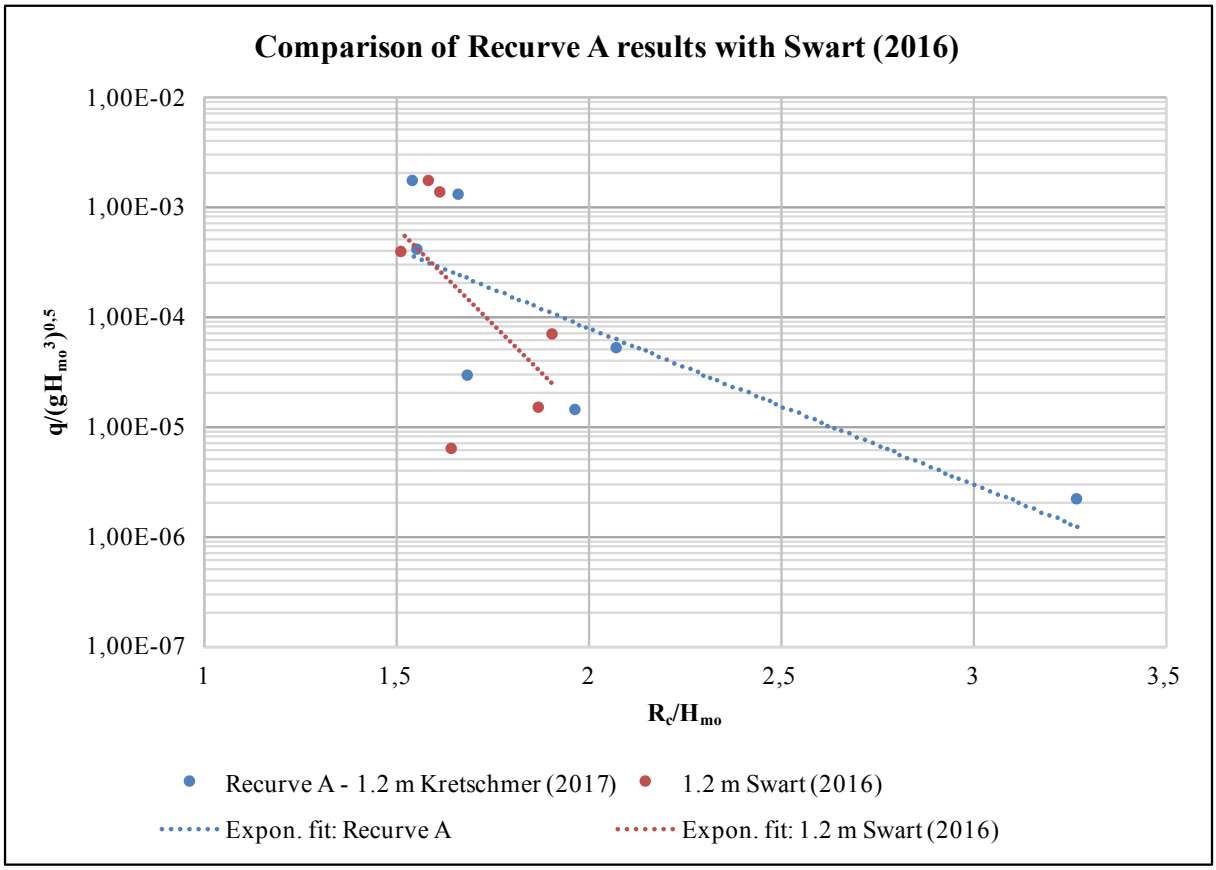

Figure 54: Comparison of Recurve A results with Swart (2016)

Overall, it can be observed from Figure 54 that the results from Recurve A correlate very well with those from the 1.2 m overhang recurve from Swart (2016), with some scatter in values along the x-axis being attributed to the difference in freeboard between the two recurve walls.

5.4 Repeatability and accuracy of tests performed

In order to ensure that the results obtained were reliable and could safely be used for comparison by future studies, test results needed to be as accurate as possible. The accuracy of test results was improved by repeating certain test conditions and evaluating the variability of the results by calculating the coefficient of variation (CoV).

In addition, before recurves with unknown overtopping reduction capabilities were tested, the accuracy of the test procedure followed was first optimised by replicating a recurve profile tested by Schoonees (2014) and Swart (2016). Combined with identical test conditions, the results of this recurve, Recurve A, were compared with those obtained by Schoonees (2014) and Swart (2016), which validated the test execution followed in this study.

The coefficient of variation of the repeated tests was calculated with the following equation:

$$CoV\ (\%) = \frac{\sigma}{\mu} \times 100$$

Where:

σ - Standard deviation of prototype overtopping rates

μ - Average of the prototype overtopping rates

The CoV was determined for two different test conditions, which were repeated three times. The first test repeated was at the 2.0 m water level with a 12 second wave period, provided in Table 10. The second repeated test condition was at the deepest water level of 2.4 m with a 10 second wave period, provided in Table 11.

The coefficients of variation of the two repeated test conditions were 12.49% and 1.91%. The reason for the high CoV of 12.49% can be attributed to the sensitivity of coefficient of variation at low overtopping rates. As the overtopping rate decreases, the effect of differences in overtopping on the CoV increases. This same trend in coefficient of variation was found by Schoonees (2014), where repeated test conditions with low overtopping rates produced CoV values of up to 38.16%.

Table 10: Accuracy of tests evaluated by CoV (Recurve A; WL_{toe} = 2 m; T_p = 12 s)

Accuracy of tests evaluated by CoV (WLtoe = 2 m; Tp = 12 s)					
Model Values	Test		A-44-2	A-44-3	A-44-4
	WL_{toe}	m	0.1	0.1	0.1
	R_c	m	0.1	0.1	0.1
	T_p	s	2.683	2.683	2.683
	Test duration	s	2683	2683	2683
	H_{mo} Avg	mm	62.29	62.48	61.53
	H_i	mm	48.26	48.41	47.65
	Overtopped Volume	l	3.89	4.44	5.00
Prototype Values	WL_{toe}	m	2.0	2.0	2.0
	R_c	m	2.0	2.0	2.0
	T_p	s	12	12	12
	H_{mo} Avg	m	1.25	1.25	1.23
	H_i	m	0.97	0.97	0.95
	Overtopped Volume	l	31111	35556	40000
	Overtopping rate	l/s/m	0.13	0.15	0.17
	CoV	%	12.49		

Table 11: Accuracy of tests evaluated by CoV (Recurve A; WL_{toe} = 2.4 m; T_p = 10 s)

Accuracy of tests evaluated by CoV (WLtoe = 2.4 m; Tp = 10 s)					
Model Value	Test		A-53-2	A-53-3	A-53-4
	WL_{toe}	m	0.12	0.12	0.12
	R_c	m	0.08	0.08	0.08
	T_p	s	2.236	2.236	2.236
	Test duration	s	2236	2236	2236
	H_{mo} Avg	mm	65.96	66.50	66.24
	H_i	mm	51.05	51.42	51.22
	Overtopped Volume	l	33.00	33.50	32.25
Prototype Values	WL_{toe}	m	2.4	2.4	2.4
	R_c	m	1.6	1.6	1.6
	T_p	s	10	10	10
	H_{mo} Avg	m	1.32	1.33	1.32
	H_i	m	1.02	1.03	1.02
	Overtopped Volume	l	264000	268000	258000
	Overtopping rate	l/s/m	1.32	1.34	1.29
	CoV	%	1.91		

According to De Rouck et al. (2005), during the CLASH project overtopping rates when repeating tests differed by up to 12%. In addition, the EurOtop Manual (EurOtop, 2007) states that test repetitions during the CLASH project showed CoV values from two wave flumes of 10% and 13%. It must be kept in mind that the CLASH project included over 10 000 overtopping tests. Therefore, considering the amount of test repetitions carried out in the present study, it can be concluded that the coefficients of variation obtained in this study are acceptable.

As an additional validation of accuracy, the final and most significant overtopping event for each recurve was repeated. The results of these repetitions are provided in Table 12, for Recurves B to E. No repetition for Recurve A under this condition was conducted due to the measure of accuracy obtained with the CoV provided in Tables 10 and 11.

As can be seen in Table 12, the overtopping volumes obtained from the repeated tests of each recurve correlate very well with their initial results, indicating a high level of accuracy among tests performed for the critical condition of highest water level and longest wave period.

Table 12: Repeatability of most significant overtopping events of Recurves B - E (model values)

Repeatability of most significant overtopping events of Recurves B - E (model values)									
Recurve		**B**		**C**		**D**		**E**	
Test		**B-55**	**B-55-2**	**C-55**	**C-55-2**	**D-55**	**D-55-2**	**E-55**	**E-55-2**
WL_{toe}	**m**	0.12	0.12	0.12	0.12	0.12	0.12	0.12	0.12
R_c	**m**	0.08	0.08	0.08	0.08	0.08	0.08	0.08	0.08
T_p	**s**	3.13	3.13	3.13	3.13	3.13	3.13	3.13	3.13
$H_{mo\ Avg}$	**mm**	63.00	63.48	64.00	63.49	64.21	64.90	66.82	66.65
H_i	**mm**	48.10	48.49	49.34	48.95	49.16	49.72	51.70	51.57
Volume	**l**	**116.07**	**114.89**	**223.07**	**228.67**	**162.34**	**170.52**	**148.17**	**149.21**

5.5 Additional aspects to consider

When deciding on the appropriate type of recurve seawall for a project, certain factors are required to first be taken into account. Some of these factors are discussed in this section, namely, safety limitations related to allowable overtopping rates, as well as constructability and feasibility of a recurve seawall.

5.5.1 Safety limitations related to allowable overtopping rates

In order to provide a safety evaluation of the recurves tested in this study in terms of their overtopping reduction capabilities, the most critical overtopping rates at each water level of all the recurves are provided in Table 13 and compared with the allowable mean overtopping discharges provided in Table 1. The values provided in Table 13 represent prototype values.

Table 13: Summary of critical overtopping rates of each recurve

Recurve A	**Test**		**A-15**	**A-25**	**A-35**	**A-45**	**A-55**
	WL_{toe}	**m**	0.6	1.0	1.6	2.0	2.4
	R_c	**m**	3.4	3.0	2.4	2.0	1.6
	T_p	**s**	14	14	14	14	14
	H_i	**m**	1.00	0.92	1.21	1.27	1.03
	Overtopped Volume	**l**	0.00	0.00	110000	1072640	1571360
	Overtopping rate	**l/s/m**	0.00	0.00	0.39	3.83	5.61
Recurve B	**Test**		**B-15**	**B-25**	**B-35**	**B-45-2**	**B-55-2**
	WL_{toe}	**m**	0.6	1.0	1.6	2.0	2.4
	R_c	**m**	3.4	3.0	2.4	2.0	1.6
	T_p	**s**	14	14	14	14	14
	H_i	**m**	1.02	0.93	0.95	0.96	0.97
	Overtopped Volume	**l**	1111	0.00	2222	51112	919096
	Overtopping rate	**l/s/m**	0.004	0.00	0.01	0.18	3.28
Recurve C	**Test**		**C-15**	**C-25**	**C-35**	**C-45**	**C-55**
	WL_{toe}	**m**	0.6	1.0	1.6	2.0	2.4
	R_c	**m**	3.4	3.0	2.4	2.0	1.6
	T_p	**s**	14	14	14	14	14
	H_i	**m**	0.98	0.90	0.98	0.99	0.99
	Overtopped Volume	**l**	0.00	0.00	75520	546640	1784560
	Overtopping rate	**l/s/m**	0.00	0.00	0.27	1.95	6.37
Recurve D	**Test**		**D-15**	**D-25**	**D-35**	**D-45**	**D-55-2**
	WL_{toe}	**m**	0.6	1.0	1.6	2.0	2.4
	R_c	**m**	3.4	3.0	2.4	2.0	1.6
	T_p	**s**	14	14	14	14	14
	H_i	**m**	0.99	0.91	0.96	1.00	0.99
	Overtopped Volume	**l**	0.00	6667	28889	151120	1364160
	Overtopping rate	**l/s/m**	0.00	0.02	0.10	0.54	4.87
Recurve E	**Test**		**E-15**	**E-25**	**E-35**	**E-45**	**E-55-2**
	WL_{toe}	**m**	0.6	1.0	1.6	2.0	2.4
	R_c	**m**	3.4	3.0	2.4	2.0	1.6
	T_p	**s**	14	14	14	14	14
	H_i	**m**	0.99	0.92	0.98	1.01	1.03
	Overtopped Volume	**l**	1111	0.00	4444	105000	1193680
	Overtopping rate	**l/s/m**	0.004	0.00	0.02	0.38	4.26

Recurve A

The performance of Recurve A in reducing overtopping would lead to some unsafe conditions for pedestrians, vehicles and buildings. It should be noted that Tests A-35 and A-45 were conducted with incorrect wave height conditions as can be seen in Table 13, but are still considered in this analysis for the sake of completeness. The conditions of Tests A-15 and A-25 will be safe for even unaware pedestrians, with no clear view of the sea. However, it would become unsafe for both unaware and aware pedestrians behind the seawall during the conditions of Tests A-35 to A-55. Overtopping conditions at the two deepest water levels of Tests A-45 and A-55 will only still be safe enough for trained staff, provided there are only low level overtopping flows and no falling jets of water.

Relating to the safety of vehicles driving behind the seawall, the conditions of only Tests A-15 and A-25 would be safe for driving at moderate or high speeds with impulsive overtopping. The remaining Tests A-35 to A-55 would provide conditions safe for driving only at low speeds with overtopping by pulsating flows at low flow depths.

Only conditions of Tests A-15 and A-25 would cause no damage whatsoever to buildings, whereas the remaining deeper water level test conditions would cause structural damage to buildings and infrastructure.

Recurve B

By analysing the overtopping results obtained, Recurve B proves to create the safest conditions behind the seawall. Tests B-15 to B-35 would provide safe conditions for unaware pedestrians behind the seawall. It would only become unsafe for both unaware and aware pedestrians under the conditions of Test B-45-2 at the second deepest water level. All the test conditions are well within the safety limitations for trained, well protected staff.

Vehicles can safely drive at moderate to high speeds under conditions from Tests B-15 to B-35. However, to ensure safe driving, speeds should be lowered under conditions from Test B-45-2.

For buildings, minor damage to fittings would occur under conditions of Test B-35 with structural damage taking place under conditions from Tests B-45-2 to B-55-2.

Recurve C

The safety evaluation of Recurve C is similar to that of Recurve A, with safe conditions for unaware pedestrians only during Tests C-15 and C-25 and unsafe conditions for both unaware and aware pedestrians from Test C-35 to C-55. Although Recurve C produced the largest overtopping rate compared to all the other recurves, during Test C-55, this condition would still be safe for trained staff to walk behind the seawall.

Vehicles could only drive safely behind the wall at moderate or high speeds during conditions of Tests C-15 and C-25. Under conditions of Tests C-35 to C-55, it would only be safe to drive at low speeds.

No damage to buildings will occur under conditions of Tests C-15 and C-25, although structural damage could take place under conditions from Tests C-35 to C-55.

Recurve D

Only Test D-15 would provide absolutely safe conditions for unaware pedestrians, with caution required during conditions of Test D-25 due to increased overtopping rates from adhesion overtopping around the bullnose overhang edge of Recurve D. Conditions from Test D-35 would start to become unsafe for aware pedestrians with a clear view of the sea and only trained staff would be safe under conditions of Tests D-45 to D-55-2.

Conditions under Tests D-15 and D-25 would be safe for vehicles to drive at moderate or high speeds, but low speeds are required to ensure safe driving while under overtopping conditions from Tests D-35 to D-55-2.

No damage to buildings or infrastructure will occur under conditions of Test D-15, but minor damage to fittings would occur during conditions of Test D-25 and structural damage would take place under conditions from Tests D-35 to D-55-2.

Recurve E

The performance of Recurve E provides similar safety standards to that of Recurve B. It would be deemed safe for unaware pedestrians who are easily upset or frightened to walk behind a recurve seawall under overtopping conditions from Tests E-15 to E-35. Only trained staff who

are well shod and protected can safely walk behind a seawall under conditions of Tests E-45 and E-55-2.

As for vehicles, moderate or high driving speeds would only be safe under conditions from Tests E-15 to E-35, provided there are no falling or high velocity water jets from impulsive overtopping. All the test conditions of Recurve E provide for safe driving at low speeds with overtopping by pulsating flows at low flow depths only and no falling water jets.

Only conditions under Test E-25 would cause no damage to buildings, with some minor damage to fittings taking place under conditions of Tests E-15 and E-35. Overtopping rates under conditions of Tests E-45 and E-55-2 could potentially cause structural damage to buildings.

5.5.2 Constructability and feasibility of a recurve seawall

After having determined the most effective recurve shape in reducing overtopping of a recurve seawall, the ease of constructing that specific recurve shape needs to be considered. When comparing the designs of Recurves, A and B, it can be assumed that the straight parapet shape of Recurve A would be easier to construct than the concave profile of Recurve B. However, once a template or formwork mould has been constructed, any shape of recurve can theoretically be produced.

When considering a cost analysis of a recurve seawall, the two most important variables that need to be taken into account are the capital expenditure (Capex) and operating expenses (Opex). The capital expenditure is based on the construction costs required to build the seawall. The operating expenses or maintenance costs are related to repairing damage to the structure due to storms occurring throughout it's lifetime. Although capital costs traditionally outweigh maintenance costs, it must be noted that maintenance costs can become a serious financial burden if the construction is not carefully executed according to design, which could lead to structural instability or premature failure.

As the construction costs of different recurves become invariable due to the use of templates, the maintenance costs will become the determining factor in the decision making process. If the two most effective recurves in reducing overtopping are to be compared, Recurves B and E, based upon their relative maintenance costs, it is expected that Recurve B would provide a

more cost-effective solution. This opinion is based on the assumption that wave forces against the slanted face of Recurve E will be larger, compared to Recurve B, due to the angular intersection between the vertical wall and the recurve face, whereas Recurve B allows for a smooth transition of water travelling across from the vertical wall to the recurve face. These additional wave forces can be expected to cause more damage to Recurve E over time and consequently lead to higher maintenance costs.

In addition to capital and maintenance costs relating to the recurve seawall, potential indirect costs should also be considered. These indirect costs are associated with damages to structures/vehicles or injuries to pedestrians behind the seawall resulting from high overtopping rates.

Chapter 6: Summary and Conclusions

6.1 General

As coastal areas around the world are experiencing a rise in sea level due to global warming, coastal developments and people residing along coastlines are being placed at risk. This has led to an increase in the demand for more effective coastal defence structures.

Impermeable vertical seawalls are traditionally used to protect the coastline from wave attack and flooding. However, the crest levels of seawalls are quite often required to be constructed very high to ensure protection against wave attack, leading to an obstruction of the sea view. Recurve seawalls can provide the same amount of overtopping reduction as a vertical wall, but with a lower crest level. Although recurve seawalls have proven to be very effective in their purpose, very limited research and guidelines on the design of recurve seawalls exists.

The objective of this project was to determine the effectiveness of the form of the overhang of a recurve seawall on reducing overtopping. To achieve this objective, this study included the execution of over 147 physical model tests on wave overtopping with varying water depths and wave periods for five different recurve forms to determine the effect of the form of a recurve on reducing overtopping of a recurve seawall.

As this study is the first of its kind in terms of its extensive variety of recurve forms tested, the findings from this study greatly contributed to the understanding and behaviour of wave overtopping of recurve seawalls with varying overhang forms.

6.2 Findings from the literature review

The literature review investigated the findings of studies on wave overtopping of recurve seawalls by researchers such as Kortenhaus et al. (2003) and Pearson et al. (2004), who contributed to the drawing up of the EurOtop Manual. In addition, reviews of more recent studies on the functionality of recurve seawalls by Schoonees (2014) and Swart (2016) were conducted.

The literature review conducted in this study concluded that numerous aspects of recurve seawalls have been researched to provide a preliminary understanding and basis for the selection of recurve seawalls as effective coastal defence structures. However, the mechanisms

describing the effectiveness of varying recurve shapes in reducing overtopping are not yet fully described and limited guidance exists on the design of more effective recurve seawalls.

Therefore, this physical model study was conducted to provide an extensive database and understanding on the effects that different recurve shapes have on reducing wave overtopping.

6.3 Findings from physical model tests

6.3.1 General

This study found that overtopping of recurve seawalls is influenced by various parameters, including the overhang shape of the recurve. The effect of these parameters on wave overtopping are concluded in Sub-sections 6.3.2 to 6.3.8, below.

6.3.2 Comparison of overall test results

An analysis of all the physical model results obtained, illustrated in Figure 39, indicated that the recurve with the convex-shaped overhang form, Recurve C, provided the least reduction in overtopping, when compared with the performances of the remaining recurves. As demonstrated in Figure 39, the majority of the recurves produced similar overtopping rates for the highest freeboard case, due to the influence of overtopping from colliding incident and reflected waves at low water levels in front of the structure.

The concave-shaped overhang of Recurve B proved to be the most effective overhang shape in reducing overtopping, with Recurve E, which had a design based on the combination of Recurves A and B, producing the second-highest reduction in overtopping. This finding is also evident from the lack of data points of Recurves B and E in Figure 39, which implies that they produced the largest amount of zero-overtopping results, as only positive overtopping values can be displayed on a semi-log graph.

6.3.3 Influence of wave return angle

The wave return angle was defined as the angle at which a reflected jet of water would leave the surface of the overhang form, which, as the designs were irregular in shape, did not correspond to the recurve angle of a typical parapet recurve wall.

Although all the recurves possessed identical overhang lengths, each recurve displayed a particular wave return angle due to its unique design. It was found that increasing the wave return angle generally decreased the reduction in overtopping, as demonstrated in Figure 41. A contradicting instance was observed with Recurve D, which possessed an identical wave return angle to that of the most effective overhang, Recurve B, yet still produced around fifty percent more overtopping than Recurve B. It was found that the poor performance of Recurve D was related to the effect of its rounded overhang edge on overtopping, as discussed in Section 5.2.7.

6.3.4 Influence of wave period

In addition to determining the influence of wave period on overtopping, this study also tested the finding of a previous study by Roux (2013), which concluded that increasing the wave period leads to an increase in overtopping up to 12 seconds, after which point a reduction in overtopping takes place.

The results from the present study clearly indicated that increasing the wave period, up to 14 seconds, leads to an increase in wave overtopping of a recurve seawall, as demonstrated in Figure 43. Although short period waves of 6 seconds lie outside the swell wave spectrum along the South African coastline, it was still included in this study. Negligibly small overtopping rates were obtained for the 6 second wave period, although this should not be disregarded as these waves generally originate from wind waves, which when combined with an onshore wind, could increase the amount of splash overtopping from colliding incident and reflected waves in front of the wall.

6.3.5 Influence of water depth

As the amount of freeboard and water depth at the base of the structure are among the most influential parameters on wave overtopping, the results indicated that increasing the water depth (which decreases the freeboard) leads to an increase in overtopping, as illustrated in Figure 44. For most of the recurves, a gradual increase in overtopping occurred at water depths increasing from 0.6 m to 2.0 m. However, the results indicated a significant increase in overtopping rate at an increase in water depth from 2.0 m to 2.4 m. This significant increase in overtopping was due to the recurve wall becoming submerged by incident waves much more regularly, greatly reducing the reflective capabilities of the recurve and allowing large amounts of green water to breach the crest of the structure. This finding led to the conclusion that caution should be taken when designing the crest level of a recurve seawall.

6.3.6 Influence of wave height

During the study, it was found that in order to achieve the design incident wave height, numerous adjustments to the input wave height were required due to the imperfect performance of active wave absorption by the wave paddle. This finding led to the conclusion that the input wave height can have a significant influence on overtopping results if not accurately adjusted to account for the limitations of the active wave absorption system.

It was also found that even after the correct input wave height was specified, tests of different recurve shapes performed under identical conditions still produced small differences in incident wave heights with large differences in overtopping. However, it was proven that these small differences in incident wave height have a negligible effect on overtopping and that it is in fact the shape of the recurve that has the largest influence on overtopping.

6.3.7 Influence of squared versus rounded overhang edge

As the design of Recurve D was identical to the design of Recurve B, with the addition of a rounded instead of a squared overhang edge, the performances of these two recurves in reducing overtopping were expected to be similar. However, it is postulated that, due to the combination of the strong adhesive forces of water and the rounded edge of the overhang, water travelling along the face of the recurve would remain adhered to the surface and, with sufficient energy, traverse around and over the crest. This type of adhesion overtopping is illustrated in Figure 47. This phenomenon led to an increase in overtopping of Recurve D, relative to Recurve B, by a factor of up to 1.49, as can be seen in Figure 40.

Overtopping in this sense increased primarily with a decrease in freeboard and increase in wave period, possibly due to more waves striking the structure providing sufficient energy for the water to remain adhered to the surface and travel around the overhang edge.

6.3.8 Influence of incident and reflected wave collisions

As previously concluded in this study, increasing the wave period leads to an increase in overtopping. However, this finding was contradicted during tests with short period waves at the two lowest water levels. It was found that as the short period waves were successfully reflected from the wall, they would collide with closely following incident waves and generate a fair

amount of splash. As these collisions occurred very close to the wall, due to the short wavelengths, the splash would breach the crest of the wall, as demonstrated in Figure 49.

In conclusion, it was found that the functionality of the recurve became negligible for short period waves in shallow water depths as overtopping would take place in the form of splash from colliding incident and reflected waves, amplified by depth-induced wave breaking, in front of the structure.

6.4 Comparison with EurOtop calculation tool and previous studies

6.4.1 General

The results from this physical model study were compared with overtopping predictions of recurve walls calculated with the EurOtop online calculation tool as well as with the measured results obtained by previous researchers, such as Schoonees (2014) and Swart (2016). It should be noted that only the results obtained from Recurve A in this study were used for comparison, as discussed in Section 5.3.1. The findings of these comparisons are concluded in Sub-sections 6.4.2 to 6.4.4, below.

6.4.2 EurOtop online calculation tool

The measured overtopping results from this study were compared with the predicted results obtained from using both the probabilistic (mean value approach) and deterministic (design approach) methods of the EurOtop online calculation tool, as illustrated in Figure 51. The calculation tool slightly over-predicted results at high freeboard cases. However, at the lowest freeboard case with longer wave periods (the most important cases) the measured results were much higher than the predicted results, as demonstrated in Figure 52.

It can therefore be concluded that the calculation tool is inadequate in predicting reliable overtopping discharges at extreme low – and high freeboards and is less sensitive to changes in wave period than a physical model.

6.4.3 Schoonees (2014)

The physical model setup used in this study was identical to the setup used by Schoonees (2014). Therefore, variables such as freeboard and water level were identical, providing the possibility of comparing overtopping results under the exact same conditions. However,

comparison of the results indicated that the measured overtopping results from this study were significantly lower than the results obtained by Schoonees (2014), as indicated in Table 8.

It was found that the significant difference in overtopping was due to the difference in wave height, as no adjustment to the input wave height was made by Schoonees (2014) to account for the imperfect performance of active wave absorption by the wave paddle, leading to increased incident wave heights.

In conclusion, it can be stated that, although the physical model setup of this study was based on that of Schoonees (2014), the results obtained from this study do not correlate well with the results obtained by Schoonees (2014) as the wave heights produced by Schoonees (2014) did not accurately simulate the chosen design wave height.

6.4.4 Swart (2016)

The dataset obtained from the study by Swart (2016) was intended to expand on the research by Schoonees (2014). Therefore, the conditions of the physical model setup used by Swart (2016) were identical to those used by Schoonees (2014) and in turn identical to those used in this study. However, it should be noted that due to uncontrollable circumstances during installation of the vertical wall into the wave flume, Swart's (2016) wall resulted in a height of 0.205 m, compared to the designed 0.2 m, adding 0.005 m of freeboard. Despite this difference in freeboard, comparison of the results from this study with those from Swart (2016) correlated very well with each other, as discussed in Section 5.3.4 and illustrated in Figure 54.

The close correlation between results of Recurve A in this study and the results from the 1.2 m overhang profile tested by Swart (2016) validated the test execution followed throughout this physical model study. Therefore, it can be concluded that the test results obtained from this study provide an accurate and reliable dataset that offers an advanced understanding on the behaviour and effects of the form of the overhang on reducing wave overtopping.

6.5 Main Conclusions

The findings from this physical model study clearly indicated that the shape of the overhang has a strong influence on the overtopping reduction capabilities of a recurve seawall. Of all the different recurve shapes tested, it was found that the concave-shaped, Recurve B, with a squared overhanging edge offered the highest reduction in overtopping. The least effective shape in reducing overtopping was found to be the convex-shaped, Recurve C, which produced up to two times more overtopping than Recurve B. In cases with high freeboards, small amounts of overtopping were observed as a result of collisions between incident and reflected waves in the close proximity of the recurve seawall. These overtopping events consisted of white water spray which, although negligibly small, should be treated with caution as the presence of an onshore wind, which was not modelled in this study, could have a significant influence on the amount of overtopping.

It was also concluded that overtopping generally increases when increasing the wave return angle of the recurve. When analysing the performances of the two different concave recurves tested, the recurve with the rounded overhanging edge produced up to 50% more overtopping, due to the adhesion of water along the rounded edge. This finding led to the conclusion that the shape of the overhanging edge is an important parameter in the reduction of overtopping. As opposed to the findings of a previous study (Roux, 2013), the results from this study showed that increasing the wave period, up to 14 seconds, consistently led to an increase in overtopping.

Chapter 7: Recommendations

7.1 General

The aim of this project was to determine the effect that different overhang forms of recurves have on reducing wave overtopping. Although the model results obtained from this study provide a very good indication of the performance of recurve overhang forms on reducing overtopping, additional investigations on wave overtopping of recurve seawalls should be conducted to further improve on the findings of this study.

This section provides discussions on the recommendations formulated after concluding the findings from this study.

7.2 Recommendations for further studies

The findings from this study indicated that the concave-shaped recurve with a square overhang edge provided the largest reduction in overtopping, when compared with the performances of the other recurve forms tested. To further improve on this finding, it is recommended that further tests should be conducted on concave-shaped recurve forms, including variations in the vertical dimension or height of the recurve.

When recurve seawall units are cast, the overhang edges are typically slightly chamfered and not perfectly square. Therefore, it is recommended that future studies on concave-shaped recurves should include and evaluate the effect of chamfered overhang edges to provide a more accurate simulation of recurve seawalls as configured in practice.

Although the wave height in this study represented a constant variable, certain conditions required adjustments to the input wave height in order to achieve the design wave. In addition, small differences in wave heights and overtopping rates were observed under identical input conditions. Therefore, it is recommended that further tests be conducted on the effects of wave height on wave overtopping of a recurve seawall.

As the beach slope remained unchanged in this project, its influence on wave overtopping of a recurve seawall could not be established. It is for this reason, that further tests on wave overtopping of recurve seawalls with varying beach slopes should be carried out.

It was initially assumed that the concave-shaped recurve with the rounded overhang edge would perform similarly to the first concave recurve tested. However, due to adhesion of water along the rounded overhang edge, this recurve produced up to fifty percent more overtopping than its squared overhang counterpart. In addition, the largest overtopping events (green water overtopping) occurred during conditions of very low freeboard levels. In these instances, the incident wave would submerge the structure, rendering the recurve ineffective in its purpose of reflecting wave energy. A possible solution to overcoming the effect of adhesion overtopping as well as green water overtopping (to an extent) would be to incorporate a square berm on top of the overhang edge of the recurve. It is therefore recommended that future studies investigate the effect that an additional berm on top of a recurve can have on reducing wave overtopping. It should be noted that such an additional berm would however defeat to some degree the big advantage of reducing the visual impact by effectively increasing the seawall height. However, it should also be kept in mind that such a berm could offer other advantages, such as potentially acting as a safety barrier for pedestrians.

As the concave-shaped recurve provided the highest reduction in overtopping, it also reflected the largest amount of wave energy. It was observed that these large amounts of wave energy often exerted substantial hydraulic forces on the recurve, which threatened the stability of the structure. In addition, it can be assumed that these substantial forces would also probably increase scouring of the beach, effectively increasing the water depth and incident wave heights, which could possibly lead to larger overtopping rates. Therefore, it is recommended that a study should be conducted on the forces that are exerted on recurve seawalls as well as on the amount of beach scouring due to these forces by incorporating a movable bed in a physical model.

References

CIRIA, CUR, CETMEF (2007). *The Rock Manual. The use of rock in hydraulic engineering (2nd edition)*. C683, CIRIA, London

CMA (Concrete Manufacturers Association), 2012. SustainableCitiesCollective. [Online] Available at: http://www.sustainablecitiescollective.com/futurecapetown/247166/what-future-sea-point-promenade [Accessed 9 September 2016]

Cox, N., 2008. Exmouth: The sea defence wall. Geograph. [Online] Available at: http://www.geograph.org.uk/photo/999039 [Accessed 6 September 2016]

De Rouck, J., Geeaerts, J., Troch, P., Kortenhaus, A., Pullen, T., Franco, L., 2005. New results on scale effects for wave overtopping at coastal structures. Proceedings of ICE05 Coastlines, Structures and Breakwaters 2005. p. 29-43. Available at: http://hdl.handle.net/1854/LU-335341

De Rouck, J., Verhaeghe, H. & Geeraerts, J., 2009. Crest level assessment of coastal structures - General overview. Coastal Engineering, 56(2), pp.99–107. Available at: http://dx.doi.org/10.1016/j.coastaleng.2008.03.014.

EurOtop, 2007. *Wave Overtopping of Sea Defences and Related Structures : Assessment Manual*., (August). [Online] Available at: http://www.overtopping-manual.com. [Accessed 7 September 2016]

Grainger, K., 2009. The sea wall, Burnham-on-Sea. Geograph. [Online] Available at: http://www.geograph.org.uk/photo/1510021 [Accessed 8 September 2016]

Hawaii Real Estate, n.d. Sturdy Concrete Sea Wall. Hawaii Oceanfront. [Online] Available at: http://www.drhank.com/kona/ [Accessed 9 September 2016]

HR Wallingford, n.d. EurOtop online calculation tool. Wave Overtopping. [Online]
Available at: http://www.overtopping-manual.com
[Accessed 9 October 2016]

Hudson, R.Y. et al., (1979) *Coastal Hydraulic Models*, SR-5, May.
Fort Belvoir, VA: U.S. Coastal Engineering Research Centre

Hughes, S.A., 1993. *Physical Models and Laboratory techniques in coastal engineering*, Singapore: World Scientific Publishing

Kobelco, 2012. Flaring seawall at Kunigami, Okinawa. [Online]
Available at:
http://www.kobelco.co.jp/english/about_kobelco/csr/environment/2012/03.html
[Accessed 9 September 2016]

Kortenhaus, A., Pearson, J., Bruce, T., Allsop, N. W .H. & van der Meer, J. W., 2003. *Influence of parapets and recurves on wave overtopping and wave loading of complex vertical walls*, Netherlands: Infram publication no. 17.

Mansard, E.P. & Funke, E.R. 1980. *The measurement of incident and reflected spectra using a least squares method*, Sydney. Proc. of 17th ICCE, pp. 154-172.

McAuley, C., 2015. Sea Defence Wall. Geograph. [Online]
Available at: http://www.geograph.org.uk/photo/4474827
[Accessed 9 September 2016]

Muller, G.V., 2016. MEng Thesis: *An appropriate size of toe rock for vertical seawalls*, Stellenbosch: University of Stellenbosch

Owen, M.W. & Steele, A.A.J., 1991. *Effectiveness of recurved wave return walls*, Wallingford. Report SR 261: HR Wallingford

Pearson, J., Bruce, T., Allsop, N. W. and Gironella, X., 2002. *Violent Wave Overtopping-Measurements at large and small scale*. Cardiff, Proc. of 28th ICCE, pp. 2227-2238.

Pearson, J., Bruce, T., Allsop, N. W. H., Kortenhaus, A. & van der Meer, J. W., 2004. *Effectiveness of recurve walls in reducing wave overtopping on seawalls and breakwaters*, Netherlands: Infram publication no.21.

Reis, M.T., Neves, M.G. & Hedges, T., 2008. *Investigating the Lengths of Scale Model Tests to Determine Mean Wave Overtopping Discharges*. Coastal Engineering Journal, 50(4), pp.441–462.
Available at: http://www.worldscientific.com/doi/abs/10.1142/S057856340800182X.

Rossouw, J., 1989. PhD Thesis: *Design waves for the South African Coastline*, Stellenbosch: University of Stellenbosch

Roux, G.B., 2013. MSc Thesis: *Reduction of seawall overtopping at the Strand*, Stellenbosch: University of Stellenbosch

Schoonees, T., 2014. MEng Thesis: *Impermeable recurve seawalls to reduce wave overtopping*, Stellenbosch: University of Stellenbosch

Schoonees, T., Toms, G. 2016. *Recurve Seawalls To Reduce Wave Overtopping*. PIANC-COPEDEC IX, 2016, Rio de Janeiro, Brazil

Swart, E. 2016. MEng Thesis: *Effect of the overhang length of a recurve seawall in reducing wave overtopping*, Stellenbosch: University of Stellenbosch

USACE, 2006. *Coastal Engineering Manual*. EM 1110-2-1100 (in 6 parts), Washington, D.C.: US Army Corps of Engineers

van der Meer, J. et al., n.d. Prediction of Overtopping. *Overtopping Manual*, pp.320-381.

West, I., 2007. Sandbanks Sand Spit, Geology of the Wessex Coast of Southern England. [Online] Available at: http://www.southampton.ac.uk/~imw/Sandbanks.htm
[Accessed 9 September 2016]

List of Appendices

Appendix A: Long-section of wave flume

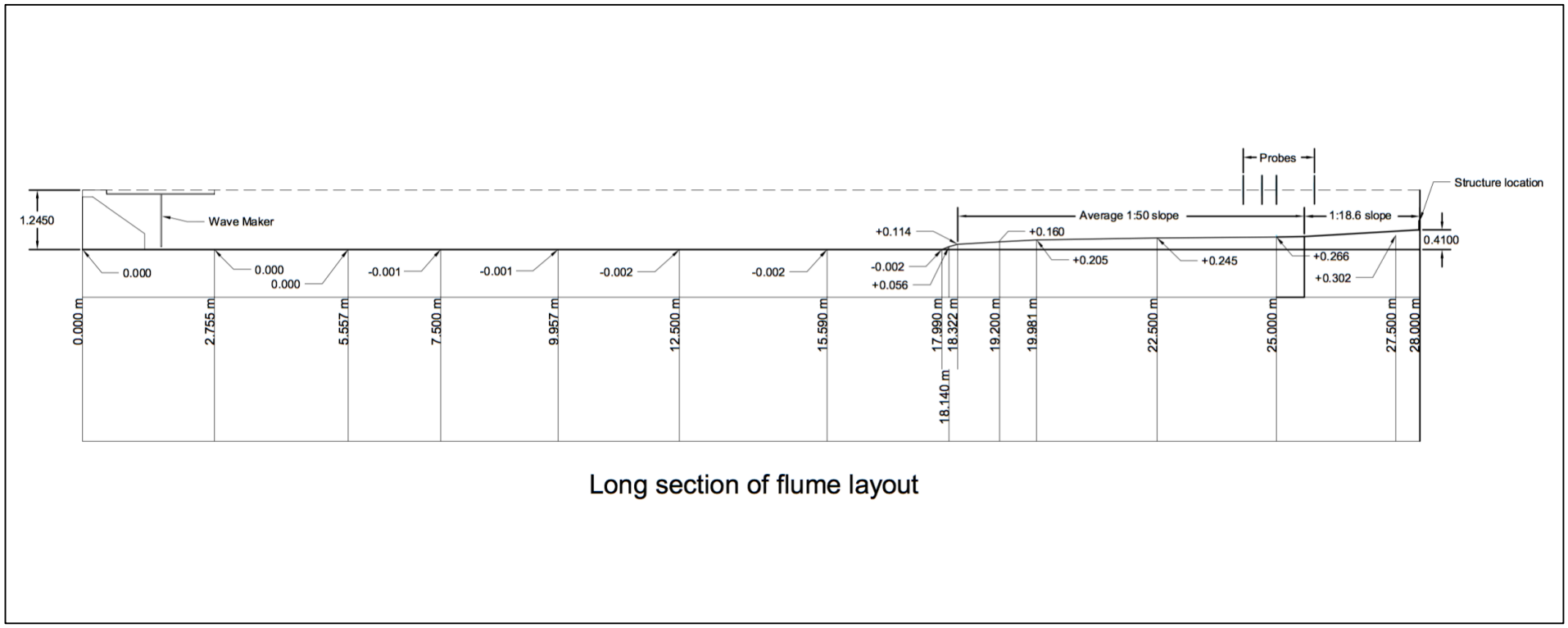

Long section of flume layout

Appendix B: Model Results

Recurve A		A-11-2	A-12-2	A-13	A-14	A-15	A-21	A-22
WL_{paddle}	m	0,446	0,446	0,446	0,446	0,446	0,466	0,466
WL_{toe}	m	0,03	0,03	0,03	0,03	0,03	0,05	0,05
R_c	m	0,17	0,17	0,17	0,17	0,17	0,15	0,15
T_p	s	1,342	1,789	2,236	2,683	3,13	1,342	1,789
Test Duration (1000 waves)	s	1342	1789	2236	2683	3130	1342	1789
$H_{mo\ (Avg)}$	mm	64,20	60,40	62,77	65,99	66,14	61,38	55,29
H_i	mm	47,53	51,90	50,48	50,62	50,17	45,89	47,03
Overtopping volume	l	0,28	0,14	0,00	0,00	0,00	0,14	0,00
WL_{toe}	m	0,6	0,6	0,6	0,6	0,6	1,0	1,0
R_c	m	3,4	3,4	3,4	3,4	3,4	3,0	3,0
T_p	s	6	8	10	12	14	6	8
$H_{mo\ (Avg)}$	m	1,28	1,21	1,26	1,32	1,32	1,23	1,11
H_i	m	0,95	1,04	1,01	1,01	1,00	0,92	0,94
Overtopping volume	l	2222	1111	0	0	0	1111	0
Overtopping rate	l/s/m	0,02	0,01	0,00	0,00	0,00	0,01	0,00

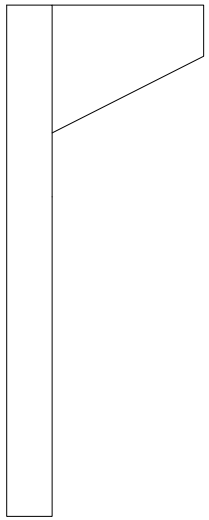

Recurve A		A-23	A-24	A-25	A-31	A-32	A-33-2	A-33-3	A-34	A-35	A-41
WL_{paddle}	m	0,466	0,466	0,466	0,496	0,496	0,496	0,496	0,496	0,496	0,516
WL_{toe}	m	0,05	0,05	0,05	0,08	0,08	0,08	0,08	0,08	0,08	0,1
R_c	m	0,15	0,15	0,15	0,12	0,12	0,12	0,12	0,12	0,12	0,1
T_p	s	2,236	2,683	3,13	1,342	1,789	2,236	2,236	2,683	3,130	1,342
Test Duration (1000 waves)	s	2236	2683	3130	1342	1789	2236	2236	2683	3130	1342
$H_{mo\ (Avg)}$	mm	57,39	59,09	57,67	67,64	72,38	61,87	61,66	76,08	76,39	68,87
H_i	mm	47,12	47,98	46,25	49,53	60,18	49,90	49,75	60,19	60,26	49,78
Overtopping volume	l	0,00	0,00	0,00	0,00	0,00	0,00	0,00	10,00	13,75	0,22
WL_{toe}	m	1,0	1,0	1,0	1,6	1,6	1,6	1,6	1,6	1,6	2,0
R_c	m	3,0	3,0	3,0	2,4	2,4	2,4	2,4	2,4	2,4	2,0
T_p	s	10	12	14	6	8	10	10	12	14	6
$H_{mo\ (Avg)}$	m	1,15	1,18	1,15	1,35	1,45	1,24	1,23	1,52	1,53	1,38
H_i	m	0,94	0,96	0,92	0,99	1,20	1,00	1,00	1,20	1,21	1,00
Overtopping volume	l	0	0	0	0	0	0	0	80000	110000	1778
Overtopping rate	l/s/m	0,00	0,00	0,00	0,00	0,00	0,00	0,00	0,33	0,39	0,01

Recurve A		A-42	A-43-2	A-43-3	A-44-2	A-44-3	A-44-4	A-45	A-51	A-52-2	A-53-2
WL_{paddle}	m	0,516	0,516	0,516	0,516	0,516	0,516	0,516	0,536	0,536	0,536
WL_{toe}	m	0,1	0,1	0,1	0,1	0,1	0,1	0,1	0,12	0,12	0,12
R_c	m	0,1	0,1	0,1	0,1	0,1	0,1	0,1	0,08	0,08	0,08
T_p	s	1,789	2,236	2,236	2,683	2,683	2,683	3,130	1,342	1,789	2,236
Test Duration (1000 waves)	s	1789	2236	2236	2683	2683	2683	3130	1342	1789	2236
$H_{mo\ (Avg)}$	mm	73,57	64,37	64,02	62,29	62,48	61,53	80,38	67,66	60,52	65,96
H_i	mm	59,79	50,93	50,63	48,26	48,41	47,65	63,63	48,64	47,28	51,05
Overtopping volume	l	1,67	1,11	1,11	3,89	4,44	5,00	134,08	0,56	1,67	33,00
WL_{toe}	m	2,0	2,0	2,0	2,0	2,0	2,0	2,0	2,4	2,4	2,4
R_c	m	2,0	2,0	2,0	2,0	2,0	2,0	2,0	1,6	1,6	1,6
T_p	s	8	10	10	12	12	12	14	6	8	10
$H_{mo\ (Avg)}$	m	1,47	1,29	1,28	1,25	1,25	1,23	1,61	1,35	1,21	1,32
H_i	m	1,20	1,02	1,01	0,97	0,97	0,95	1,27	0,97	0,95	1,02
Overtopping volume	l	13360	8889	8889	31111	35556	40000	1072640	4444	13333	264000
Overtopping rate	l/s/m	0,08	0,04	0,04	0,13	0,15	0,17	3,83	0,04	0,08	1,32

Recurve A		A-53-3	A-53-4	A-54-2	A-55
WL_{paddle}	m	0,536	0,536	0,536	0,536
WL_{toe}	m	0,12	0,12	0,12	0,12
R_c	m	0,08	0,08	0,08	0,08
T_p	s	2,236	2,236	2,683	3,130
Test Duration (1000 waves)	s	2236	2236	2683	3130
$H_{mo\ (Avg)}$	mm	66,50	66,24	62,26	66,63
H_i	mm	51,42	51,22	48,00	51,72
Overtopping volume	l	33,50	32,25	110,56	196,42
WL_{toe}	m	2,4	2,4	2,4	2,4
R_c	m	1,6	1,6	1,6	1,6
T_p	s	10	10	12	14
$H_{mo\ (Avg)}$	m	1,33	1,32	1,25	1,33
H_i	m	1,03	1,02	0,96	1,03
Overtopping volume	l	268000	258000	884480	1571360
Overtopping rate	l/s/m	1,34	1,29	3,69	5,61

Recurve B		B-11	B-12	B-13	B-14	B-15	B-21	B-22
WL_{paddle}	m	0,446	0,446	0,446	0,446	0,446	0,466	0,466
WL_{toe}	m	0,03	0,03	0,03	0,03	0,03	0,05	0,05
R_c	m	0,17	0,17	0,17	0,17	0,17	0,15	0,15
T_p	s	1,342	1,789	2,236	2,683	3,13	1,342	1,789
Test Duration (1000 waves)	s	1342	1789	2236	2683	3130	1342	1789
$H_{mo\ (Avg)}$	mm	65,00	62,13	65,59	68,37	67,48	62,70	56,48
H_i	mm	48,19	52,78	52,68	52,22	50,86	46,97	47,92
Overtopping volume	l	0,14	0,28	0,00	0,14	0,14	0,14	0,00
WL_{toe}	m	0,6	0,6	0,6	0,6	0,6	1,0	1,0
R_c	m	3,4	3,4	3,4	3,4	3,4	3,0	3,0
T_p	s	6	8	10	12	14	6	8
$H_{mo\ (Avg)}$	m	1,30	1,24	1,31	1,37	1,35	1,25	1,13
H_i	m	0,96	1,06	1,05	1,04	1,02	0,94	0,96
Overtopping volume	l	1111	2222	0	1111	1111	1111	0
Overtopping rate	l/s/m	0,01	0,01	0,00	0,005	0,004	0,01	0,00

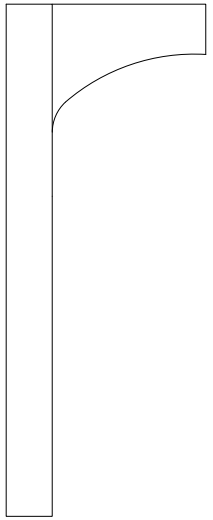

Recurve B		B-23	B-24	B-25	B-31	B-32	B-33	B-34	B-35	B-41	B-42
WL_{paddle}	m	0,466	0,466	0,466	0,496	0,496	0,496	0,496	0,496	0,516	0,516
WL_{toe}	m	0,05	0,05	0,05	0,08	0,08	0,08	0,08	0,08	0,1	0,1
R_c	m	0,15	0,15	0,15	0,12	0,12	0,12	0,12	0,12	0,1	0,1
T_p	s	2,236	2,683	3,13	1,342	1,789	2,236	2,683	3,130	1,342	1,789
Test Duration (1000 waves)	s	2236	2683	3130	1342	1789	2236	2683	3130	1342	1789
$H_{mo\ (Avg)}$	mm	59,00	60,32	58,12	67,68	57,52	63,32	60,51	59,72	64,80	56,10
H_i	mm	48,38	48,79	46,45	49,51	47,21	51,09	47,75	47,32	46,49	44,34
Overtopping volume	l	0,00	0,28	0,00	0,00	0,00	0,00	0,00	0,28	0,00	0,00
WL_{toe}	m	1,0	1,0	1,0	1,6	1,6	1,6	1,6	1,6	2,0	2,0
R_c	m	3,0	3,0	3,0	2,4	2,4	2,4	2,4	2,4	2,0	2,0
T_p	s	10	12	14	6	8	10	12	14	6	8
$H_{mo\ (Avg)}$	m	1,18	1,21	1,16	1,35	1,15	1,27	1,21	1,19	1,30	1,12
H_i	m	0,97	0,98	0,93	0,99	0,94	1,02	0,96	0,95	0,93	0,89
Overtopping volume	l	0	2222	0	0	0	0	0	2222	0	0
Overtopping rate	l/s/m	0,00	0,01	0,00	0,00	0,00	0,00	0,00	0,01	0,00	0,00

Recurve B		B-43	B-44	B-45-2	B-51	B-52	B-53	B-53-2	B-54	B-55	B-55-2
WL_{paddle}	m	0,516	0,516	0,516	0,536	0,536	0,536	0,536	0,536	0,536	0,536
WL_{toe}	m	0,1	0,1	0,1	0,12	0,12	0,12	0,12	0,12	0,12	0,12
R_c	m	0,1	0,1	0,1	0,08	0,08	0,08	0,08	0,08	0,08	0,08
T_p	s	2,236	2,683	3,130	1,342	1,789	2,236	2,236	2,683	3,130	3,130
Test Duration (1000 waves)	s	2236	2683	3130	1342	1789	2236	2236	2683	3130	3130
$H_{mo\ (Avg)}$	mm	61,31	58,87	61,56	63,59	56,33	62,43	62,30	58,86	63,00	63,48
H_i	mm	48,32	45,32	48,14	45,67	43,53	48,02	47,92	44,95	48,10	48,49
Overtopping volume	l	0,00	1,11	6,39	0,00	0,28	14,50	14,25	54,22	116,07	114,89
WL_{toe}	m	2,0	2,0	2,0	2,4	2,4	2,4	2,4	2,4	2,4	2,4
R_c	m	2,0	2,0	2,0	1,6	1,6	1,6	1,6	1,6	1,6	1,6
T_p	s	10	12	14	6	8	10	10	12	14	14
$H_{mo\ (Avg)}$	m	1,23	1,18	1,23	1,27	1,13	1,25	1,25	1,18	1,26	1,27
H_i	m	0,97	0,91	0,96	0,91	0,87	0,96	0,96	0,90	0,96	0,97
Overtopping volume	l	0	8889	51112	0	2222	116000	114000	433760	928560	919096
Overtopping rate	l/s/m	0,00	0,04	0,18	0,00	0,01	0,58	0,57	1,81	3,32	3,28

Recurve C		C-11	C-12	C-13	C-14	C-15	C-21	C-22
WL_{paddle}	m	0,446	0,446	0,446	0,446	0,446	0,466	0,466
WL_{toe}	m	0,03	0,03	0,03	0,03	0,03	0,05	0,05
R_c	m	0,17	0,17	0,17	0,17	0,17	0,15	0,15
T_p	s	1,342	1,789	2,236	2,683	3,13	1,342	1,789
Test Duration (1000 waves)	s	1342	1789	2236	2683	3130	1342	1789
$H_{mo\ (Avg)}$	mm	63,41	59,60	62,61	65,03	64,77	59,85	54,63
H_i	mm	46,78	51,31	50,45	49,94	49,11	44,66	46,39
Overtopping volume	l	0,14	0,14	0,00	0,14	0,00	0,14	0,00
WL_{toe}	m	0,6	0,6	0,6	0,6	0,6	1,0	1,0
R_c	m	3,4	3,4	3,4	3,4	3,4	3,0	3,0
T_p	s	6	8	10	12	14	6	8
$H_{mo\ (Avg)}$	m	1,27	1,19	1,25	1,30	1,30	1,20	1,09
H_i	m	0,94	1,03	1,01	1,00	0,98	0,89	0,93
Overtopping volume	l	1111	1111	0	1111	0	1111	0
Overtopping rate	l/s/m	0,01	0,01	0,00	0,005	0,00	0,01	0,00

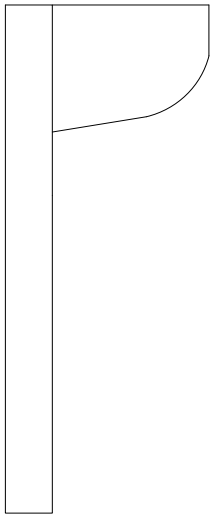

Recurve C		C-23	C-24	C-25	C-31	C-32	C-33	C-34	C-35	C-41	C-42
WL_{paddle}	m	0,466	0,466	0,466	0,496	0,496	0,496	0,496	0,496	0,516	0,516
WL_{toe}	m	0,05	0,05	0,05	0,08	0,08	0,08	0,08	0,08	0,1	0,1
R_c	m	0,15	0,15	0,15	0,12	0,12	0,12	0,12	0,12	0,1	0,1
T_p	s	2,236	2,683	3,13	1,342	1,789	2,236	2,683	3,130	1,342	1,789
Test Duration (1000 waves)	s	2236	2683	3130	1342	1789	2236	2683	3130	1342	1789
$H_{mo\ (Avg)}$	mm	56,25	58,82	56,20	65,38	58,16	61,93	62,84	61,67	66,08	57,32
H_i	mm	46,26	47,65	45,09	47,78	47,84	49,99	49,58	49,00	47,58	45,37
Overtopping volume	l	0,00	0,00	0,00	0,00	0,14	0,56	1,81	9,44	1,25	1,11
WL_{toe}	m	1,0	1,0	1,0	1,6	1,6	1,6	1,6	1,6	2,0	2,0
R_c	m	3,0	3,0	3,0	2,4	2,4	2,4	2,4	2,4	2,0	2,0
T_p	s	10	12	14	6	8	10	12	14	6	8
$H_{mo\ (Avg)}$	m	1,13	1,18	1,12	1,31	1,16	1,24	1,26	1,23	1,32	1,15
H_i	m	0,93	0,95	0,90	0,96	0,96	1,00	0,99	0,98	0,95	0,91
Overtopping volume	l	0	0	0	0	1111	4444	14444	75520	10000	8889
Overtopping rate	l/s/m	0,00	0,00	0,00	0,00	0,01	0,02	0,06	0,27	0,08	0,06

Recurve C		C-43	C-44	C-45	C-51	C-52	C-53	C-54	C-55	C-55-2
WL_{paddle}	m	0,516	0,516	0,516	0,536	0,536	0,536	0,536	0,536	0,536
WL_{toe}	m	0,1	0,1	0,1	0,12	0,12	0,12	0,12	0,12	0,12
R_c	m	0,1	0,1	0,1	0,08	0,08	0,08	0,08	0,08	0,08
T_p	s	2,236	2,683	3,130	1,342	1,789	2,236	2,683	3,130	3,130
Test Duration (1000 waves)	s	2236	2683	3130	1342	1789	2236	2683	3130	3130
$H_{mo\ (Avg)}$	mm	63,46	61,38	62,95	65,30	57,29	62,94	59,29	64,00	63,49
H_i	mm	50,18	47,58	49,56	46,94	44,62	48,69	45,64	49,34	48,95
Overtopping volume	l	13,50	38,33	68,33	13,00	14,88	51,11	146,84	223,07	228,67
WL_{toe}	m	2,0	2,0	2,0	2,4	2,4	2,4	2,4	2,4	2,4
R_c	m	2,0	2,0	2,0	1,6	1,6	1,6	1,6	1,6	1,6
T_p	s	10	12	14	6	8	10	12	14	14
$H_{mo\ (Avg)}$	m	1,27	1,23	1,26	1,31	1,15	1,26	1,19	1,28	1,27
H_i	m	1,00	0,95	0,99	0,94	0,89	0,97	0,91	0,99	0,98
Overtopping volume	l	108000	306640	546640	104000	119000	408880	1174720	1784560	1829360
Overtopping rate	l/s/m	0,54	1,28	1,95	0,87	0,74	2,04	4,89	6,37	6,53

Recurve D		D-11	D-12	D-13	D-14	D-15	D-21	D-22
WL_{paddle}	m	0,446	0,446	0,446	0,446	0,446	0,466	0,466
WL_{toe}	m	0,03	0,03	0,03	0,03	0,03	0,05	0,05
R_c	m	0,17	0,17	0,17	0,17	0,17	0,15	0,15
T_p	s	1,342	1,789	2,236	2,683	3,13	1,342	1,789
Test Duration (1000 waves)	s	1342	1789	2236	2683	3130	1342	1789
$H_{mo\ (Avg)}$	mm	63,24	59,95	63,13	65,84	65,20	60,47	54,75
H_i	mm	46,94	51,45	50,82	50,49	49,38	45,08	46,15
Overtopping volume	l	0,14	0,14	0,00	0,14	0,00	0,28	0,28
WL_{toe}	m	0,6	0,6	0,6	0,6	0,6	1,0	1,0
R_c	m	3,4	3,4	3,4	3,4	3,4	3,0	3,0
T_p	s	6	8	10	12	14	6	8
$H_{mo\ (Avg)}$	m	1,26	1,20	1,26	1,32	1,30	1,21	1,09
H_i	m	0,94	1,03	1,02	1,01	0,99	0,90	0,92
Overtopping volume	l	1111	1111	0	1111	0	2222	2222
Overtopping rate	l/s/m	0,01	0,01	0,00	0,005	0,00	0,02	0,01

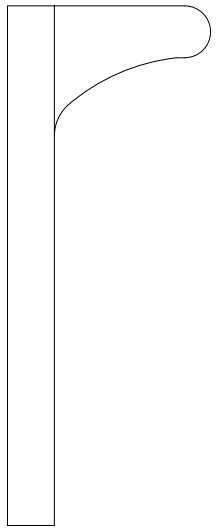

Recurve D		D-23	D-24	D-25	D-31	D-32	D-33	D-34	D-35	D-41	D-42
WL_{paddle}	m	0,466	0,466	0,466	0,496	0,496	0,496	0,496	0,496	0,516	0,516
WL_{toe}	m	0,05	0,05	0,05	0,08	0,08	0,08	0,08	0,08	0,1	0,1
R_c	m	0,15	0,15	0,15	0,12	0,12	0,12	0,12	0,12	0,1	0,1
T_p	s	2,236	2,683	3,13	1,342	1,789	2,236	2,683	3,130	1,342	1,789
Test Duration (1000 waves)	s	2236	2683	3130	1342	1789	2236	2683	3130	1342	1789
$H_{mo\ (Avg)}$	mm	57,12	58,87	56,58	66,08	58,23	61,80	61,85	60,55	66,23	58,25
H_i	mm	46,88	47,78	45,42	48,22	47,95	49,87	48,86	48,04	47,59	46,16
Overtopping volume	l	0,56	0,83	0,83	0,97	1,39	1,67	3,06	3,61	1,67	1,67
WL_{toe}	m	1,0	1,0	1,0	1,6	1,6	1,6	1,6	1,6	2,0	2,0
R_c	m	3,0	3,0	3,0	2,4	2,4	2,4	2,4	2,4	2,0	2,0
T_p	s	10	12	14	6	8	10	12	14	6	8
$H_{mo\ (Avg)}$	m	1,14	1,18	1,13	1,32	1,16	1,24	1,24	1,21	1,32	1,17
H_i	m	0,94	0,96	0,91	0,96	0,96	1,00	0,98	0,96	0,95	0,92
Overtopping volume	l	4444	6667	6667	7778	11111	13333	24444	28889	13333	13333
Overtopping rate	l/s/m	0,02	0,03	0,02	0,06	0,07	0,07	0,10	0,10	0,11	0,08

Recurve D		D-43	D-44	D-45	D-51	D-52	D-53	D-54	D-54-2	D-55	D-55-2
WL_{paddle}	m	0,516	0,516	0,516	0,536	0,536	0,536	0,536	0,536	0,536	0,536
WL_{toe}	m	0,1	0,1	0,1	0,12	0,12	0,12	0,12	0,12	0,12	0,12
R_c	m	0,1	0,1	0,1	0,08	0,08	0,08	0,08	0,08	0,08	0,08
T_p	s	2,236	2,683	3,130	1,342	1,789	2,236	2,683	2,683	3,130	3,130
Test Duration (1000 waves)	s	2236	2683	3130	1342	1789	2236	2683	2683	3130	3130
$H_{mo\ (Avg)}$	mm	63,30	61,11	63,50	65,50	58,04	63,97	60,29	60,51	64,21	64,90
H_i	mm	49,91	47,23	49,77	46,99	44,88	49,27	46,09	46,37	49,16	49,72
Overtopping volume	l	3,89	7,22	18,89	1,94	3,06	28,75	90,96	96,80	162,34	170,52
WL_{toe}	m	2,0	2,0	2,0	2,4	2,4	2,4	2,4	2,4	2,4	2,4
R_c	m	2,0	2,0	2,0	1,6	1,6	1,6	1,6	1,6	1,6	1,6
T_p	s	10	12	14	6	8	10	12	12	14	14
$H_{mo\ (Avg)}$	m	1,27	1,22	1,27	1,31	1,16	1,28	1,21	1,21	1,28	1,30
H_i	m	1,00	0,94	1,00	0,94	0,90	0,99	0,92	0,93	0,98	0,99
Overtopping volume	l	31111	57760	151120	15556	24444	230000	727680	774400	1298720	1364160
Overtopping rate	l/s/m	0,16	0,24	0,54	0,13	0,15	1,15	3,03	3,23	4,64	4,87

Recurve E		E-11	E-12	E-13	E-14	E-15	E-21	E-22
WL_{paddle}	m	0,446	0,446	0,446	0,446	0,446	0,466	0,466
WL_{toe}	m	0,03	0,03	0,03	0,03	0,03	0,05	0,05
R_c	m	0,17	0,17	0,17	0,17	0,17	0,15	0,15
T_p	s	1,342	1,789	2,236	2,683	3,13	1,342	1,789
Test Duration (1000 waves)	s	1342	1789	2236	2683	3130	1342	1789
$H_{mo\ (Avg)}$	mm	64,45	60,63	63,54	66,87	65,76	61,36	54,96
H_i	mm	47,86	52,08	51,05	51,13	49,73	45,79	46,40
Overtopping volume	l	0,14	0,14	0,14	0,14	0,14	0,14	0,00
WL_{toe}	m	0,6	0,6	0,6	0,6	0,6	1,0	1,0
R_c	m	3,4	3,4	3,4	3,4	3,4	3,0	3,0
T_p	s	6	8	10	12	14	6	8
$H_{mo\ (Avg)}$	m	1,29	1,21	1,27	1,34	1,32	1,23	1,10
H_i	m	0,96	1,04	1,02	1,02	0,99	0,92	0,93
Overtopping volume	l	1111	1111	1111	1111	1111	1111	0
Overtopping rate	l/s/m	0,01	0,01	0,01	0,005	0,004	0,01	0,00

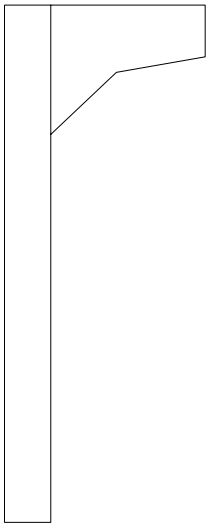

Recurve E		E-23	E-24	E-25	E-31	E-32	E-33	E-34	E-35	E-41	E-42
WL_{paddle}	m	0,466	0,466	0,466	0,496	0,496	0,496	0,496	0,496	0,516	0,516
WL_{toe}	m	0,05	0,05	0,05	0,08	0,08	0,08	0,08	0,08	0,1	0,1
R_c	m	0,15	0,15	0,15	0,12	0,12	0,12	0,12	0,12	0,1	0,1
T_p	s	2,236	2,683	3,13	1,342	1,789	2,236	2,683	3,130	1,342	1,789
Test Duration (1000 waves)	s	2236	2683	3130	1342	1789	2236	2683	3130	1342	1789
$H_{mo\ (Avg)}$	mm	57,23	59,29	57,27	66,26	59,50	62,39	62,56	61,62	67,48	58,88
H_i	mm	46,95	48,00	45,84	48,40	48,97	50,32	49,42	48,92	48,68	46,74
Overtopping volume	l	0,00	0,00	0,00	0,00	0,00	0,00	0,00	0,56	0,00	0,00
WL_{toe}	m	1,0	1,0	1,0	1,6	1,6	1,6	1,6	1,6	2,0	2,0
R_c	m	3,0	3,0	3,0	2,4	2,4	2,4	2,4	2,4	2,0	2,0
T_p	s	10	12	14	6	8	10	12	14	6	8
$H_{mo\ (Avg)}$	m	1,14	1,19	1,15	1,33	1,19	1,25	1,25	1,23	1,35	1,18
H_i	m	0,94	0,96	0,92	0,97	0,98	1,01	0,99	0,98	0,97	0,93
Overtopping volume	l	0	0	0	0	0	0	0	4444	0	0
Overtopping rate	l/s/m	0,00	0,00	0,00	0,00	0,00	0,00	0,00	0,02	0,00	0,00

Recurve E		E-43	E-44	E-45	E-51	E-52	E-53	E-54	E-54-2	E-55	E-55-2
WL_{paddle}	m	0,516	0,516	0,516	0,536	0,536	0,536	0,536	0,536	0,536	0,536
WL_{toe}	m	0,1	0,1	0,1	0,12	0,12	0,12	0,12	0,12	0,12	0,12
R_c	m	0,1	0,1	0,1	0,08	0,08	0,08	0,08	0,08	0,08	0,08
T_p	s	2,236	2,683	3,130	1,342	1,789	2,236	2,683	2,683	3,130	3,130
Test Duration (1000 waves)	s	2236	2683	3130	1342	1789	2236	2683	2683	3130	3130
$H_{mo\ (Avg)}$	mm	64,46	62,29	64,30	67,52	59,41	65,64	62,05	62,28	66,82	66,65
H_i	mm	50,93	48,23	50,41	48,56	46,21	50,66	47,65	47,87	51,70	51,57
Overtopping volume	l	0,56	2,22	13,13	0,14	0,69	21,25	76,39	76,94	148,17	149,21
WL_{toe}	m	2,0	2,0	2,0	2,4	2,4	2,4	2,4	2,4	2,4	2,4
R_c	m	2,0	2,0	2,0	1,6	1,6	1,6	1,6	1,6	1,6	1,6
T_p	s	10	12	14	6	8	10	12	12	14	14
$H_{mo\ (Avg)}$	m	1,29	1,25	1,29	1,35	1,19	1,31	1,24	1,25	1,34	1,33
H_i	m	1,02	0,96	1,01	0,97	0,92	1,01	0,95	0,96	1,03	1,03
Overtopping volume	l	4444	17778	105000	1111	5556	170000	611112	615520	1185360	1193680
Overtopping rate	l/s/m	0,02	0,07	0,38	0,01	0,03	0,85	2,55	2,56	4,23	4,26

Appendix C: Influence of wave period

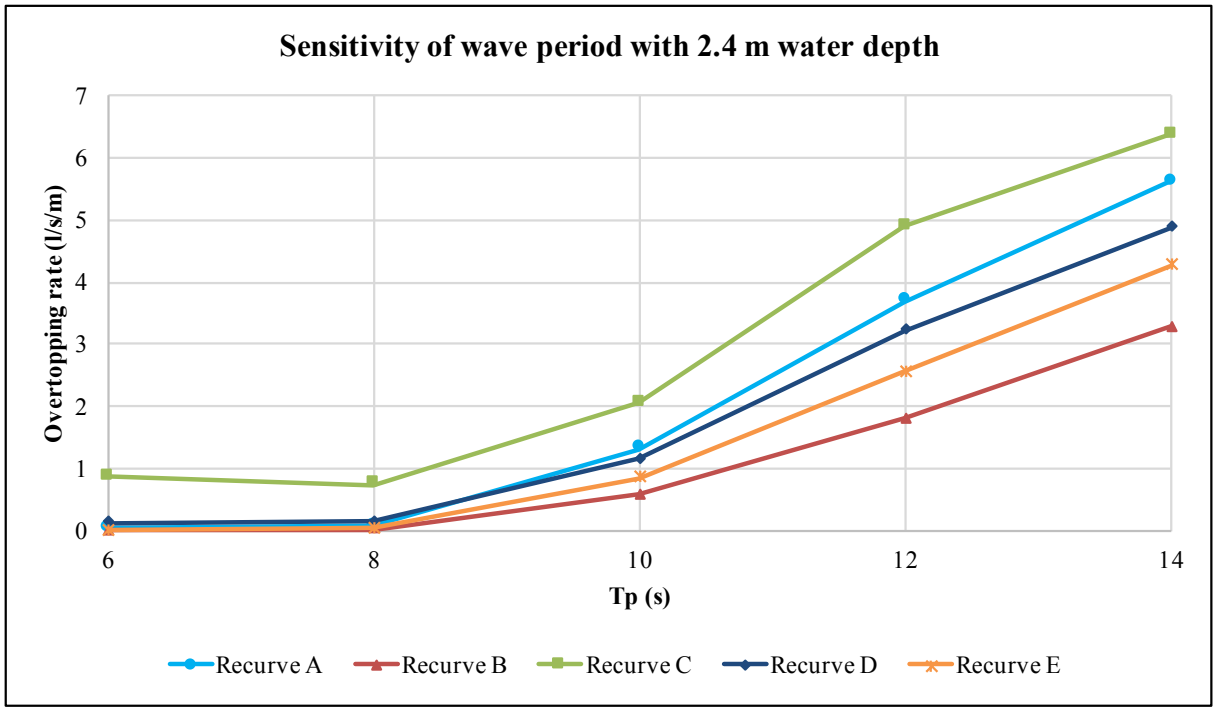

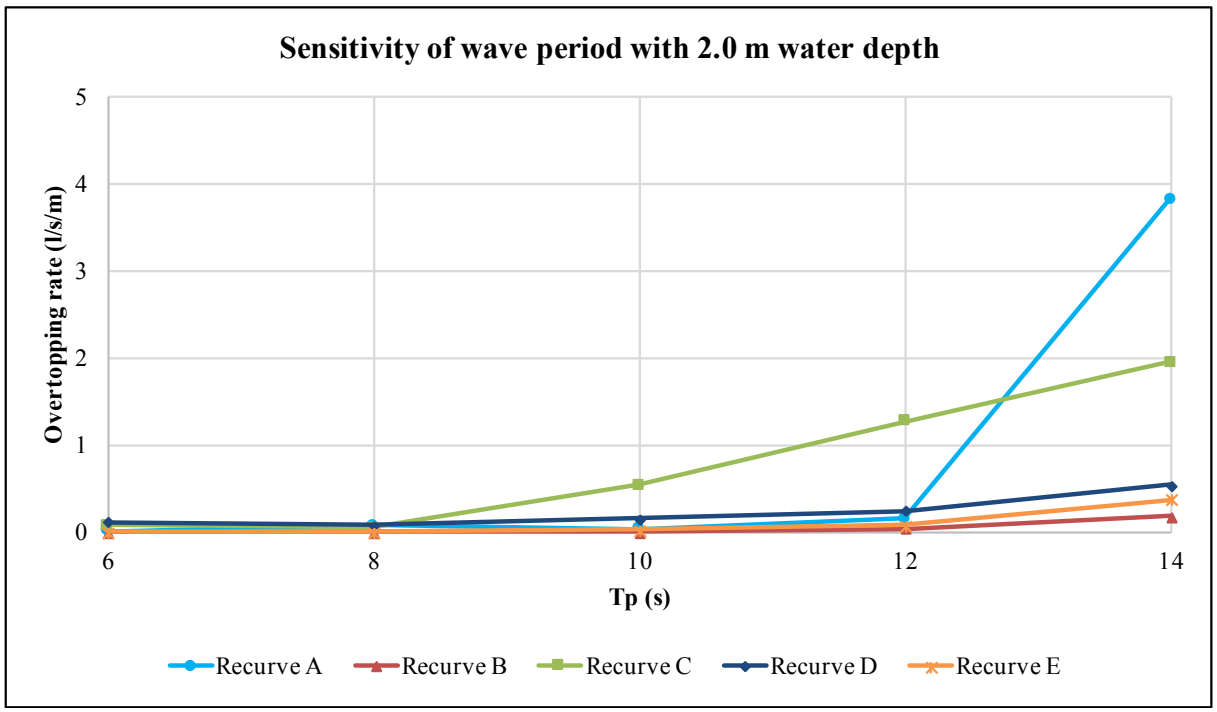

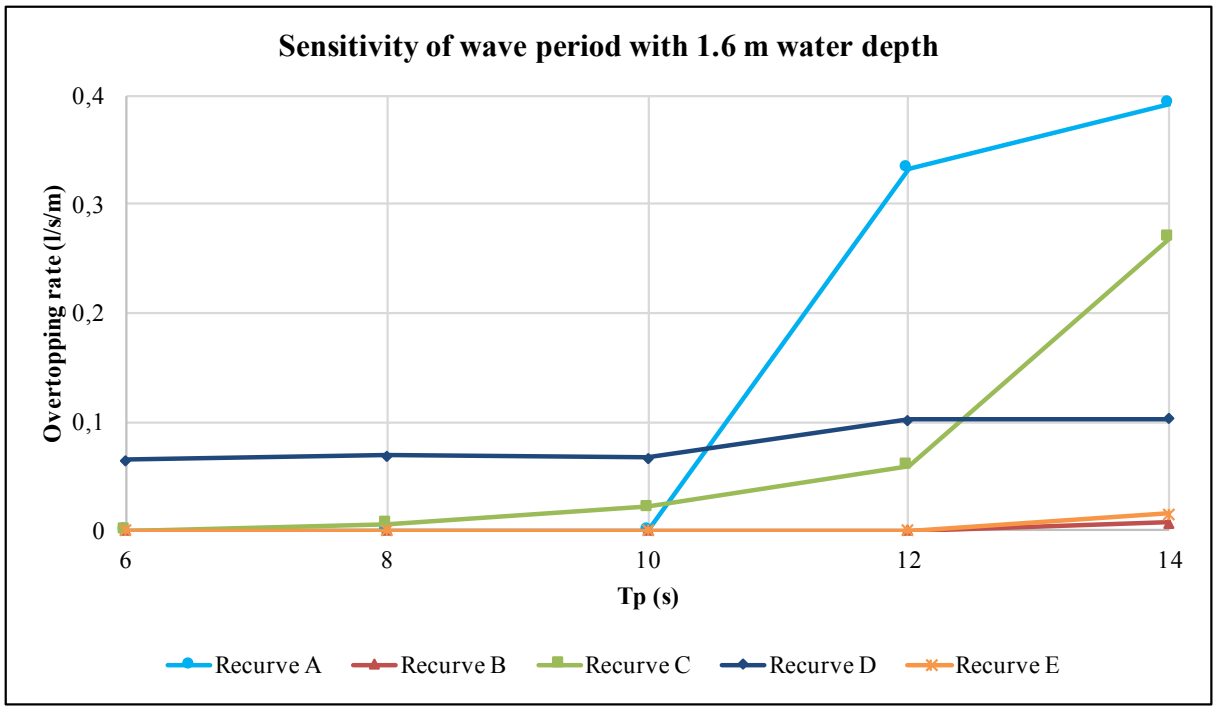

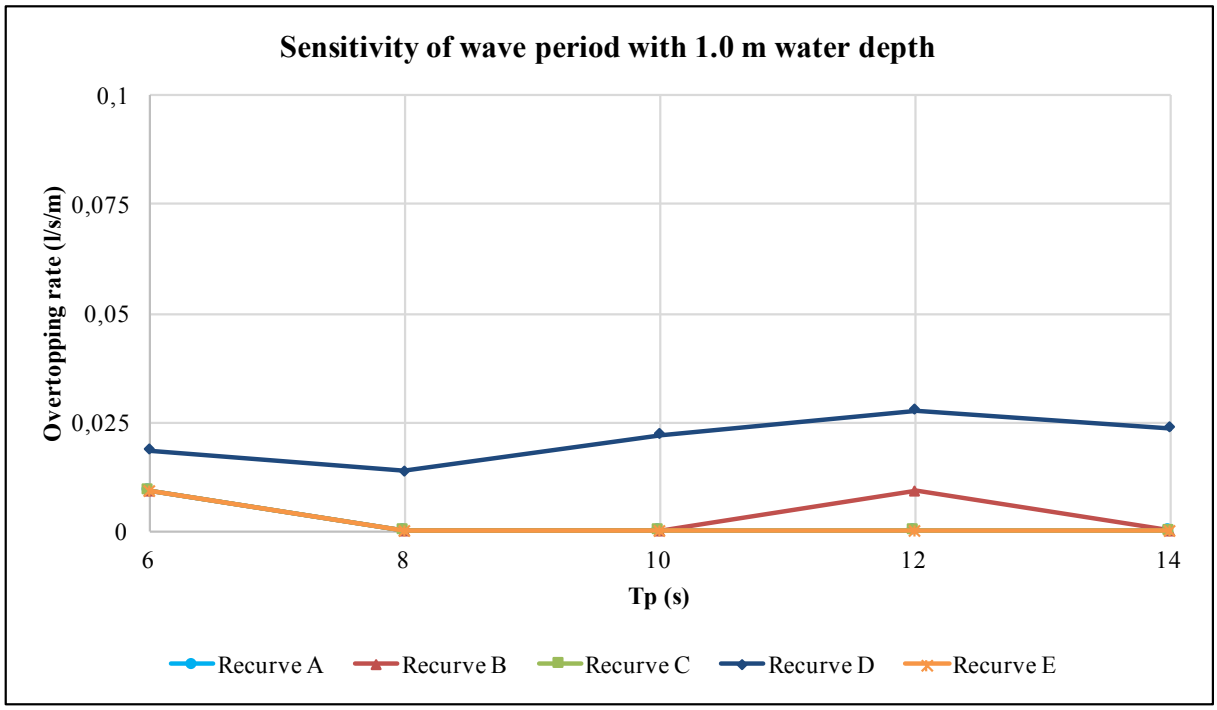

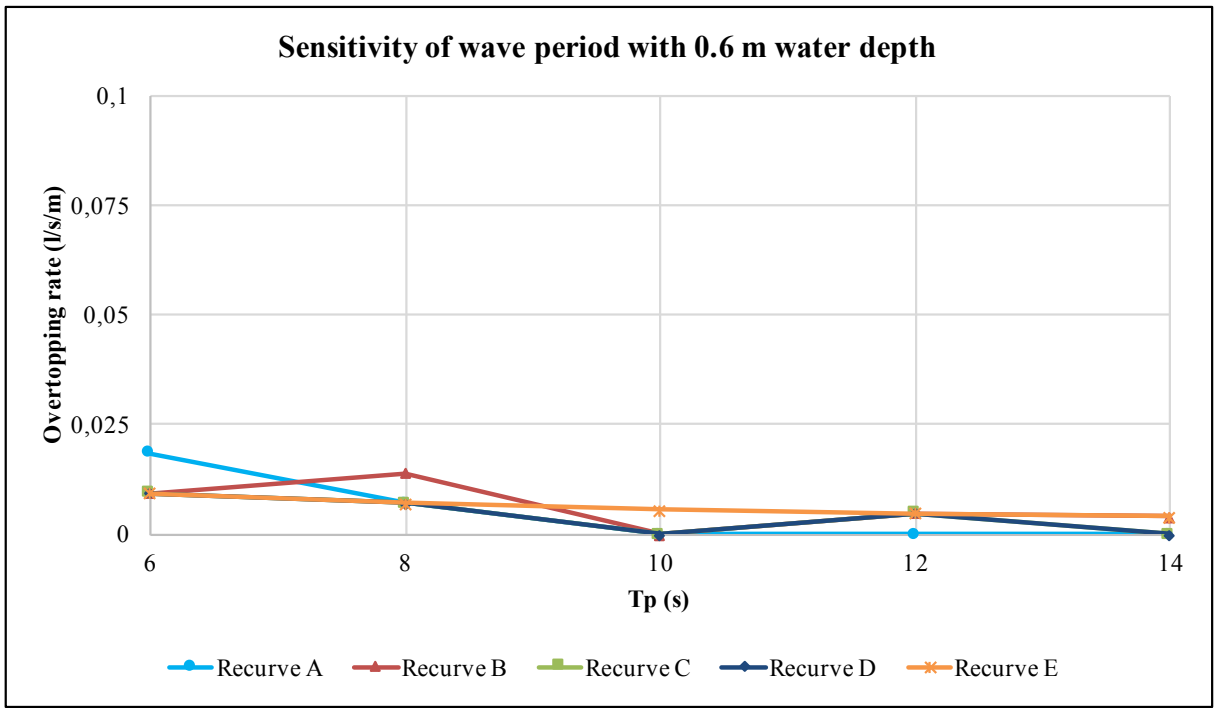

Appendix D: Influence of water depth